METHANE EMISSIONS FROM LAKES IN NORTHEAST SIBERIA AND ALASKA

A

DISSERTATION

Presented to the Faculty

of the University of Alaska Fairbanks

in Partial Fulfillment of the Requirements

for the Degree of

DOCTOR OF PHILOSOPHY

By

Katey Marion Walter, B.A., M.S.

Fairbanks, Alaska

May 2006

UMI Number: 3229744

INFORMATION TO USERS

The quality of this reproduction is dependent upon the quality of the copy submitted. Broken or indistinct print, colored or poor quality illustrations and photographs, print bleed-through, substandard margins, and improper alignment can adversely affect reproduction.

In the unlikely event that the author did not send a complete manuscript and there are missing pages, these will be noted. Also, if unauthorized copyright material had to be removed, a note will indicate the deletion.

UMI®

METHANE EMISSIONS FROM LAKES IN NORTHEAST SIBERIA AND ALASKA

By

Katey Marion Walter

RECOMMENDED:

Advisory Committee Chair

Assistant Chair, Department of Biology and Wildlife
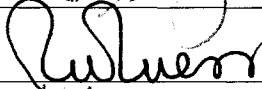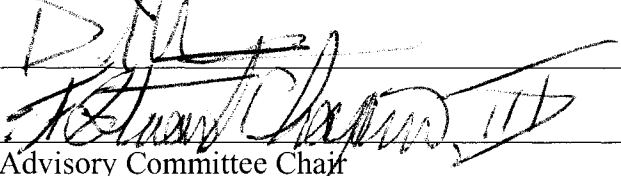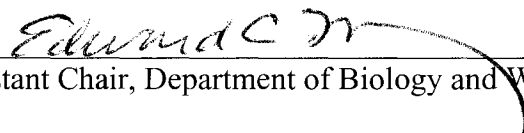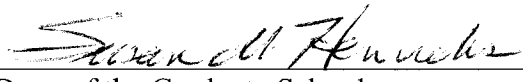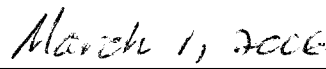
APPROVED:

Dean, College of Natural Science and Mathematics

Dean of the Graduate School

March 1, 2006

Date

ABSTRACT

Large uncertainties in the budget of atmospheric methane (CH_4), an important greenhouse gas whose relative greenhouse effect is 23 times stronger than that of carbon dioxide (CO_2), limit the accuracy of climate-change projections. Concentrations of atmospheric CH_4 have been rising during recent decades, particularly at high northern latitudes. The causes of this increase are not well understood. Here I describe and quantify an important source of methane—bubbling from northern lakes—that has not been incorporated in previous regional or global methane budgets.

I introduce a new method to accurately measure ebullition (bubbling), which accounted for 95% of CH_4 emissions from North Siberian thaw lakes. Documenting the patchiness of ebullition increased previous estimates of CH_4 flux from lakes 5-fold in Siberia and 2.5- to 14-fold in Alaska.

Extrapolating estimates of measured fluxes, I show that North Siberian yedoma (Pleistocene-aged organic-rich loess) thaw lakes emit 3.8 Tg CH_4 yr^{-1}. An independent mass-balance approach based on carbon lost from permafrost that thawed beneath lakes revealed that lakes emit 4-5 Tg CH_4 yr^{-1}. Adding these emissions significantly increases present estimates of northern wetland contributions (<6-40 Tg yr^{-1}) to the atmospheric CH_4 budget.

Thermokarst (thaw) erosion was the primary driver of CH_4 emissions in lakes. A 14.7% expansion of thaw lakes from 1974 to 2000 increased lake CH_4 emissions by 58% in Siberia, demonstrating a positive feedback to climate warming. The Pleistocene age of CH_4 (^{14}C age 35,570-42,800 years in Siberia and 14,760-26,020 years in Alaska) emitted from hotspots along active thermokarst margins of lakes demonstrated that recruitment of a previously sequestered carbon source contributes to this feedback.

Finally, reconstruction of yedoma's distribution at the Last Glacial Maximum together with compilation of thaw lake basal ages that developed at the onset of Holocene warming, suggested that thaw lake development contributed up to 70% of the rapid increase in atmospheric CH_4 during deglaciation.

About 425 Gt C remain preserved in the yedoma ice complex in North Siberia. If this Siberian permafrost warms more rapidly in the future as projected, the positive feedback of ebullition from expanding thaw lakes could increase the rate of high-latitude warming.

TABLE OF CONTENTS

LIST OF FIGURES

LIST OF TABLES

ACKNOWLEDGEMENTS

It is my pleasure to express gratitude to the many people from whom I have learned during the course of this research.

I thank my coauthors for their individual contributions to the science presented in these four chapters. Use of the word "we" in the manuscripts represents the team effort behind this research.

Terry Chapin, my adviser, contributed largely to the critical thinking and discussion of the content of these manuscripts, as well as to the financial support of the effort. Terry has taught me to find the constructive and positive side of any argument that allows me to proceed confidently with my work. I am grateful for all of the time, encouragement and mentorship that Terry has provided. His example has influenced my aspirations not only as a scientist and future adviser to students, but also to emulate his humility, consideration and generosity towards others.

Sergei Zimov, director of the Northeast Science Station in Cherskii, Siberia, where much of this research was conducted, served as a secondary adviser to me. I spent more than 14 months at the Northeast Science Station during this project. Sergei taught me to seek and prioritize the large and important questions in scientific research. He has strived to teach me to economize my efforts through forethought in projects. Sergei's brilliance and creativity in scientific thinking across a range of disciplines mark him as one of the truest geniuses I've met in my lifetime. Sergei contributed to this research from the earliest stages through to publication as a co-author by helping me to define my research objectives, providing logistical support at the Northeast Science Station, and providing intellectual contributions to the manuscripts, particularly with the mass balance calculations of methane produced over millennial time scales based on carbon loss beneath lakes.

Contributions from other co-authors are as follows: Dave Verbyla helped me with the GIS analysis of lake area change for Chapter 1. Qianlai Zhuang used my lake emission estimates in the Terrestrial Ecosystems Model to calculate the influence of

adding lakes to prior estimates of methane emissions from wetlands land in Northeast Siberia for Chapter 2. Mary Edwards contributed significantly to the development of the paleolakes paper (Chapter 3). She constructed the circumpolar map of yedoma distribution at the Last Glacial Maximum and the present day based on literature that we collected as a team. She also pulled together a large number of basal age dates for lakes in Siberia and Alaska, and has provided excellent critical reviews for each revision of the manuscript. Jeff Chanton provided laboratory support for me to conduct stable isotope analyses, and analyzed a large number of samples for this project himself. He has also provided constructive reviews of Chapters 1 and 4. Ted Schuur and Koushik Dutta also provided me lab space, support, and assistance for preparation of graphite targets from methane gas samples. Ted has provided constructive reviews of Chapters 1 and 4 as well.

Each of the members of my academic committee has enhanced my growth as a scientist during the years of my Ph.D. I am grateful to Dave Valentine for inspiring me always to dig deeper and explore interesting questions through discussion. His excellent and challenging critique of each of my manuscripts has substantially improved the product. I am grateful to Roger Ruess for encouraging me each time he saw me, and for making the life of a biology professor look pretty-darn-good. Bruce Finney was very supportive throughout the project, loaning me sediment coring instruments to take to Siberia despite the risk that they might never return, and providing a helpful perspective on lakes and isotopes based on his own rich history of research on Alaskan lakes.

I would like to thank each of the personnel at the Northeast Science Station, namely Sergei and Galya Zimov, and Sergei and Anja Davidov for their hospitality, help with measurements, and a wonderful experience collaborating on Russian soil. I hope that we will continue to work together several more decades to come.

This project would not have been possible without the energy and moral-boosting in field assistance from the following persons: Dmitri Draluk (2002-2004), Catherine Copass Thompson (2004), Edward Ricter (2004), Kaarle Strailey (2004), Erin Carr

(2003), Jason Vogel (2002), Dan Nidzgorski (2002), Nikita Zimov (2001), and Catherine Chan (2001).

I am thankful to Mimi Chapin for opening her home and sharing her love of Russia with me. Spending time with Mimi helped me to transition culturally between Alaska and Russia after spending many long months in Siberia.

My field work at the Toolik Lake Field Station was subsidized by Brian Barnes, who provided user days for me. Andrew Balser and Lael Rogan assisted me with GIS data.

Thoughtful manuscript reviews were provided by Donie Bret-Harte, Ed Dlugokencky and John Hobbie.

Finally, I am thankful for the love and support from my family in the lower 48, and to all of my friends and colleagues in the Fairbanks community who have become like a family to me during the past five years. In particular I'd like to thank my dear friends Jenny Rohrs Ritchie, Susanne Lyle, Anja Kade, Vera Wadsworth, Martin Wilmking and Eddie Ricter. I'd like to acknowledge Jason Vogel, Jill Johnstone, and Cath Copass Thompson for "showing me the ropes" of graduate school and setting rigorous examples of hard work and achievement as senior graduate students.

GENERAL INTRODUCTION

Methane (CH_4), the second-most important greenhouse gas after carbon dioxide, is responsible for ~20% of the direct radiative forcing from all long-lived greenhouse gases [Intergovernmental Panel on Climate Change (IPCC) 2001]. Methane was a major component of Earth's early atmosphere and is the most abundant organic gas in the atmosphere today. In addition to its effect on the Earth's energy balance through its infrared properties, CH_4 is chemically reactive, influencing concentrations of ozone (O_3), hydroxyl radicals (OH), and carbon monoxide (CO) in the troposphere. In the stratosphere, CH_4 concentration influences ozone and chlorine chemistry (Cicerone and Oremland 1988). The largest sink of atmospheric CH_4 is photochemical oxidation by the reactant, the hydroxyl radical, a reaction that produces CO, carbon dioxide (CO_2), water (H_2O), hydrogen (H_2) and formaldehyde (CH_2O). Half of stratospheric H_2O vapor comes from CH_4 oxidation.

During the past 150 years, the concentration of CH_4 in the atmosphere has more than doubled from 0.7 ppbv to ~1.8 ppbv (Etheridge *et al.*, 1998), due primarily to the rise of anthropogenic activities that release methane as a byproduct: ruminant animal husbandry, rice agriculture, natural gas production, coal mining, biomass burning, and landfills. In total, anthropogenic emissions account for ~60% of global CH_4 sources (IPCC 2001). Bacterial production of CH_4 under anaerobic conditions in wetlands is the largest natural source of atmospheric CH_4, accounting for ~15-47% of global emissions (IPCC 2001, Mikaloff Fletcher 2004). Bacterial CH_4 production also occurs in the guts of termites and zooplankton. Other recognized, though poorly quantified, sources of atmospheric CH_4 include bacterial production in ocean sediments and destabilization of gas hydrates in marine and permafrost strata. Methane oxidation in aerobic water columns and soils greatly decreases the magnitude of the emission sources. Oxidation of CH_4 by the OH radical in the troposphere accounts for ~90% of total destruction. The remaining sink is partitioned by methanotrophic bacteria in aerobic soils and by reaction with OH, Cl, and O ($_1$D) in the stratosphere.

Concentrations of atmospheric CH_4 are highest in the Arctic, where the greatest areal extent of wetlands also occurs (Fung et al., 1991, Mathews and Fung 1987, Aselmann and Crutzen 1989), and lowest in the Antarctic. The latitudinal gradient of atmospheric CH_4 is well documented (Rasmussen and Khalil 1984, Steele et al. 1987, Fung 1991). Analyses of ice cores extracted from Greenland and Antarctica show that northern sources of CH_4 have been important for hundreds of thousands of years before the industrial revolution (Rasmussen and Khalil 1984, Severinghaus and Brook 1999, Smith et al. 2004). Tropical sources are also large; however, substantial photolytic production of the OH radical in the tropics prevents buildup of tropical atmospheric CH_4 concentration to the degree that occurs in the north, where CH_4 sources are less balanced by sinks.

The increase in global atmospheric CH_4 results from an imbalance between sources and sinks, which have been identified, but poorly quantified due to difficulties in assessing high variability in emission rates (Fung et al., 1991, IPCC, 2001, Mikaloff Fletcher 2004). Although bogs and tundra have been identified as major sources of atmospheric CH_4 at northern high latitudes, contributing to the high late-summer and autumn increases in global CH_4 (Nisbet et al. 1988), uncertainties in the areal extent of wetlands and large spatial and temporal variability of short-term local CH_4 emission measurements result in a wide range in emission estimates (<6 -40 Tg CH_4 yr^{-1}) (Reeburgh et al. 1998, Worthy et al. 2000, Mikaloff Fletcher et al. 2004). Lakes are also a prominent landscape feature in the north, occupying up to 30% of the land surface area in some regions (Mathews and Fung 1987, Zimov et al. 1997, Hinkel et al. 2003). However model estimates of northern wetland emissions have yet to include ebullition (bubbling) from lakes (Zhaung et al. 2004, Mikaloff Fletcher et al. 2004a, b).

There is widespread interest in improving estimates and understanding controls of northern wetland CH_4 emissions because future climate projections of high latitude warming will further destabilize permafrost and accelerate thermokarst erosion (ground thaw and subsidence) (Osterkamp et al. 2000, Jorgenson et al. 2001, ACIA 2004, Sazonova et al. 2004), which releases organic matter previously sequestered in

permafrost into anaerobic decomposition environments of lakes and wetlands, enhancing methanogenesis (Zimov *et al.* 1997).

Local emissions from most lakes and wetlands can vary by several orders of magnitude on scales of a few meters or several hours. Heterogeneity in ebullition is a major contributor to this variability, and the spatial and temporal patchiness of ebullition challenges efforts to quantify this mode of emission. As a result, many studies of CH_4 emissions from lakes and wetlands report only emissions *via* molecular diffusion and aquatic plant transport (Whalen and Reeburgh 1990, Kling *et al.* 1992, Rudd 1993, Roulet *et al.* 1994, Bastviken *et al.* 2004). Studies that aimed to assess ebullition with greater accuracy have shown that ebullition, particularly from lakes, is a dominant, yet inadequately quantified mode of CH_4 emission, leading to a systematic underestimation of aquatic CH_4 sources globally (Casper *et al.*, 2000, Bastviken 2004).

The majority of this research was conducted on North Siberian thaw lakes, where degradation of permafrost in Pleistocene-aged, organic-rich loess, termed 'yedoma', leads to thaw lake expansion and CH_4 emissions over a 10^6 km^2 territory of North Siberia (Zimov *et al.* 1997). Earlier work identified North Siberian yedoma lakes as a source of atmospheric CH_4 with $^{14}C_{CH4}$ age up to 27,000 years. Zimov *et al.* (1997) used a method common among lake methane studies whereby annual ebullition estimates were derived from measurements using a few (1-4) randomly placed bubble traps periodically deployed. In this study of the same lakes, I couple continuous year-round monitoring of randomly-placed bubble traps that measure 'background' ebullition, with mapping of new types of bubbling, which have particularly high flux rates that have never before been quantified: 'point-source' and 'hotspot' ebullition. The aim is to determine how much of total lake CH_4 emissions 'background' bubbling accounts for when point- source and hotspot bubbling are also included. My hypothesis is that documentation of ebullition patchiness improves accuracy of lake emission estimates for the same lakes previously studied, and has important implications for improving and increasing estimates of global methane emissions from lakes, which have been largely derived with inadequate sampling of ebullition.

Specifically, the objectives of this work were to: (1) develop a new method for accurate quantification of ebullition from lakes based on year-round, continuous flux measurements coupled with mapping of bubbling point sources and hotspots in lake ice (Chapters 1 and 2); (2) demonstrate that northern lake emissions are important at the global scale (Chapters 1 and 2), not only in current budgets of atmospheric CH_4, but also during times of deglaciation when thaw lakes appeared on unglaciated northern landscapes in response to rapid climate warming and wetting (Chapter 3); (3) assess thermokarst erosion as a major landscape-scale process that enhances CH_4 emissions from expanding thaw lakes and serves as an important positive feedback to climate warming (Chapters 1-4); (4) investigate uncertainties associated with scaling emissions from lake-level to regional estimates (Chapter 1); and (5) link maps of bubble-source distributions in lakes with long-term, continuous flux measurements and isotope compositions of bubbles to provide annual whole-lake and regional CH_4 isofluxes (flux-weighted averages of isotope signatures) from Siberian thaw lakes for use in inverse models to help quantify lake ebullition as a newly recognized source of atmospheric CH_4 (Chapter 4).

CHAPTER 1

Methane bubbling from Siberian thaw lakes: A positive feedback to climate warming†

Abstract

Large uncertainties in the budget of atmospheric methane (CH_4), which has half the radiative forcing of carbon dioxide, limit the accuracy of climate-change projections[1,2]. We introduce a new method to accurately measure ebullition (bubbling), which accounted for 95% of CH_4 emissions from North Siberian thaw lakes. By documenting the patchiness of CH_4 emissions, accurate ebullition measurements increased previous estimates of CH_4 flux from the same lakes 5-fold[3]. Extrapolating our measured fluxes, we show that North Siberian thaw lakes emit 3.8 Tg CH_4 yr^{-1}. An independent mass-balance approach based on the loss of organic carbon from thawed permafrost beneath lakes produced a similar estimate (4-5 Tg CH_4 yr^{-1}). This significantly increases present estimates of northern wetland contributions (<6-40 Tg yr^{-1}) (ref. 1,2,4-6) to the atmospheric CH_4 budget. Thermokarst (thaw) erosion accounted for 79-90% of total CH_4 emissions. A 14.7% expansion of thaw lake area from 1974 to 2000 increased lake CH_4 emissions by 58%. The Pleistocene age (35-43 kyBP) of CH_4 emitted from hotspots along active thermokarst margins of lakes demonstrates that recruitment of a previously sequestered carbon source is a large cause of this positive feedback to climate warming.

†*This manuscript is in review at Nature.*

Understanding the role of North Siberian thaw lakes in the global atmospheric methane (CH_4) budget is important because the concentration of atmospheric CH_4, a potent greenhouse gas, is highest at 65 to 70°N (ref. 7,8), has risen during recent decades[9], and exhibits an unexplainably large seasonal amplitude at high northern latitudes with bimodal maxima in winter and spring[7,8], times when wetlands are frozen, but unfrozen lake sediments actively produce and emit CH_4. This study shows that ebullition from Siberian thaw lakes is a large and increasing source of atmospheric CH_4 as Siberian thaw lakes continue to expand.

Thaw lakes comprise 90% of the lakes in the Russian permafrost zone[10]. Many North Siberian lakes differ from lakes in America and Europe because they are underlain by *yedoma*, an organic-rich (~2% carbon (C) by mass) Pleistocene-age loess permafrost whose ice content is 50-90% by volume[3,11-13]. Thermokarst erosion occurs along lake margins when massive, subsurface ground ice wedges melt, causing the ground surface to subside. Labile organic matter from permafrost erodes into anaerobic lake bottoms upon thaw of yedoma, enhancing methane production and emission[3]. In this study we used remote sensing, aerial surveys and year-round, continuous measurements of CH_4 flux to (a) quantify CH_4 emissions from North Siberian lakes, paying particular attention to the role of ebullition, and (b) document the role of thermokarst erosion as a landscape process that fuels CH_4 production and feeds back to climate warming.

Ebullition is often the dominant pathway of CH_4 release from aquatic ecosystems[14,15], yet it is seldom measured due to its extreme temporal and spatial patchiness. Siberian lakes provide a unique opportunity to assess ebullition flux more accurately. As ice forms in autumn, bubbles released from lake sediments are frozen in place, allowing accurate mapping of ebullition 'point sources' across lake surfaces. We used random and selective placement of underwater/ under-ice bubble traps to make daily measurements of 'background', 'point-source' (moderately high bubble flux from discrete points in lake sediments) and 'hotspot' (open holes in ice due to extremely high bubble flux from discrete points in lake sediments) fluxes from April 2003 through May

2004 on two intensively studied lakes in North Siberia (Supplementary Information). We extrapolated fluxes regionally using the distribution of hotspots in aerial photographs.

Ebullition comprised 95 ± 1% of the CH_4 flux from the intensively studied lakes, with molecular diffusion contributing the remainder (Table 1-1). Emergent plants were absent as a conduit in our lakes. Point sources other than hotspots of bubbling comprised the largest proportion (59 ± 12%) of total CH_4 emissions (Table 1-1). Ebullition rates were highest in traps selectively placed over hotspots along thermokarst margins of lakes (Fig. 1-2)(hotspots <1% of lake area), contributing 11 ± 7% of the total CH_4 flux (Table 1-1) with a maximum rate of 18,835 mg CH_4 d^{-1} (>30 L d^{-1}) in March. This exceeds most published CH_4 flux rates for lakes and wetlands by several orders of magnitude[4,5,14-19]. Hotspot bubbling represents point sources of CH_4 produced from a large volume of unfrozen lake sediments that is vented through small (<2 cm) holes in the sediment surface.

Hotspots were visible as "black holes" in lake ice along thermokarst margins in ground and aerial surveys of lakes (Supplementary Information). Half of 60 lakes surveyed in our study region (including our two intensively studied lakes) had modest thermokarst erosion, marked by banks with gentle slopes and stable vegetation and hotspots distributed primarily in a 15-m wide belt along thaw margins. The remaining lakes had more intense thermokarst erosion, with steep muddy banks, occasional exposed ice wedges, and a >30 m wide belt of hotspot emissions at the lake margins. The two lake types were interspersed across our 300-km aerial transect.

Forty-four percent of annual CH_4 emissions from Siberian lakes occurs in winter and spring when CH_4 trapped as bubble clusters in lake ice is released to the atmosphere during (a) high temperature anomalies[20], (b) overflow events when lake water is forced through lenses of ice clusters and open holes after heavy snowfall[20], and (c) springtime thaw of lake ice[19,20] (Table 1-1).

When background, point-source, and hotspot ebullition fluxes were aggregated to a whole-lake basis, the annual flux was 24.9 ± 2.3 g m^{-2} yr^{-1} from the intensive study lakes. Our estimate is conservative because it neglects other extreme expulsions of CH_4

from lakes, which were not measured because of their rarity (Supplementary Information). Fluxes from the 15-m band of active thermokarst on the eroding edge of lakes (15.8% of lake area, 128 ± 24 g m^{-2} yr^{-1}) accounted for 79% of total lake emissions (Table 1-1). In the other 50% of the region's lakes, we extrapolated the thermokarst margin flux to the >30-m band where hotspots were observed (31.6% of lake area). In these lakes we estimate that thermokarst margins accounted for 90% of the lake-averaged annual flux of 43.7 ± 3.2 g CH$_4$ m^{-2} yr^{-1}.

These emission rates exceed those reported in previous work on the same lakes (6.8 g m^{-2} yr^{-1})(ref. 3), other high-latitude lakes and ponds (0.5 to 9.2 g CH$_4$ m^{-2} yr^{-1}) (ref. 21,22) and 11.3 g CH$_4$ m^{-2} d^{-1} for the 120 day ice free season in beaver ponds[23], and North Siberian wetlands (0.9-14.3 g CH$_4$ m^{-2} yr^{-1} (ref. 24), 11.7 g CH$_4$ m^{-2} yr^{-1} (ref. 25) and 6.4 ± 3.4 g CH$_4$ m^{-2} yr^{-1}, [n = 8 chambers measured biweekly from June-October in 2003, this study]).

Our lake estimate likely exceeds others not only because of the prevalence of thermokarst activity in North Siberia, but also because our stratified sampling design with continuous measurements and mapping point sources and hotspots accounted for the patchiness of bubbling. The few studies that previously measured ebullition estimated fluxes from a few randomly placed bubble traps that were periodically deployed[3,14,15,26]. In our study random placement of up to 14 traps per lake with continuous year-round monitoring revealed that this 'background' bubbling accounted for only $24 \pm 6\%$ of the total emissions. To our knowledge, this is the first study to quantify the spatial and temporal patchiness of ebullition in any lake, thereby reducing uncertainty in a highly sporadic mode of methane emission.

We extrapolated our lake estimate to the yedoma region of North Siberia using 11% lake area measured in our GIS study, which is conservative given the range of lake area estimates for this region (8.5 to >30%) (ref. 3,10,27), yielding a regional flux of 3.8 Tg CH$_4$ yr^{-1}. Adding our results of ebullition from North Siberian lakes (3.8 Tg yr^{-1}), which have not yet been included in global estimates of CH$_4$ emissions from wetlands[2,17,18,28], to a range of estimates for northern wetland flux (<6-40 Tg CH$_4$ yr^{-1})

(ref. 1,2,4-6) increases current estimates of northern wetland CH_4 emissions by 10-63%. The uncertainty analysis is provided as Supplementary Information. Since yedoma lakes are only a fraction of northern lakes, ebullition measurements in other lake regions would likely further increase CH_4 emission estimates.

To assess the plausibility of our CH_4 flux estimate of 3.8 Tg CH_4 yr^{-1} we used an independent mass-balance approach based on Holocene C loss associated with thermokarst lake development. The C content beneath former thermokarst lakes (30 Kg C m^{-3}) is 30% less than in undisturbed yedoma (42 Kg C m^{-3}) (detailed data not presented), and we assumed half of this C was converted to CH_4 based on the stoichiometry of methane production from cellulose degradation[29]. Applying this 15% C loss due to methanogenesis beneath lakes to yedoma territory of North Siberia (1×10^6 km^2, 25-m average thickness, 50% ice content)[3,12,27], which has been degraded by migratory lakes whose scars cover 50% of the region[11,27], yields a release of 53 Gt CH_4 during the Holocene (10,000-13,000 years) or on average, ~4-5 Tg CH_4 yr^{-1}. This estimate is conservative because it does not include CH_4 derived from Holocene-age lake deposits. Given the uncertainties associated with both flux estimates, their rough correspondence lends support to our conclusion that North Siberian lakes are a globally significant source of atmospheric CH_4.

In areas of discontinuous permafrost, recent permafrost degradation associated with warming has led to lake area loss[30]. However, in the zone of continuous permafrost, which presently comprises about half of arctic permafrost[31], warming[32] has caused thaw lakes to grow in number and size[30]. Using Geographical Information Systems (GIS) analysis of 1974 MSS and 2000 ETM Landsat imagery we measured a 14.7% increase in lake area (from 9.6% to 11% lakes) for a 12,000 km^2 territory including our study region along the Kolyma River near Cherskii, Russia (Fig. 1-3). This is similar to the 12% increase in lake area observed in continuous permafrost zones of West Siberia during recent decades[30]. The years of the images analyzed had temperature and precipitation values typical of the 20th century for our study region[33]. We assumed flux rates for lakes in 1974 were the same as current rates of our two intensive study lakes (24.9 g CH_4 m^{-2}

yr^{-1}). Applying this modest rate to 50% of the region's lakes in 2000 and higher rates (43.7 g CH$_4$ m^{-2} yr^{-1}) to the other half of the region's lakes, where intense erosion has led to the observed 14.7% increase in lake area, resulted in an estimated 58% increase in lake CH$_4$ emissions, or 1.4 Tg CH$_4$ yr^{-1} between 1974 (2.4 Tg yr^{-1}) and 2000 (3.8 Tg yr^{-1}) if extrapolated regionally.

Isotopic analyses reveal that methane collected from ebullition in Siberian thaw lakes during 2001-2004 is of biogenic origin (δ^{13}CH$_4$ = –61‰ to –82‰, δD-CH$_4$ = -466‰ to -425‰). The wide range indicates that methanogenesis substrates or pathways differed among zones of ebullition (Table 1-1; Chapter 4). Ebullition hotspots had ^{14}C-ages ranging from 35-42.8 kyBP (0.49-0.81 % modern carbon- pMC), reflecting the importance of recently thawed Pleistocene-age permafrost soils as a source of labile organic matter for methanogenesis deep within the thaw bulb of lakes[3,34] (Fig. 1-2). Non-hotspot sources of bubbling had younger radiocarbon ages, 1,385 to 22,050 years. (6.4-85 pMC), indicating greater influence of Holocene organic sources for methane production. Weighting the radiocarbon signature of point-source types by their abundance in lakes yielded an average annual ^{14}CH$_4$ age of 16,520 years, signifying that Pleistocene sediments deposited 20,000 to 40,000 years ago constitute 41-83% of the CH$_4$ emitted from Siberian lakes. The δD-CH$_4$ and radiocarbon age of CH$_4$ sampled from our North Siberian thaw lakes are distinct from other arctic lakes and wetlands, including the East Siberian alasses situated on sandy soils, whose δD-CH$_4$ and ^{14}C-CH$_4$ are -363 ± 20‰ and 95-123 pMC respectively[35]. Therefore the unique ^{14}C-depleted CH$_4$ signature of ebullition from yedoma lakes should be considered in future studies that estimate the fraction of total atmospheric CH$_4$ emissions derived from fossil fuels.

In conclusion, we have shown that North Siberian lakes are a significantly larger source of atmospheric CH$_4$ than previously recognized. Emissions are dominated by ebullition, a mode of emission that we have quantified using the new technique of mapping bubbling point sources. This CH$_4$ source is largely fueled by thermokarst, and we have linked the expansion of thermokarst lakes during recent decades with a 58% increase in lake CH$_4$ emissions, demonstrating a new feedback to climate warming.

Though the recent increase in flux due to lake expansion is modest relative to anthropogenic emissions[1,2,7,8], the ~500 Gt of labile Pleistocene-aged C in ice-rich yedoma permafrost[13] could fuel a powerful positive feedback to high-latitude warming through CH_4 ebullition from thermokarst lakes if northeast Siberia continues to warm in the future, as projected[32].

Methods

All numbers following a ± sign are standard deviations unless otherwise noted.

Ebullition measured by bubble traps

We measured ebullition using umbrella-shaped floating bubble traps (~1-m diameter, 25 traps randomly placed, 16 traps fixed over point sources and hotspots of bubbling) from April 26, 2003 through June 1, 2004 at two lakes (max depth 16.5-m and 11-m, area 0.11 km^2 and 0.06 km^2) near the Northeast Science Station in Cherskii (68°45'36" N, 161°,20'34" E). During winter, we measured every 3-4 days the volume of gas collected continuously in bubble traps suspended beneath the ice. We made 2,981 individual measurements of bubble volumes collected in bubble traps. Methane concentration of bubbles was 79.6 ± 1.1% CH_4 (n=36), as measured by gas chromatography using a thermal conductivity detector (TCD Shimadzu 8A) and a flame ionization detector (FID Shimadzu 6A). To verify that our intensively studied lakes were regionally representative of thermokarst lakes on yedoma territory, we made ground surveys of 35 other lakes and took aerial photographs of 60 lakes in Northern Siberia.

Mapping bubble clusters in lake ice as 'point sources' of ebullition.

We removed snow from lake surfaces along six 50-m x 1-m transects per lake (Fig. 1-1) in early winter to count the number and type of bubble clusters in lake ice that represent 'point sources' of ebullition. We categorized four types of bubble patterns in lake ice and measured winter methane flux rates (mg CH_4 d^{-1} per point) associated with each 'point-source' category using under-ice floating traps from 10/9-10/29/2003 (n=6-8 traps per category): *kotenok* (stacks of small individual, unmerged bubbles, 25 ± 12), *koshka* (merged bubbles clustered in multiple layers of ice, 190 ± 172), *kotara* (single large pockets of merged bubbles in ice, 825 ± 348) and open-hole *hotspots* (2175 ± 1195) (ANOVA, F=16.23$_{3,27}$ p<.0001). Average emissions from point sources were extrapolated to entire lakes based on transects of bubble cluster and hotspot densities in ice over shallow, medium, and deep water depths in thermokarst and non-thermokarst areas of lakes. Unlike other point sources, seasonal averages for hotspots were derived from year-round measurements using bubble traps (1754 ± 690 mg CH_4 d^{-1}, n=4 traps summer; 2125 ± 1222 mg CH_4 d^{-1}, n=10 traps winter). In contrast, average flux by molecular diffusion was 10 ± 1.8 mg CH_4 m^{-2} d^{-1} during the summer.

The CH_4 concentration in point-source bubbles trapped in lake ice (53.6 ± 1.6 % CH_4; n=3) in spring before any thawing occurred was similar to earlier observations (50% CH_4, n=8 koshkas) (ref. 3) and 33% less than in fresh lake bubbles (80%). When applying CH_4 concentrations to the bubble volume measurements, we used 54% CH_4 in our calculation of wintertime 'point-source' and 'background' ebullition, and 80% for all other ebullition.

We include the estimated flux from point sources in addition to the randomly placed bubble trap flux (background ebullition) because traps covered less than 0.03% of the lake area and there was no overlap between values of point source fluxes and values of background ebullition.

Equations

We estimate whole-lake CH_4 emissions M_{ltot} as the average of two intensively studied lakes, $(24.9 \pm 2.3 \text{ mg } CH_4 \text{ m}^{-2} \text{ yr}^{-1})$: where

$$M_{ltot} = \sum_{z=1}^{3} A_z \left(M_{dz} + M_{hz} + M_{pz} + M_{bz} \right) \tag{1}$$

z = The 3 major lake zones: shallow thermokarst margins, non-thermokarst margins, and the deeper center of lakes.

A_z = area of each zone (fraction of lake area).

M_d = Diffusive flux estimated from biweekly surface water concentrations of CH_4 measured during the ice-free summer period in the lake center[16] (mg CH_4 m^{-2} yr^{-1}).

M_h = Density of hotspots (No. points m^{-2}) * mean flux per hotspot (mg CH_4 season^{-1}) for summer (n=4 hotspots) and winter (n=10 hotspots).

$$M_p = t \sum_{s=1}^{3} \rho_s M_s \tag{2}$$

where ρ_s is the density of each point source (No. points m^{-2}, s = point source type: kotenok (1), koshka (2), or kotara (3); M_s is the mean flux per point source (mg CH_4 day^{-1} in October; n = 6-8 traps per point source type); and t is 365 days per year. This extrapolation is conservative because October point source ebullition appeared to be lower than at other times of year (data not shown).

M_b = Average seasonal bubble fluxes determined for randomly situated traps (background ebullition) as a summation of interpolation of daily fluxes during winter and summer. Background traps were monitored year round with 2-10 traps per lake zone.

The complete table of North Siberian methane emission sources detailed for each lake is provided in Supplementary Information.

Regional extrapolation

Regional estimates M_{yedoma} (3.8 Tg CH_4 yr^{-1}) were extrapolated from whole lake fluxes as follows:

$$M_{yedoma} = A_{yedoma} * P_{lakes} * 0.5(M_{1tot} + M_{2tot}) \tag{3}$$

Where A_{yedoma} is 1×10^6 km^2; P_{lakes} is 0.11 fractional lake cover; M_{1tot} is 24.9 g CH_4 m^{-2} yr^{-1}, representing half of the region's lakes with modest erosion; and M_{2tot} is 43.7 CH_4 m^{-2} yr^{-1}, the flux from the other half of the region's lakes with intense thermokarst erosion and extensive hotspots.

This 11% lake cover estimate, based on our GIS analysis, is conservative relative to the range reported in the literature (8.5 to >30%) (ref. 3,10,27). To lend support to the assumption that our estimates of CH_4 flux are representative, we verified that 2003-2004 had temperature and precipitation inputs typical of the period 1980-2004 based on observations made at the Cherskii Meteorological Station (data not shown).

Methane isotopes procedures.

Gas samples were collected directly into glass serum vials from ebullition flux, sealed with Butyl rubber stoppers, and stored at 4° C until isotopic analyses. We measured $^{13}C/^{12}C$ of CH_4 by direct injection with a syringe using gas chromatography/mass spectrometry (Hewlet-Packard 5890 Series II GC coupled to a Finnigan MAT Delta S). A subsample of gas was combusted to CO_2 and catalytically reduced to graphite[34], and its $^{14}C/^{12}C$ values measured by atomic mass spectrometry at the Keck Carbon Cycle AMS Facility at the University of California, Irvine. We determined D/H of CH_4 on a Finnigan MT delta +XP using a Trace GC with a poroplot column and the reduction column set at 1450°C.

References

1. Intergovernmental Panel on Climate Change (IPCC). *The Scientific Basis.* Cambridge Univ. Press, New York (2001).

2. Mikaloff Fletcher, S. E., Tans, P. P., Bruhwiler, L. M., Miller, J. B., & Heimann, M. CH_4 source estimated from atmospheric observations of CH_4 and its $^{13}C/^{12}C$ isotopic ratios: 1. Inverse modelling of source processes. *Global Biogeochem. Cycles* **18**, GB4004, doi:10.1029/2004GB002223 (2004).

3. Zimov, S. A. *et al.*, North Siberian lakes: A methane source- fuelled by Pleistocene Carbon. *Science* **277**, 800-802 (1997).

4. Roulet, N. T. *et al.* Role of Hudson Bay lowland as a source of atmospheric methane. *J. Geophys. Res.* **99**, 1439-1454 (1994).

5. Reeburgh, W. S. *et al.* A CH_4 emission estimate for the Kuparuk River basin, Alaska. *J. Geophys. Res.* **103**, 29,005- 29,013 (1998).

6. Worthy, D. E., Levin, J., I., Hopper, F., Ernst, M. K., & Trivett, N. B. A. Evidence for a link between climate and northern wetland methane emissions. *J. Geophys. Res.* **105**, 4031-4038 (2000).

7. Fung, I. *et al.*, Three-dimensional model synthesis of the global methane cycle. *J. of Geophys. Res.* **96**, 13,033- 13,065 (1991).

8. Dlugokencky, E. J., Steele , L. P., Lang, P. M., & Masarie , K. A. The growth rate and distribution of atmospheric methane. *J. of Geophys. Res.* **99**, 17,021- 17,043 (1994).

9. Dlugokencky, E. J., Masarie, K.A., Lang, P.M., & Tans, P.P. Continuing decline in the growth rate of the atmospheric methane burden. *Nature* **393**, 447-450 (1998).

10. Mostakhov, S. E. in *Mezhdunarodnaia conferentsiia po merzlotovedeniiu, Podzemnye vody kriolitosfery* (ed. Tolstikhin, N. I.) (Iakustkoe Knizhnoe Izdeatel'stvo, Iakutsk, Russia, 1973).

11. Tomirdiaro, S.V., in *Paleoecology of Beringia* (eds. Hopkins, D. M. , Matthews J. V. Jr., Schweger, C. E., Young , S. B.) (Academic Press, New York, 1982).

12. Romanovskii, N. N. *et al.* Thermokarst and Land-Ocean Interactions, Laptev Sea Region, Russia. *Perm. & Periglac. Process.* **11**: 137-152 (2002).

13. Zimov, S. A. Pleistocene Park: Return of the Mammoth's Ecosystem. *Science* **308**, 796-798 (2005).

14. Keller, M. & Stallard. R. F. Methane emission by bubbling from Gatun Lake, Panama *J. Geophys. Res.* **99**, 8307- 8319 (1994).

15. Casper, P., Maberly, S. C., Hall, G. H., & Finlay, B. J. Fluxes of methane and carbon dioxide from a small productive lake to the atmosphere. *Biogeochemistry* **49**, 1-19 (2000).

16. Kling, G., Kipphut, G. W., & Miller, M. C. The flux of CO_2 and CH_4 from lakes and rivers in arctic Alaska. *Hydrobiologia* **240**, 23-36 (1992).

17. Mathews, E. & Fung, I. Methane emission from natural wetlands: Global distribution, area, and environmental characteristics of sources. *Global Biogeochem. Cycles* **1**, 61-86 (1987).

18. Aselmann, I. & Crutzen, P. J. Global distribution of natural freshwater wetlands, rice paddies, their net primary productivity, seasonality, and possible methane emissions. *J. of Atm. Chem.* **8**, 307-358 (1989).

19. Phelps, A. R. Peterson , K. M., & Jeffries, M.O. Methane efflux from high-latitude lakes during spring ice melt. *J. Geophys. Res.* **103**, 29,029-29,036 (1998).

20. Zimov, S. A. *et al.*, in *Permafrost Response on Economic Development, Environmental Security and Natural Resources* (Eds. Paepe, R. & Melnikov, V.) (Kluwer Academic Publishers, the Netherlands, 2001).

21. Whalen, S. C. & Reeburgh, W. S. A methane flux transect along the trans-Alaska pipeline haul road. *Tellus* **42**, 237-249 (1990).

22. Bartlett, K. B., Crill, P. M., Sass, R. L., Harriss, R. C., & Dise , N. B. Methane emissions from tundra environments in the Yukon-Kuskokwim Delta, Alaska. *J. Geophys. Res.* **97**, 16,645-16,660 (1992).

23. Roulet, N. T., Crill, P. M., Comer, N.T., Dove, A. & Boubonniere, R. A. CO_2 and CH_4 flux between a boreal beaver pond and the atmosphere. *J. Geophys. Res.* **102**, 29,313-29,3193 (1997).

24. Nakayama, T. Estimation of methane emission from natural wetlands in Siberian Permafrost Area, Doctoral Dissertation, Division of Geophysics, Graduate School of Science, Hokkaido University, 100 pp. (1995).

25. Corradi, C., Kolle, O., Walter, K., Zimov, S. A., Schulze, E.-D. Carbon dioxide and methane exchange of a north-east Siberian tussock tundra. Global Change Biology **11**, 1910-1925 (2005).

26. Bastviken, D., Cole, J., Pace, M., & Tranvik, L. Methane emissions from lakes: Dependence of lake characteristics, two regional assessments, and a global estimate. *Global Biogeochem. Cycles* **18**, GB3010, doi:10.1029/2004GB002238 (2004).

27. Czudek, T. & Demek, J. Thermokarst in Siberia and its influence on the development of lowland relief. *Quat. Res.* **1**, 103-120 (1970).

28. Zhuang, Q. *et al.* Methane fluxes between terrestrial ecosystems and the atmosphere at northern high latitudes during the past century: A retrospective analysis with a process-based biogeochemistry model. *Global Biogeochem. Cycles* **18**, GB3010, doi:10.1029/2004GB002239 (2004).

29. Conrad, R., Klose, M., and Clause, P. Pathway of CH_4 formation in anoxic rice field soil and rice roots determined by 13C-stable isotope fractionation. *Chemosphere* **47**, 797 (2002).

30. Smith, L. C., Y. Sheng, G. M. MacDonald, & L. D. Hinzman. Disappearing arctic lakes. *Science* **308**: 1429 (2005).

31. Brown, J., Ferrians Jr., O. J., Heginbottom, J. A. & Melnikov, E. S. Circum-Arctic map of permafrost and ground-ice conditions, U.S. Geological Survey Circum-Pacific Map CP- 45, 1:10,000,000, Reston, Virginia. (1997).

32. Sazonova, T. S., Romanovsky, V. E., Walsh, J. E. & Sergueev, D. O. Permafrost dynamics in the 20th and 21st centuries along the East Siberian transect. *J. Geophys. Res.* **109**, doi:10.1029/2003JD003680 (2004).

33. New, M., Lister, D., Hulme, M., & Makin, I. A high-resolution data set of surface climate over global land areas. *Climate Research* **21,** 1-25 (2002).

34. M. Stuiver, M. and H. Polach. Reporting of ^{14}C data. *Radiocarbon.* **19**, 355-363 (1977).

35. Nakagawa, F., Yoshida, N., Nojiri, Y., & Makarov, V.N. Production of methane from alases in eastern Siberia: Implications from its ^{14}C and stable isotope compositions. *Global Biogeochem. Cycles* **16**(3), doi.10.1029/2000GB001384 (2002).

Figure 1-1. Photographs of CH₄ bubbles trapped in lake ice. The distribution of ebullition point sources was measured along transects on lake ice (a), recognizing four distinct categories of bubble clusters [b. kotenok, c. koshka, d. kotara, e. hotspot) with associated CH₄ emission rates (*Methods*)].
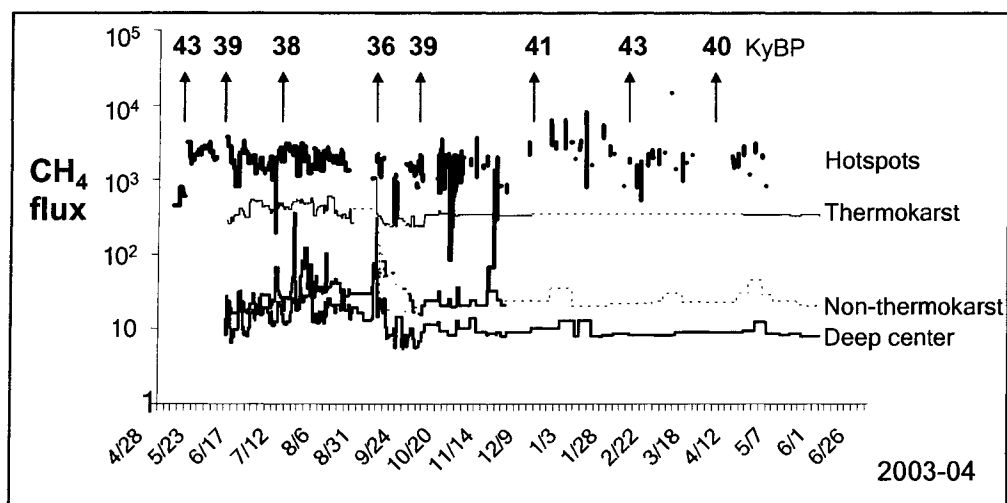
Figure 1-2. Average ebullition rates for representative areas of lakes. Ebullition rates along thermokarst margins (15.8 ± 2.2% of lake area) were an order of magnitude greater than ebullition rates along non-thermokarst margins (4.4 ± 1.4% of lake area) and at various depths throughout the lake center (79.8 ± 0.8% of lake area). Hotspots (<1% of lake area) are presented here separately. Breaks in the hotspot line are periods of no data (Supplementary Information). Numbers above hotspot data indicate the radiocarbon ^{14}C age (KaBP) of CH_4 bubbles collected from a particular hotspot repeatedly throughout the study period. We interpolated fluxes (dashed lines) if less than 25% of the total traps were operating due to temporary mechanical failures.

* Units of hotspot emission are mg CH_4 d^{-1} per tiny (<2 cm diameter) emission vent because they represent CH_4 emitted from a larger volume of lake sediments.
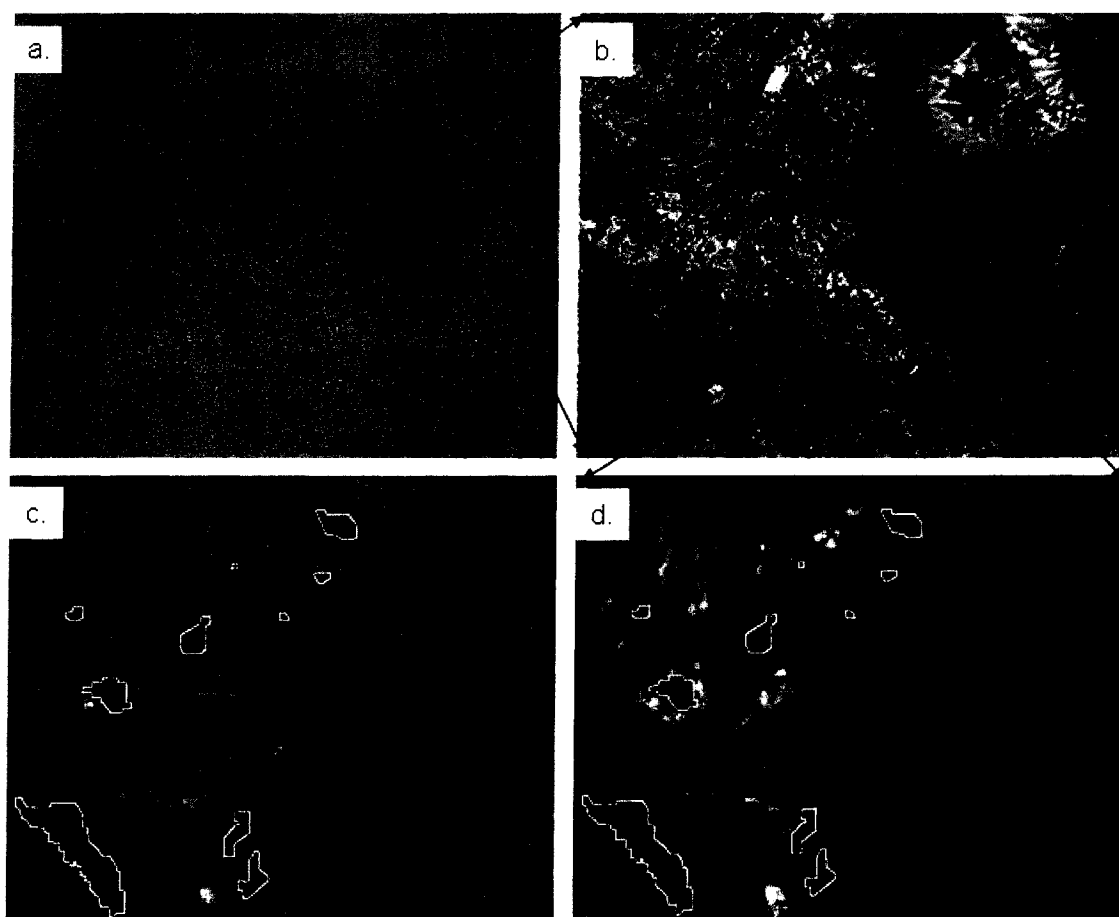
Figure 1-3. Thermokarst lake expansion. The schematic a shows yedoma distribution (blue shading - continuous distribution, blue triangles - sporadic distribution) in North Siberia (courtesy of N. N. Romanovskii). The Landsat image b (~120 km^2) represents the region of our GIS lake change analysis from 1974 (image c) to 2000 (image d). The shorelines from 1974 are delineated as white polygons, while some areas of expansion of thaw lakes are indicated by arrows and formation of new lakes by circles on the 2000 image d.

Table 1-1. Summary of CH_4 flux and isotopes in bubbles from North Siberian thermokarst lakes. Error estimates are half of the absolute difference between measurements for two intensive study lakes. Sources of variability are shown in Supplementary Table 1.

Season 2003-04	Flux Component	Whole-lake $(g\,CH_4\,m^{-2}\,yr^{-1})$	% of annual flux	Thermokarst Margins $(g\,CH_4\,m^{-2}\,yr^{-1})$	$^{14}CH_4$ age years	$^{14}CH_4$ % modern carbon	$\delta^{13}C\text{-}CH_4$	$\delta D\text{-}CH_4$
Summer (open water June-Sept.)	Background ebullition	5.7 ± 2.0	22 ± 6%	27.7 ± 14	1,345 to 5,350	51 to 85%	-61.2‰ to 63.2‰	
	Point source	6.2 ± 0.7	25 ± 5%	34.7 ± 0.7	5,590 to 12,285	22 to 50%	-62.8‰ to 76.7‰	-466‰ to -425‰
	Hotspots	1.0 ± 0.7	4 ± 2%	5.4 ± 3.9	37,920 to 38,670	0.81 to 0.89%	-79.6‰	-443‰ to -436‰
	Molecular Diffusion	1.3 ± 0.1	5 ± 1%	1.3 ± 0.1				
Winter (ice cover Oct.-May)	Background ebullition	0.5 ± 0	2 ± 0%	0.7 ± 0				
	Point source	8.3 ± 0.9	34 ± 7%	46.9 ± 0.9	22,050	6.40%		
	Hotspots	2.0 ± 1.3	8 ± 5%	11.1 ± 7.7	39,120 to 42,900	0.49 to 0.77%	-80.4‰	-459‰ to -450‰
Total		24.9 ± 2.3	100%	127.8 ± 24.0	16,520†			

‰, parts per mil

† Sum of the mean radiocarbon age of each flux component weighted by each component's proportion of total annual emissions.
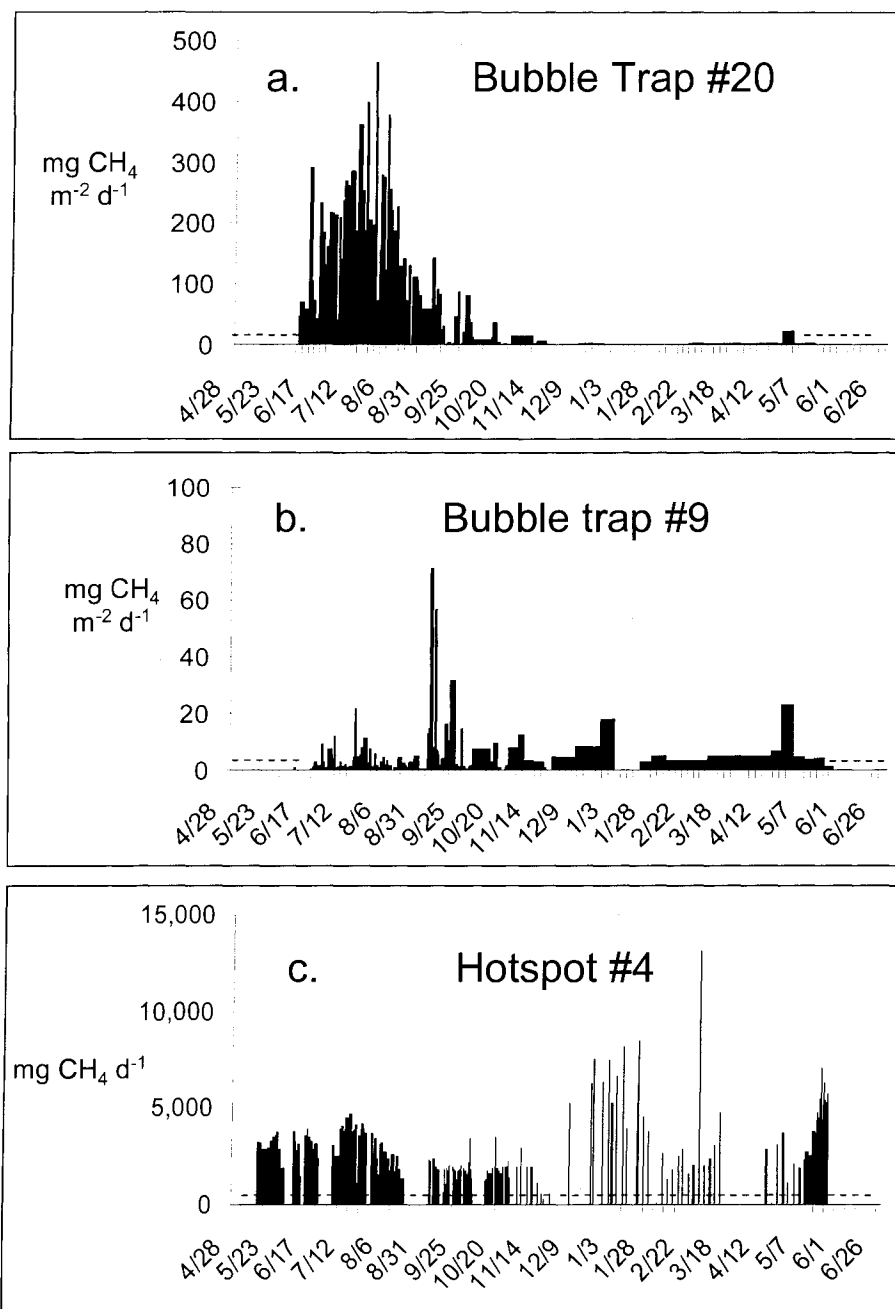
Supplementary Figure 1-1. Ebullition dynamics captured by daily measurements during 2003-04 in single bubble traps floating at randomly located points where water was 2-m deep (a) and 10-m deep (b). We secured traps over individual hotspots (c). In summer, hotspot traps were sampled daily as they filled often with >15L of gas each day; but in winter when logistics necessitated less frequent sampling, we measured hotspot fluxes over the course of several hours to prevent umbrellas from overflowing and freezing into the ice. We verified that hourly flux rates were not different from daily flux rates. Dashed lines represent periods of 'no-data'.

Supplementary Figure 1-2. Photograph of hotspots along thermokarst lake margin. Methane emissions along thermokarst margins (128 g CH_4 m^{-2} yr^{-1}) exceeded whole lake average emissions (24.9 g CH_4 m^{-2} yr^{-1}) in the intensive study lakes because of a higher abundance of hotspots and point sources of ebullition in the thermokarst zone. Hotspots in the photograph, which was taken in October 2003 at Shuchi Lake, are open holes in ice inside the dark rings of wet snow.
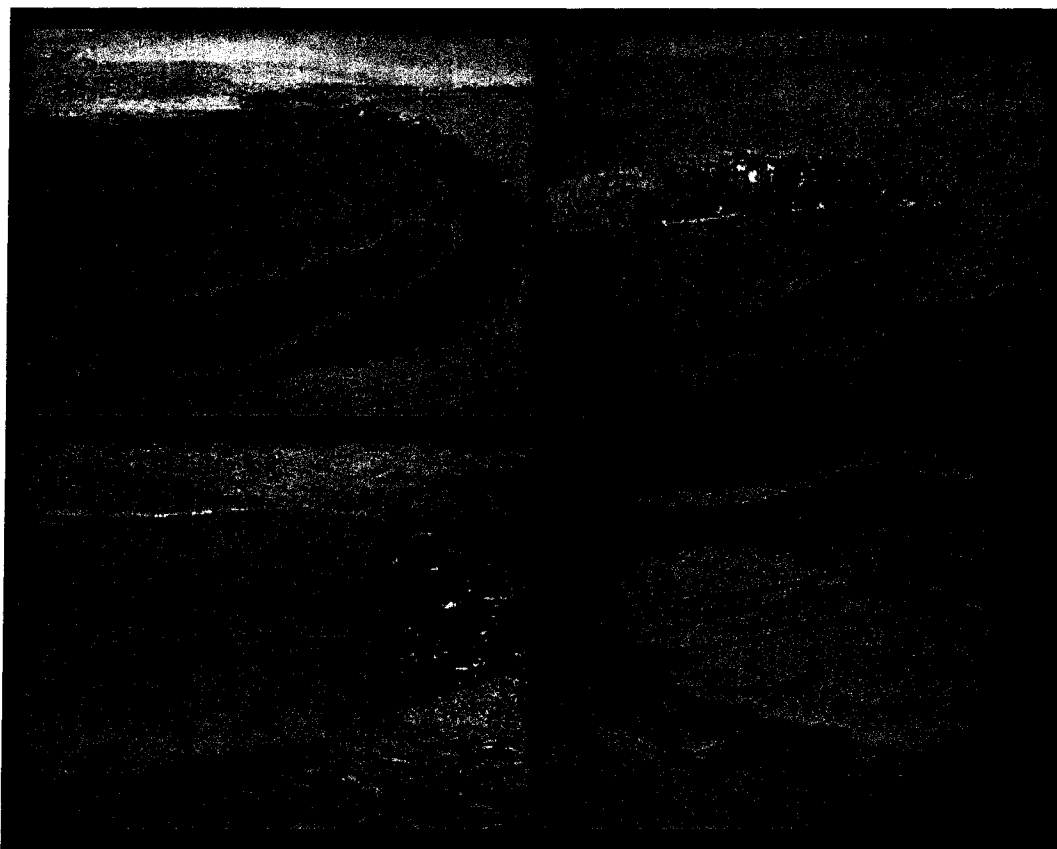
Supplementary Figure 1-3. Black-hole hotspots (dark round spots) mark the zone of enhanced methane emissions due to thermokarst erosion. We sorted aerial photographs of 60 lakes into two categories reflecting lakes with moderate and intense thermokarst erosion. Half of the lakes exhibited moderate erosion, with black-hole hotspots occurring primarily in a narrow zone 15-m from the thermokarst margin (panels a and b, as well as our two intensive study lakes). This zone was $15.8 \pm 2.2\%$ of lake area in our intensive study lakes. Black-hole hotspots extended >30-m into the lake away from thaw margins in the other half of the photos (panels c and d), suggesting that these lakes have a recent history of more intense thermokarst erosion. Due to a lack of coordinates for lakes in aerial photographs we were unable to directly link the GIS lake change analysis to hotspot distributions in the photographs. To extrapolate CH_4 fluxes to these lakes, we applied flux rates measured along thermokarst margins of our intensive study lakes (128 g CH_4 m^{-2} yr^{-1}) to a doubly large zone of thermokarst influence (31.6% of lake area).

Supplementary Figure 1-4. Large, rare emission events. Some CH_4 emission events are unpredictable, but may be of large magnitude. Three times we observed geysers of lake gas released during a >30-second episode, which created an eruption cone that stood several centimeters above the lake water surface (not shown). In August of 2002 and 2003 we used video and photography to document large plumes of CH_4 that lifted thick peat mats (12 m^2) from the bottom of thermokarst lakes 4-8 m to the surface (below). These lake bottom islands floated at the lake surface for 3-6 days releasing CH_4, before sinking back to the lake bottom. Methane bubbled out from the mat when we disturbed it with a pole.
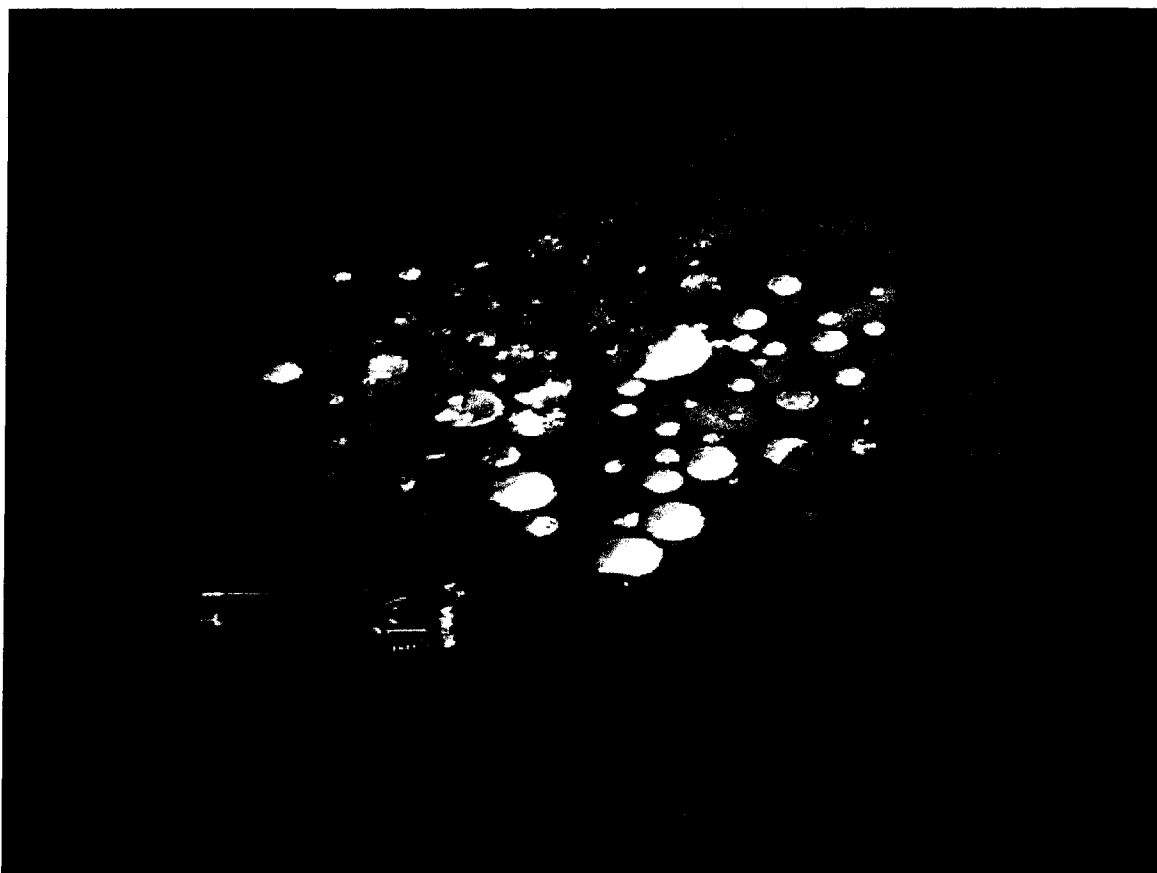
Supplementary Figure 1-5: Proposed cover illustration for Nature. Methane bubbles trapped in lake ice during the first few days of ice formation on a Siberian thermokarst lake in October 2003.

Supplementary Table 1-1. Sources of variability in our estimate of Siberian thaw lake CH_4 emissions for yedoma territory. By documenting ebullition patchiness, we were able to assess sources of uncertainty in our regional estimate of CH_4. Within-lake sources of variability, such as errors associated with point source fluxes, led to a smaller range of variability for regional estimates (2.4-5.1 Tg CH_4 yr^{-1}) than percentage of the region occupied by lakes (2.9-10.3 Tg CH_4 yr^{-1}). Since our extrapolation is based on the conservative estimate of lake area, actual regional emissions could be higher.

   Calculations are based on mean values of point source density per unit lake area and the mean flux per point source type in our intensive study lakes. Here we present the potential effect of the largest sources of variability around the whole-lake and regional means (34.3 g CH_4 m^{-2} yr^{-1}, 3.8 Tg CH_4 yr^{-1}) that are not accounted for in Equations 1-3, assuming that emissions from half of the region's lakes are the same as our study lakes (24.9 g CH_4 m^{-2} yr^{-1} with 15.8% thermokarst zone area), and emissions from the other half of the region's lakes reflect a 2-times larger thermokarst zone (43.7 g CH_4 m^{-2} yr^{-1} with 31.6% thermokarst zone area). Since lake area (as a percent of the yedoma region) is the largest source of variability influencing regional estimates of lake CH_4 emissions, we used a low-end estimate (11% lake area) in our calculations to be conservative. Other potential sources of variation that we have not estimated include the aerial extent of yedoma, CH_4 flux and thermokarst erosion variation among lakes in different yedoma sub-regions, intra-lake flux variation for lakes with intense erosion, and interannual variation.

Source of variability	Range of variability	Intensive study lakes g CH_4 m^{-2} yr^{-1}	Average regional lakes g CH_4 m^{-2} yr^{-1}	Regional flux Tg CH_4 yr^{-1}
Flux per point source[†]	36%	16.0 to 33.5	21.6 to 46.5	2.4 to 5.1
Density of point sources[α]	16%	22.9 to 31.4	30.4 to 42.2	3.3 to 4.6
Between zones within lakes[β]		*Accounted for in calculations*		
Between intensive study lakes	9%	22.7 to 27.2		
Between lakes with modest *vs.* intense thermokarst		*Accounted for in calculations*		
Lake area (percent of region)[γ]	46%			2.9 to 10.3

† The range shown in the table is the mean flux minus the standard deviation for each point source category in each lake zone and the mean flux plus the standard deviation for each point source category in each lake zone using the mean density of point source types—i.e., the variation in flux among replicate bubble traps for a given point source type in a given lake zone.

α The range shown in the table applies the mean flux for each point source category to the mean density minus the standard deviation of density for each point source type in each lake zone and the mean density plus the standard deviation of density for each point source type in each lake zone—i.e., the variation in flux due to variation in density of a given point source type in a given lake zone.

β We accounted for variation between zones in our calculations (Supplementary Table 1-2). Methane emissions from the zone of shallow thermokarst margins had the highest flux.

γ Lake area estimates for sub-regions of yedoma territory are reported as 8.5% to >30%.

Supplementary Table 1-2. Detailed calculation of annual CH₄ emissions from two intensive study lakes. Whole-lake methane emissions are the area-weighted sum of emissions for each zone of the lake (thermokarst margins, deep center, and non-thermokarst margins). Methane fluxes are the sum of molecular diffusion and ebullition. The patchiness of ebullition is accounted for by quantifying 'background', 'point-source' and 'hotspot' bubbling. We calculated emission estimates for half of the region's lakes with intense thermokarst erosion, which are not represented by our intensive study lakes, by doubling the area of thermokarst zones in this table and subtracting the difference from the deep center zone.

Lake	Zone within lake	Area	% Annual emissions	Area weighted mg CH_4 m^{-2} yr^{-1} summer	winter	← Subsection mg CH_4 m^{-2} yr^{-1} summer	winter	= Diffusion mg CH_4 m^{-2} yr^{-1} summer	+ Hotspots mg CH_4 m^{-2} yr^{-1} summer	winter	+ Point sources mg CH_4 m^{-2} yr^{-1} summer	winter	+ Background mg CH_4 m^{-2} yr^{-1} summer	winter	Bubble traps n
Tube Dispenser	Thermokarst	14%	76%	11,733	8,910	86,272	65,515	1,213	9,316	18,782	34,066	46,026	41,677	707	3
	Deep center	81%	21%	3,891	1,768	4,828	2,193	1,213	182	366	1,049	1,417	2,384	410	6
	Non-thermokarst	6%	3%	409	507	7,046	8,739	1,213	3,838	7,739	184	248	1,811	752	2
	Whole lake	100%	100%	16,033	11,185			1,213	1,636	3,298	5,489	7,416	7,695	471	
	% of annual flux			59%	41%			4%	18%		47%		30%		
	Total			27,218				1,213	4,934		12,905		8,165		
Shuchi	Thermokarst	18%	82%	9,337	9,355	51,889	51,986	1,425	1,448	3,450	35,369	47,786	13,647	750	2
	Deep center	79%	17%	2,694	1,065	3,410	1,349	1,425	42	101	601	812	1,342	436	10
	Non-thermokarst	3%	1%	162	45	5,373	1,480	1,425	111	264	309	417	3,528	799	2
	Whole lake	100%	100%	12,193	10,465			1,425	297	709	6,849	9,253	3,622	503	
	% of annual flux			54%	46%			6%	4%		71%		18%		
	Total			22,658				1,425	1,006		16,101		4,126		

CHAPTER 2

Methane bubbles in lake ice: A new method to evaluate emissions from arctic and sub-arctic lakes[†]

In his Russian Christmas story, A.N. Tolstoy wrote about children ice-skating on frozen lakes and pausing to light methane bubbles trapped in lake ice to heat their tea. Although Russian children have been reading about these bubbles in ice for more than a century, recognition of their importance as an atmospheric methane source is only now being made in the scientific literature.

Methane (CH_4) is an important greenhouse gas whose relative greenhouse effect is 23 times stronger than that of carbon dioxide (CO_2) (IPCC 2001). Although atmospheric methane concentrations have been increasing, particularly at high northern latitudes, the causes of these increases are not well understood. In this paper we describe and quantify an important source of methane—bubbling from northern lakes—that has not been incorporated in previous regional or global methane budgets (Cicerone and Oremland 1998, IPCC 2001, Zhuang *et al.* 2004). The methane emitted in bubbles is challenging to measure because bubbles occur sporadically and haphazardly across the surface of lakes so that minor variations in the location of sampling chambers causes large variability and errors in the resulting estimate. Such errors also make it difficult to detect statistically significant differences among treatments or ecosystems. However, such bubbling events are the dominant pathway of methane release from lakes and may be an important pathway of methane emission globally (Casper *et al.* 2000).

Lakes are a prominent landscape feature in the Arctic and sub-Arctic, occupying up to 30% of land surface area (Zimov *et al.* 1997, Semiletov 1999). Arctic and boreal lakes are known to be net emitters of carbon dioxide and methane (Kling *et al.* 1992,

Zimov *et al.* 1997, 2001, Semiletov 1999). As is true worldwide, fluxes related to bubbling, also called "ebullition", have not been well quantified in the North, but the ice cover resulting from the extreme cold of the polar region allowed us to develop a new field-based technique to quantify ebullition from arctic lakes (Chapter 1). This method uses the spatial patchiness of ebullition as a basis for stratifying ebullition measurements, thereby providing a rigorous platform for scaling methane fluxes to entire lakes and regions.

This article has three goals: (1) to describe a method for accurate measurement of ebullition flux from arctic and sub-arctic lakes, (2) to examine the role of thermokarst (thaw) erosion as a landscape-scale process that supplies high-quality organic substrates to fuel methanogenesis in lake sediments, and (3) to demonstrate the potential importance of lake bubbling as source of atmospheric methane at high latitudes.

Methane production and emission in northern ecosystems

Methanogens are an ancient group of anaerobic microorganisms that evolved before the Earth's atmosphere was oxygenated. Bacterial methane production today is restricted to anaerobic environments, such as lake sediments, where methanogens use end products of organic matter fermentation to produce methane. Methane production is enhanced by warm temperature, intermediate pH, extremely low redox state (Eh <-244 mv), and the availability of labile organic matter as a substrate for decomposition (Smith and Lewis 1992, Valentine *et al.* 1994, Grant and Roulet 2002, Zimov *et al.* 1997). Recent climate change in the Arctic has altered environmental conditions in ways that enhance methane production. Changes include higher mean annual temperatures, increases in precipitation, and the release of labile organic matter from frozen soils upon thaw of permafrost (Zimov *et al.* 1997, IPCC 2001, Peterson *et al.* 2002, ACIA 2004).

Methane emission from lakes can occur *via* three pathways: molecular diffusion, bubbling (ebullition), and transport through gas-conducting tissues of emergent plants

(Chanton 2004). Emergent plants are important conduits in shallow, productive lakes where they dominate; but many arctic and sub-arctic lakes are open water bodies where methane emission occurs primarily by bubbling and molecular diffusion (Kling 1992, Zimov 1997, 2001) (Table 2-1). Bubbling is a particularly effective mode of emission because it transports methane directly from sediments to the atmosphere, largely bypassing oxidation that can occur in the water column or in the oxygenated soils adjacent to plant roots (Chanton 2004).

Methane is only sparingly soluble in water, so methane produced in sediments quickly reaches saturation and comes out of solution as bubbles. Bubbles are released sporadically in response to changes in bottom currents (Joyce and Jewell 2003), decreases in hydrostatic pressure caused by a reduction in water level (Bartlett et al. 1988), decline in atmospheric pressure during storms, or when bubble buoyancy exceeds a threshold (Mattson and Likens 1990, Casper et al. 2000, Glaser et al. 2004).

Generally, ebullition is episodic and difficult to quantify for several reasons. First, some chamber-based studies discard the occasional extremely high fluxes caused by bubbling as "outliers" (Grant and Roulet 2002), even though these might represent an important contribution to total methane flux. Secondly, exceptionally high rates of methane bubbling occur during storm events (Mattson and Likens 1990), when there is a dramatic reduction in barometric pressure; but scientists often miss these events choosing instead to make short-term chamber measurements on "better weather" days. Finally, even long-term continuous measurements using permanent underwater bubble traps placed randomly throughout a lake can underestimate the bubbling flux from lakes because of low likelihood of placement over rare discrete, fixed points of high bubble emissions, which can account for the majority of annual lake emissions (Zimov et al. 1997, Chapter 1). Given these difficulties, many past efforts using chambers have not adequately quantified the contribution of point-source bubbling to the total methane budget of lakes and wetlands. In work where ebullition has been studied in detail, it dominated methane efflux from temperate and tropical lakes (Keller and Stallard 1994, Casper et al. 2000). We propose that careful investigation of bubbling from lakes will

reveal that lakes are much more important contributors to the global atmospheric methane budget than previously thought.

Selective sampling of bubbling points: a new technique

The majority of lake methane emission studies is based on estimates of diffusive flux, which can be calculated using a boundary-layer model based on measurements of the dissolved methane concentration in the surface water (Kling et al. 1992). Bubble fluxes can be measured with floating chambers or underwater bubble traps (Keller and Stallard 1994). Most measurements of bubbling have been made for only a few minutes to hours. To the best of our knowledge, this is the first study to present long-term, continuous measurements of methane fluxes from lakes, taking into consideration the patchiness of bubbling. Table 2-1 summarizes the methods and methane emission rates reported from lakes globally in the scientific literature.

In our work we used several approaches to quantify methane emissions from Siberian and Alaskan lakes. In the yedoma (icy, Pleistocene-age, organic-rich loess permafrost) region of North Siberia, where the majority of our work was conducted (Table 2-2), we made weekly measurements of diffusive emission throughout the entire open-water period (June-September 2003) using surface water methane concentrations and the boundary layer model with meteorological assumptions of Kling (1992). We also made daily measurements of ebullition flux in 25 bubble traps that were placed randomly throughout two thaw lakes from April 26, 2003 through June 1, 2004 (Chapter 1). Randomly placed bubble traps covered less than 0.03% of the lake area and were constructed from a weighted copper wire ring (~1-m diameter), woven through a circle of polyethylene film (0.15mm thick). The center of the polyethylene circle was sealed around the mouth of an inverted polycarbonate soft-drink bottle (Fig. 2-1). A hole drilled into the top of the inverted bottle allowed the trapped gas to be released through tygon tubing and a stopcock into a graduated cylinder for bubble volume measurement. Bubble

traps were attached to ropes and anchored to the bottom of the lake in random locations. We sampled the underwater bubble traps daily from a rowboat in summer and from the ice in winter. In winter, we accessed bubble traps from the ice (Fig. 2-1) by first carefully penetrating the ice with an ice-pick. Figure 2-2 shows the daily dynamics of bubbling captured by three individual underwater bubble traps. Methane concentration of bubbles collected from traps within two hours of capture in traps was $79.6 \pm 1.1\%$ (n=36, mean $\pm$ SD), as measured by gas chromatography using a thermal conductivity detector (TCD Shimadzu 8A) (Chapter 1).

In addition to random placement of underwater bubble traps, we took advantage of the unique opportunity that northern, seasonally-ice covered lakes provide to assess the spatial patchiness of bubbling. After locating point sources of ebullition by removing snow from and walking along lake-surface transects in early winter, we mapped the locations of bubbles trapped in the ice (Table 2-3). Transects revealed that bubbles were not randomly dispersed but occurred in distinct clusters. Much like a time-lapse photograph, the ice literally froze into place the bubbles that had been produced since ice cover had formed. Initially ice forms with relatively uniform thickness across lakes so methane bubbles emitted from lake sediments rise to the surface, becoming trapped in ice directly above. As ice thickens throughout winter, insulatory factors such as snow redistribution and gas bubble accumulation cause ice to thicken unevenly across the lake's surface. Bubbles released from sediments later in winter travel along the uneven lower surface of lake ice, accumulating in places of higher elevation where ice is thinnest. For this reason early autumn surveys of bubble cluster distributions in ice produce the least biased maps of point-sources of bubbling across lakes.

Placing bubble traps beneath the ice where bubble clusters occurred, we selectively sampled these fixed 'point sources' of bubbling. Their general Russian name, 'koshka', translates to English as 'cat', likely reflecting the resemblance between the bubble cluster patterns and a cat's paw print. We categorized three types of point-source bubble patterns in lake ice and measured methane fluxes during 21 days in October 2003 from two lakes associated with each cluster type using under-ice floating bubble traps

(Chapter 1) (Table 2-3). We exploited the richness of the Russian language, which contains many expressions of 'cat' for naming the three categories of bubble cluster types: Kotenok, the weakest of the bubble classes, might translate as 'kitten'; 'koshka' as a typical 'tomcat', and 'kotara', which might imply 'a big, fat grandfather cat that sits on the woodstove'. Occasionally the flux from kotara point sources was extremely high, as high as a fourth bubbling category called 'hotspots'; however, during intervening low-flux days ice reformed solidly over kotaras causing large pockets of bubbles to build up under the ice. Our ice observations and flux measurements indicated that the location of these point sources tended to remain in the same place for at least a year, and summer dives showed that the bubbles emerged from small vents with diameters ranging from several millimeters to two centimeters. We assume that these vents connect to a system of fissures that collect methane from a substantial volume of sediments.

In addition to point sources, we located ebullition 'hotspots', whose bubble emissions also originated from a small hole in the sediment surface. Hotspot bubbling maintained permanently ice-free holes (0.5-1m diameter) above the sediment vent throughout winter due to the convection of warm lake water carried to the surface by constant high rates of bubbling (Fig 2-2c). The fact that holes can remain ice-free even during extended periods of -40°C air temperature attests to the vigorous nature of this bubbling dynamic. Muskrat activity and the occasional overburden of heavy snowfall, which forces lake water to overflow onto the lake's surface, also help maintain ice-free pathways of hotspot emissions in winter.

To estimate an area-based flux for each transect, we counted the number of each bubble cluster class (representing point sources) and hotspots in lake ice along transects (Table 2-4). These early-winter ebullition fluxes were extrapolated to entire lakes based on transects of bubble cluster densities over shallow, medium, and deep water depths along thermokarst and non-thermokarst margins of lakes. Lake-ice bubbles were 53.6 ± 1.6 % CH_4 (n=3) in spring before any thawing occurred (Chapter 1). We extrapolated the mean daily flux rates for each point source type (bubble cluster category) and hotspots to the entire year to generate annual estimates of emission from point-source and hotspot

bubbling (Table 2-5). Uncertainty analysis and details of the extrapolation are provided in Chapter 1. Calculations subtract the 34% decrease in methane concentration that occurs during the long winter before bubble cluster gas is released to the atmosphere when ice thaws in spring (Chapter 1), which is appropriate if the loss is due to microbial oxidation of methane into carbon dioxide. However, analysis of other bubble gas constituents (nitrogen, oxygen, carbon dioxide) revealed that the composition of gas bubbles in ice shifted in the direction of atmospheric compositions during entrapment, suggesting a significant part of the methane decrease is due to diffusion from the bubble pockets rather than oxidation (data not shown; Chapter 4).

In general, point-source and hotspot emissions should be added to emissions measured using randomly placed bubble traps (background bubbling) because the flux rates measured by these two types of sampling did not overlap (Fig. 2-3). In addition, the probability of capturing point-source or hotspot bubbling points using random placement of bubble traps was only 0.001% based on the average area-weighted coverage of point sources and hotspots across the whole lake surface (3.7% of lake area), multiplied by the coverage provided by random placement of 14 traps (<0.03% of lake area). The probability of capturing point-sources or hotspots using randomly placed bubble traps differed according to particular zones within lakes (Fig. 2-3), but was consistently low. Throughout the lake center (80% of lake area) and along the shallow margins without thermokarst activity (4% of lake area), the probabilities were 1.5×10^{-7} and 2.7×10^{-6}. In the shallow area along active thermokarst margins (16% of lake area), point sources and hotspot were more common, and the probability of capturing them with randomly placed bubble traps was higher (6.9×10^{-5}).

To validate the extrapolation of point source measurements made during October to the entire year, we compared the October fluxes to fluxes of six individual point sources that were monitored year-round in two intensively studied lakes. Based on this comparison, we learned that the October point-source ebullition appeared to be lower than at other times (Fig. 2-4), making our temporal extrapolation conservative. Unlike

for point-sources, daily emissions of 4-10 hotspots were measured year-round using bubble traps.

Summing the contributions of the various sources of methane emissions from lakes (Chapter 1), random placement of bubble traps accounted for 24% of annual lake emissions, while 6% of emission occurred *via* molecular diffusion. The majority of methane (70%) was emitted by discrete, fixed points of bubbling (point-sources and hotspots), which, due to their rarity, were unlikely to occur under randomly placed bubble traps. This suggests that bubbling point sources and hotspots have been systematically missed as a source of atmospheric methane in previous studies. The simple new technique introduced in this article can be used to measure point sources ebullition in other lakes where winter ice forms and thereby improve estimates of lake methane emissions.

Application of method to other arctic and sub-arctic lakes

To demonstrate application of this method to other lake systems, we conducted bubble cluster surveys on autumn ice to estimate point-source ebullition from the following sites: lakes on the Holocene alluvium sediments of the Kolyma River floodplain in Siberia; sand lakes in North-central Siberia on the banks of the Lena River; boreal thaw lakes on Pleistocene-age, retransported loess in interior Alaska; and tundra lakes on glacial substrates on the north slope of Alaska's Brooks Range (Tables 2-2 through 2-5). Surveys of bubble clusters trapped in lake ice revealed that ebullition from lakes is ubiquitous in the Arctic (Fig. 2-5). The least bubbling occurred in the large sand lakes of the Lena River region and in Toolik Lake, Alaska, where organic-poor sediments lack substrates to fuel methanogenesis. Point-source ebullition was also relatively unimportant at Grass Lake, a stabilized yedoma thaw lake that lacks thermokarst erosion and was filling in with dense beds of aquatic mosses. At the other extreme, lakes with active thermokarst had particularly high rates of methane emission.

Importance of point source bubbling in lakes of Alaska and Siberia

To evaluate the importance of point-source and hotspot bubbling, we compared methane emission estimates derived from bubble cluster surveys on lake ice with previous estimates that ignored point sources and hotspots. Applying the daily methane flux estimates associated with each point-source type to the distribution of point sources measured on Alaskan tundra lakes in October 2004 (Table 2-5), we estimated an average daily bubbling of 35.0 ± 48.4 mg CH_4 m^{-2} of lake for 7 lakes (n = 20 transects, mean $\pm$ SD). Despite the large variability in bubbling within and among lakes, ebullition emissions through "point sources" significantly increased the average daily emission estimate previously reported for the same arctic lakes by Kling *et al.* 1992, which was 6.5 $\pm$ 1.1 mg CH_4 m^{-2} of lake (n=11) for July and August 1991 (One-way ANOVA, $F=6.01_{1,26}$, $p=0.02$). Excluding Toolik Lake, an exceptionally large, deep lake where we did not find bubbles in ice, the mean bubbling rate for the remaining 6 small lakes was 41.2 ± 50.3 mg CH_4 m^{-2} of lake d^{-1} (n = 17 transects). Rocky substrates of glacial origin with low organic matter content likely provided insufficient substrate to support high rates of methane production in Toolik Lake. Extrapolating daily methane fluxes to 365 days in the year, we estimated 1.6 g CH_4 m^{-2} of lake yr^{-1} (including Toolik Lake) and 9.3 g CH_4 m^{-2} of lake yr^{-1} for small lakes (excluding Toolik Lake)[1] for the north slope of Alaska's Brooks Range. The large difference in flux estimate, depending on whether Toolik Lake is included, suggests that future studies that determine the relative abundance of different lake types in Alaska would greatly reduce the uncertainty in this flux estimate. This inclusion of methane bubbling in these estimates increases the earlier

---

[1] We estimated the average regional emission from lakes by weighting the point-source-derived fluxes by the area of individual lakes (1.3 g CH_4 m^{-2} yr^{-1} including Toolik Lake, and 7.2 g CH_4 m^{-2} yr^{-1} for small lakes if Toolik Lake is excluded). Based on relative contribution of point source and hotspot emissions (70% of the total) to total annual emissions from North Siberian lakes, we added an additional 30% to the point source emission estimate derived by mapping point sources on Alaska's North Slope to account for diffusion and background bubbling fluxes, making the total: 1.6-9.3 g CH_4 m^{-2} yr^{-1}.

diffusion-derived regional estimate of summertime methane emissions from lakes of 0.67 g CH_4 m^{-2} of lake yr^{-1} (Kling *et al.* 1992) by 2.5- to 14-fold.

Conducting a similar calculation for the two intensively studied yedoma lakes in Siberia, we conclude that consideration of point sources and hotspots (17.1-17.8 g CH_4 m^{-2} of lake yr^{-1}) yielded a 11- to 14-fold increase in the estimate of CH_4 emissions above estimates based on diffusion alone (1.2-1.4 g CH_4 m^{-2} of lake yr^{-1}), and 2- to 3-fold increase above estimates that would be derived by only measuring diffusion and ebullition with randomly placed chambers (5.5-9.4 g CH_4 m^{-2} of lake yr^{-1}). Our calculations are conservative because they are based on early winter measurements of point-source ebullition, a season when bubble rates were particularly low (Fig. 2-4). Given that warmer surface sediments in summer enhance methane production rates, we might expect higher rates of bubbling in summer (Miller and Oremland 1988).

Implications for modeling lake bubble emissions

Given the paucity of adequate ebullition studies in the literature, lake contributions have, until now, been considered negligible in the global atmospheric methane budget. Consequently, lake processes have not been incorporated in biogeochemical models that simulate methane emissions from northern wetlands . We ran a modeling experiment with the Terrestrial Ecosystem Model (TEM) (Zhuang *et al.* 2004) to test the hypothesis that including estimates of methane emitted from lakes based the technique introduced in this article would significantly increase prior model estimates of regional emissions that ignored lakes. Adding the methane emission estimate from North Siberian yedoma lakes (35 g CH_4 m^{-2} of lake yr^{-1})(Chapter 1) to the regional net methane emissions estimated by TEM for the ice-rich loess area of Northeast Siberia increased the regional flux estimate 2.8- to 8.5-fold from 0.1 Tg CH_4 yr^{-1} to 0.38-0.95 Tg CH_4 yr^{-1}. The range reflects variation in estimates of lake area (10-30% lake area) for North Siberia (Mostakhov 1970, Zimov *et al.* 1997, Chapter 1). Given that lake processes are not

included in TEM, we expect that if ebullition is ubiquitous among arctic and boreal lakes, incorporating lake methane emissions into models like TEM will have important implications for the magnitude and seasonality of source estimates of greenhouse gas emissions throughout the Arctic.

Hotspots of methane bubbling around the Arctic linked to thawing permafrost

Since methane is formed as a byproduct of anaerobic decomposition of organic matter, lakes with high sediment organic content produce more methane than lakes with low sediment organic content (Smith and Lewis 1992, Michmerhuizen *et al.* 2002). Primary production in lakes by littoral macrophyte communities and phytoplankton is a well-documented source of organic substrates to lake sediments (Aselmann and Crutzen 1990, Whiting and Chanton 1992). Similarly, small East Siberian lakes surrounded by wetlands with high plant biomass had higher emissions than large lakes with fewer wetlands (Nakayama *et al.* 1994). Because most of the Earth's lakes are small with large ratios of littoral zone area to lake area (Wetzel 2001), processes that govern littoral zone carbon contributions to lake sediments are key to methane production in lakes.

Thermokarst is another important but rarely documented source of labile organic matter to lake sediments (Zimov *et al.* 1997, 2005). Radiocarbon ages of methane emitted from thaw lakes in North Siberia (up to 43,000 years, Zimov *et al.* 1997, Chapter 1) and interior Alaska (up to 26,000 years; Chapter 4) suggest that thawing permafrost along lake margins supplies ancient, labile organic substrates that enhance methanogenesis in lake sediments. Organic matter released from thawing yedoma in our Siberia study region is Pleistocene-age (20,000-40,000 years, Zimov et al 1997) as is that of the retransported silt permafrost that characterizes our study lakes in interior Alaska (12,500-40,000 years, Hamilton *et al.* 1988).

Aerial photographs taken in autumn 2003 of more than 60 Siberian yedoma lakes showed that hotspots of ebullition occurred in the shallow areas of all lakes along active

thermokarst margins (Fig. 2-6). We measured maximal rates of hotspots of ebullition, 18 g CH_4 spot^{-1} d^{-1} in a Siberian yedoma lake and 25 g CH_4 spot^{-1} d^{-1} during short-term spot sampling of thaw lakes in interior Alaska. Although the study lakes in Alaska were not situated on yedoma, they were subject to thermokarst erosion, which supplies ancient organic substrates from the organic-rich retransported silt that characterizes their locations (Hamilton *et al.* 1998). These measured hotspot emission rates exceed most published methane flux rates for lakes and wetlands by at least two orders of magnitude (Table 2-1). Ground surveys of hotspot distributions on Siberian lakes revealed that the number of hotspots increased exponentially from the lake center towards thermokarst margins (Fig. 2-7). Hotspots of ebullition were absent from non-thermokarst margins of lakes. We did not observe hotspots on the sand-bottom lakes near the Lena River or on Alaska's North Slope tundra lakes that were situated on organic-poor glacial deposits. In interior Alaska, where we surveyed both thermokarst and non-thermokarst lakes, hotspots occurred throughout thermokarst lakes (Fig. 2-8), but were absent from non-thermokarst lakes. Based on these observations, we conclude that thermokarst erosion is a particularly important landscape process that fuels methane production and emission where it occurs in permafrost regions of the North.

Arctic and sub-arctic lake bubbling as a source of methane to the atmosphere

The concentration of methane in the atmosphere is highest at 65-70°N and has been increasing in recent decades (Fung *et al.* 1991, Dlugokencky *et al.* 1998), but its sources are still not all well defined (IPCC 2001, Keppler *et al.* 2006). At northern high latitudes, seasonal maxima occur in early winter and spring, when wetlands are freezing or already frozen (Fung *et al.* 1991). Meteorology may influence these seasonal patterns because during summer emissions are mixed throughout the atmospheric boundary layer and in winter they mix only in a shallow surface layer because of strong inversions. Consequently, it is unclear the extent to which seasonal atmospheric patterns reflect

seasonal variation in sources of emissions or errors in models of atmospheric transport (Mikaloff Fletcher 2004). Our work improves bottom-up estimates of methane sources from a process that has until now been overlooked in the global atmospheric methane budget, that is, bubbling from lakes. Unlike wetlands, lake sediments remain unfrozen year-round, producing and emitting methane.

Two pulses of methane loss have been recognized from most northern lakes (Michmerhuizen *et al.* 1996): In autumn, methane that accumulated in the hypolimnion (the deep water) of lakes during summer stratification is released to the atmosphere during fall turnover. Similarly, methane stored in lake water during winter is released to the atmosphere at the time of spring turnover. Our study suggests that an additional source of lake methane is important in spring- the release of a large volume of methane trapped in ice as bubbles when lake ice begins to thaw. A better understanding of this new high-latitude source of methane, whose large springtime pulse-release coincides with the seasonal maximum of atmospheric methane, could help resolve uncertainties in models of global methane dynamics.

Challenge for the future

The arctic system is changing and plays a prominent role in the debate regarding global climate change (Serreze *et al.* 2000, Moritz 2002, Peterson 2002). Observed changes that coincide with 20th-century warming include the retreat of glaciers, thawing of permafrost and melting of sea ice, increase in river discharge, and alteration of terrestrial and aquatic ecosystems (Overpeck *et al.* 1997, IPCC 2001, Peterson *et al.* 2002, ACIA 2004), including changes in lake area (Labrecque *et al.* 2006, Riordan 2004, Smith 2005, Chapter 1). The projected increase in global temperature during the next century will likely lead to further permafrost degradation in the north, thereby subjecting the vast amounts of organic carbon currently stored in permafrost to mineralization and greenhouse gas production (Post *et al.* 1982, IPCC 2001, Zimov *et al.* 2005).

Degradation of discontinuous permafrost often results in lake area loss due to catastrophic lake drainage (Smith *et al.* 2005); however, in ice-rich, continuous-permafrost areas of the Arctic and sub-Arctic we expect that permafrost thaw and ground-surface subsidence will lead to lake expansion and creation of new methane-producing lakes (Smith *et al.* 2005, Chapter 1).

Until now, methane fluxes from northern wetlands have been underestimated because of a lack of methods for assessing the patchiness of bubbling from lakes. Introduction of this simple new technique of counting methane bubble clusters in lake ice to map point sources of ebullition has great potential to improve scientists' ability to quantify lake methane emissions. This paper demonstrated the importance of ebullition for estimating methane emissions from individual lakes as well as for including lakes in regional estimates of methane emissions. Given the prominence of lakes in the Arctic and sub-Arctic, and their role in greenhouse gas emissions, the challenge now stands to accurately assess methane bubbling from a broader spectrum of arctic and sub-arctic lakes in order to better understand dynamics of the atmospheric methane budget at high latitudes.

References

Arctic Climate Impact Assessment (ACIA): Overview Report. Cambridge Univ. Press, New York (2004).

Aselmann I, Crutzen PJ. 1989. Global distribution of natural freshwater wetlands, rice paddies, their net primary productivity, seasonality, and possible methane emissions. Journal of Atmospheric Chemistry 8: 307-358.

Baker-Blocker A, Donahue TM, Mancy KH. 1977. Methane flux from wetland areas. Tellus 29: 245-250.

Barber LE, Ensign JC. 1979. Methane formation and release in a small Wisconsin lake. Geomicrobiology Journal 1: 341-353.

Bartlett KB, Crill PM, Sebacher DI, Harriss RC, Wilson JO, Melack JM. 1988. Methane flux from the Central Amazonian Floodplain. Journal of Geophysical Research 93: 1571-1582.

Casper P, Maberly SC, Hall GH, Finlay BJ. 2000. Fluxes of methane and carbon dioxide from a small productive lake to the atmosphere. Biogeochemistry 49: 1-19.

Chanton JP. 2004. The effect of gas transport mechanism on the isotope signature of methane in wetlands. Organic Geochemistry 100(5): 753-768.

Cicerone RJ, Oremland RS. 1998. Biogeochemical aspects of atmospheric methaneGlobal Biogeochemical Cycles 2(4):299-327

Dlugokencky EJ, Masarie KA, Lang PM, Tans PP. 1998. Continuing decline in the growth rate of the atmospheric methane burden. Nature 393: 447-450.

Fallon RD, Harris S, Hanson RS, Brock TD. 1980. The role of methane in internal carbon cycling in Lake Mendota during summer stratification. Limnology and Oceanography 25: 357-360.

Fung I, John J, Lerne J, Mathew E, Prather M, Steele LP, Fraser PJ. 1991. Three-dimensional model synthesis of the global methane cycle. Journal of Geophysical Research 96: 13,033-13,065.

Glaser PH, Chanton JP, Morin P, Rosenberry KO, Seigel DI, Ruud O, Chasar LI, and
Reeve AS. 2004. Surface deformations as indicators of deep ebullition fluxes in
a large northern peatland. Global Biogeochemical Cycles 18,

Grant RF, Roulet NT. 2002. Methane efflux from boreal wetlands: Theory and testing of
the ecosystem model Ecosys with chamber and tower flux measurements. Global
Biogeochemical Cycles 16, 1054, doi:10.1029/2001GB001702.

Hamilton TD, Craig JL, Sellmann PV. 1988. The Fox permafrost tunnel: A late
Quaternary geologic record in central Alaska. Geological Society of America
Bulletin 100, 948-969.

Intergovernmental Panel on Climate Change (IPCC). *The Scientific Basis*. Cambridge
Univ. Press, New York (2001).

Joyce J, Jewell PW. 2003. Physical controls on methane ebullition from reservoirs and
lakes. Environmental and Engineering Geoscience 9(2): 167-178.

Keller M, Stallard RF. 1994. Methane emission by bubbling from Gatun Lake, Panama.
Journal of Geophysical Research 99: 8307-8319.

Kling GW, Kipphut GW, Miller MC. 1992. The flux of CO2 and CH4 from lakes and
rivers in arctic Alaska. Hydrobiologia 240: 23-36.

Labrecque S, Duguay CR, Hawkings J, and Lauriol B. 2005. Contemporary changes in
the aerial extent of thaw lakes in the Old Crow Flats, Yukon Territory, Canada.
Arctic, Antarctic and Alpine Research *in review*.

Mattson MD, Likens GE. 1990. Air pressure and methane fluxes. Nature 347.

Michmerhuizen CM, Striegl RG, McDonald ME. 1996. Potential methane emission
from north-temperate lakes following ice melt. Limnology and Oceanography 41:
985-991.

Mikaloff Fletcher SE, Tans PP, Bruhwiler LM, Miller JB, Heimann M. 2004. CH_4
source estimated from atmospheric observations of CH_4 and its $^{13}C/^{12}C$ isotopic
ratios: 1. Inverse modeling of source processes. Global Biogeochemical Cycles
18: GB4004, doi:10.1029/2004GB002223.

Miller LG, Oremland RS. 1988. Methane efflux from the pelagic regions of four lakes. Global Biogeochemical Cycles 2: 269-277.

Moritz RE, Bitz CM, Steig EJ. 2002. Dynamics of recent climate change in the Arctic. Science 297, 1497-1502.

Naiman RJ, Manning T, Johnston CA. 1991. Beaver population fluctuations and tropospheric methane emissions in boreal wetlands. Biogeochemistry 12: 1-15.

Nakayama T, Nojiri Y, Zeng Y. 1994. Measurement of methane flux from alasses around Yakutsk, eastern Siberia in 1993. in Proceedings of the Second Symposium on the Joint Siberian Permafrost Studies Between Russia and Japan in 1993, edited by G. Inoue, pp. 40-44 Natl. Inst. for Environ. Stud., Tsukuba, Japan.

Overpeck JT *et al.* 1997. Arctic and environmental change of the last four centuries. Science 278: 1251-1256.

Peterson BJ, Holmes RM, McClelland JW, Vorosmarty CJ, Lammers RB, Shiklomanov AI, Rahmstorf S. 2002. Increasing river discharge to the Arctic Ocean. Science 298: 2171-2173.

Post WM, Emmanuel WR, Zinke PJ and Strangenburger AG. 1982. Soil carbon pools and world life zones. Nature 298, 156-159.

Riordan B, Verbyla D, McGuire D. 2004. Decrease in surface water across a warming subarctic landscape. The Earth Observer 16: 3-4.

Roulet NT, Jano A, Kelly CA, Klinger LF, Moore TR, Protz R, Ritter JA, Rouse WR. 1994. Role of Hudson Bay lowland as a source of atmospheric methane. Journal of Geophysical Research 99, 1439-1454.

Roulet NT, Crill PM, Comer NT, Dove A, Boubonniere RA. 1997. CO_2 and CH_4 flux between a boreal beaver pond and the atmosphere. Journal of Geophysical Research 102: 29,313-29,319.

Rudd JWM, Hamilton RD. 1978. Methane cycling in a eutrophic shield lake and its effects on whole lake metabolism. Limnology and Oceanography 23: 337-348.

Rudd JWM, Harris R, Kelly CA, Hecky RE. 1993. Are hydroelectric reservoirs significant sources of greenhouse gases? Ambio 22: 246-248.

Semiletov IP. 1999. Aquatic sources and sinks of CO_2 and CH_4 in the polar regions. Journal of Atmospheric Sciences 56: 286-306.

Serreze MC, Walsh JE, Chapin III FS, Osterkamp T, Dyurgerov M, Romanovsky V, Ochel WC, Morison J, Zhang T, Barry RG. 2000. Observational evidence of recent change in the northern high-latitude environment. Climatic Change 46: 159-207.

Smith LK, Lewis Jr. WM. 1992. Seasonality of methane emissions from five lakes and associated wetlands of the Colorado Rockies. Global Biogeochemical Cycles 6: 323-338.

Smith LC, Sheng Y, MacDonald GM, Hinzman LD. 2005. Disappearing arctic lakes. Science 308: 1429.

Strayer RF, Tiedje JM. 1978. *In situ* methane production in a small, hypereutrophic, hard-water lake: Loss of methane from sediments by vertical diffusion and ebullition. Limnology and Oceanography 23: 1201-1206.

Valentine DW, Holland EA, Schimel DS. 1994. Ecosystem and physiological controls over methane production in northern wetlands. Journal of Geophysical Research 99: 1563-1571.

Wetzel RG.2001. Limnology: Lake and River Ecosystems. San Diego: Academic Press.

Whalen SC, Reeburgh WS. 1990. A methane flux transect along the trans-Alaska pipeline haul road. Tellus 22B: 237-249.

Whiting GJ, Chanton JP. 1992. Plant-dependent CH4 emission in a subarctic Canadian fen. Global Biogeochemical Cycles 6: 225-331.

Zhuang Q, Melillo J, Kicklighter DW, Prinn TG, McGuire AD, Steudler PA, Felzer BS, Hu S. 2004. Methane fluxes between terrestrial ecosystems and the atmosphere at northern high latitudes during the past century: A retrospective analysis with a process-based biogeochemistry model. Global Biogeochemical Cycles 18: 1-23.

Zimov SA, Voropaev YV, Semiletov IP, Davidov SP, Prosiannikov SF, Chapin III FS,
Chapin MC, Trumbore S, Tyler S. 1997. North Siberian lakes: A methane
source- fueled by Pleistocene Carbon. Science 277: 800-802.

Zimov SA, Voropaev YV, Davidov SP, Zimova GM, Davydova AI, Chapin III FS,
Chapin MC. 2001. Flux of methane from North Siberian aquatic systems:
Influence on atmospheric methane. Pages 511-524 in Paepe R, Melnikov V, eds.
Permafrost Response on Economic Development, Environmental Security and
Natural Resources. Netherlands: Kluwer Academic Publishers.

Zimov SA. 2005. Pleistocene Park: Return of the Mammoth's Ecosystem. Science 308:
796-798.
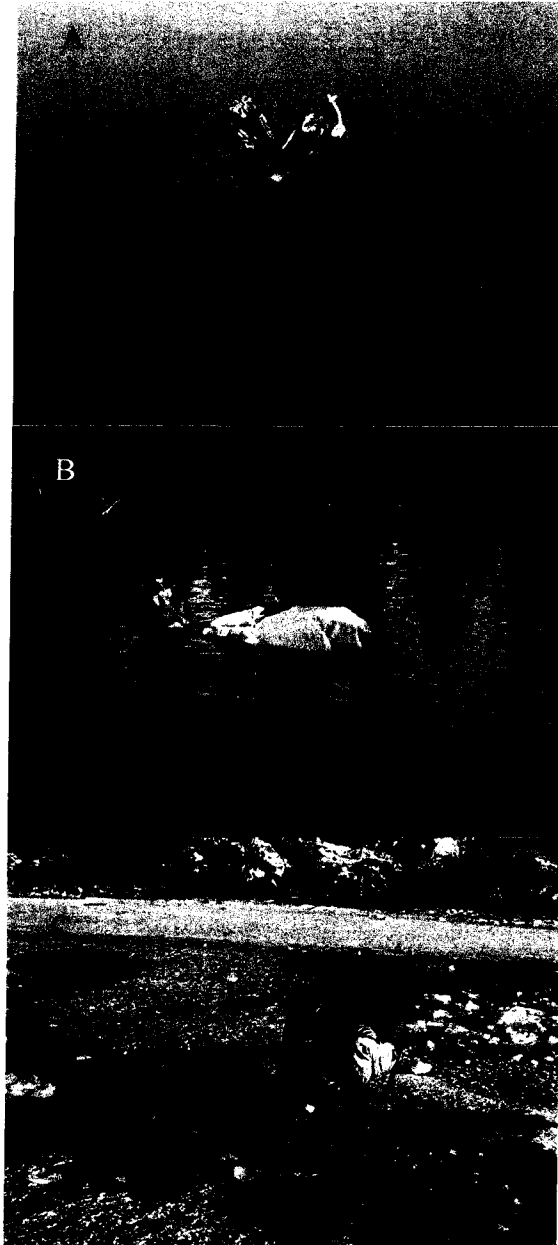
Figure 2-1. Floating bubble traps tethered to an anchor on the lake bottom in summer placed randomly to measure background bubbling rates (panel A), and over point sources of bubbling (panel B). The large volume of gas in the point source trap accumulated in less than 14 hours. In winter, traps hang from Larch tree poles that lay on the surface of the ice (panel C).
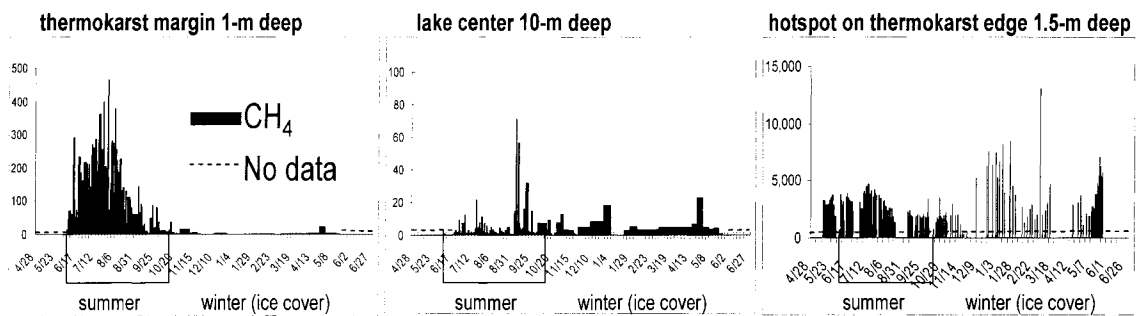
Figure 2-2. Examples of temporal variation of CH_4 ebullition (mg CH_4 m^{-2} d^{-1}, scale on y-axes varies) captured in single bubble traps in 2003-04. Panels A and B show bubbling in traps randomly placed in the shallow thermokarst margin zone (A) and at depth in the lake center (B). Panel C is an example of hotspot bubbling, which was continuously high. During some times of the year, we made repeated short-term measurements of hotspot bubbling instead of continuous bubble collection because leaving the traps in place for too many hours unattended would result in them filling with gas and overturning. Times of no data are indicated by a dashed line.

October 9-29, 2003	Background emission $g \, CH_4 \, m^{-2} \, yr^{-1}$	Background area (percent of whole lake area)	Point source & hotspot emission $g \, CH_4 \, m^{-2} \, yr^{-1}$	Point source & hotspot area (percent of area in each lake section)
Non-therm. margin	3.4 ± 0.9	4.4%	6.6 ±5.5	0.9%
Lake center	2.4 ± 0.5	79.8%	2.3 ±0.7	0.05%
Thermokarst margin	28.4 ± 14.0	15.8%	98.1 ±10.1	23%
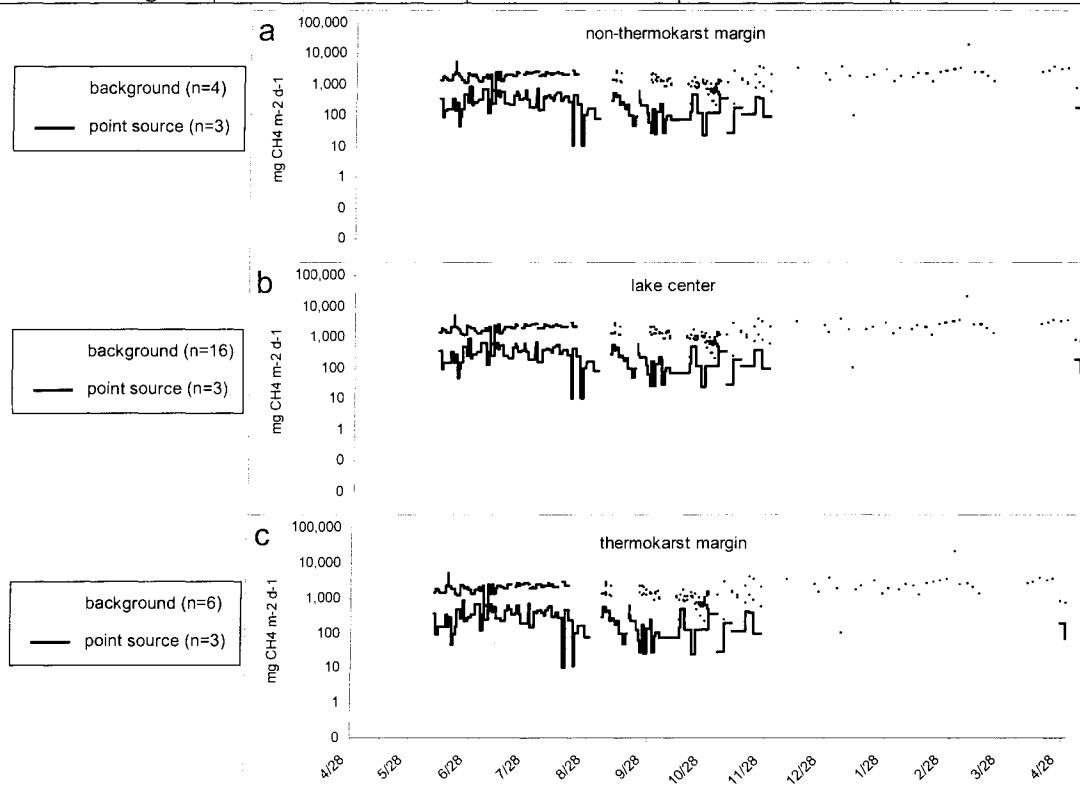
Figure 2-3. Background bubbling *vs.* discrete bubbling points. Traps placed strategically over point sources and hotspots measured significantly higher rates of methane bubbling (mg $CH_4 \, m^{-2} \, yr^{-1}$, log scale) than traps placed randomly (background) in shallow non-thermokarst areas of lakes (A), throughout the lake center (B), and along shallow thermokarst margins (C) in the two intensively studied Siberian lakes. Because the density of point-source bubbling was much higher along shallow thermokarst margins, the probability of capturing point-source bubbling in randomly placed traps in the thermokarst area was higher than the rest of the lake where point sources were rarer.
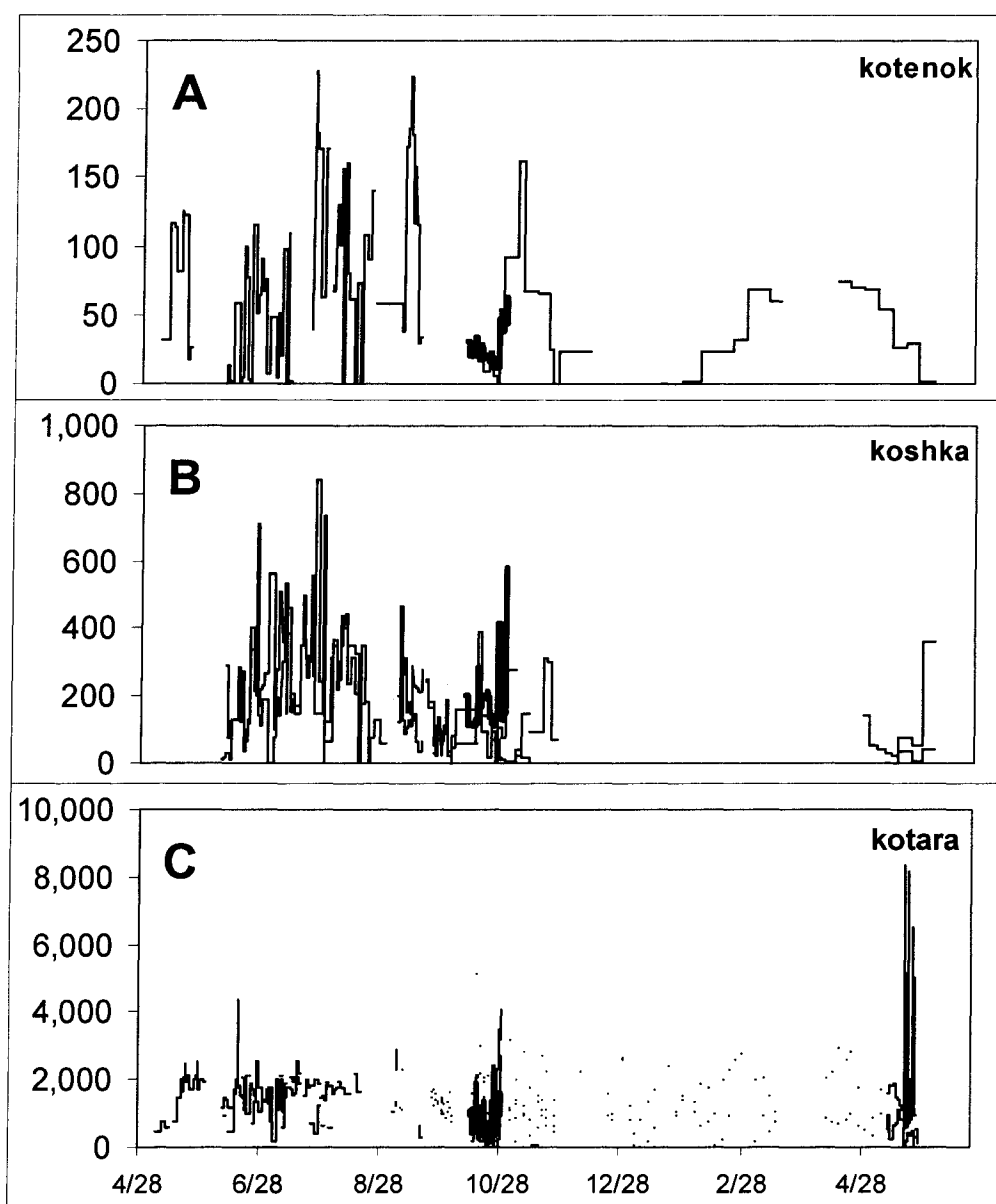
Figure 2-4. Short term *vs.* long term measurements of point-source ebullition. Point source bubbling during 21-day measurement period in October 2003 (red line, mean of 6-8 bubble traps) and long-term (black, individual traps) for three categories of point sources: (A) kotenok (n = 6 short term, n = 1 long term); (B) koshka (n = 8 short term, n = 2 long term); and (C) kotara (n = 7 short term, n = 7) from April, 2003 through May, 2004. Due to a small sample size of long-term point source traps, mean ebullition rates measured during the October study were extrapolated to 365 days per year; a conservative extrapolation since October ebullition was lower than at other times of the year. Rates of bubbling are presented as mg CH_4 spot^{-1} d^{-1} on the y-axis with different scales for A-C.
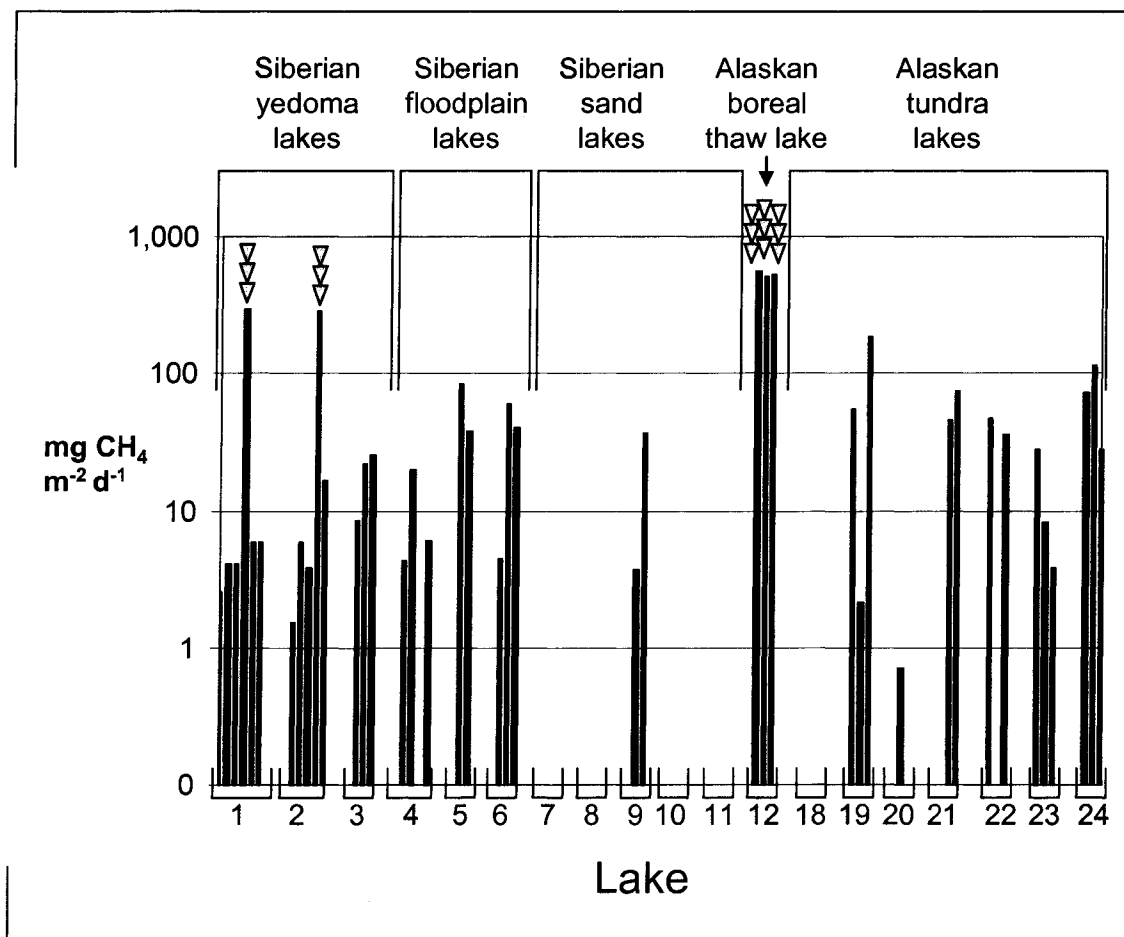
Figure 2-5. Methane bubbling by point sources as measured by surveys of bubble clusters along individual transects on ice of Siberian and Alaskan lakes. Three stacked triangles indicate the presence of thermokarst erosion, which enhances methane production and bubble emissions in the Alaskan thaw pond and certain transects on the Siberian lakes. Rates of methane bubbling are shown as a log scale on the y-axis.
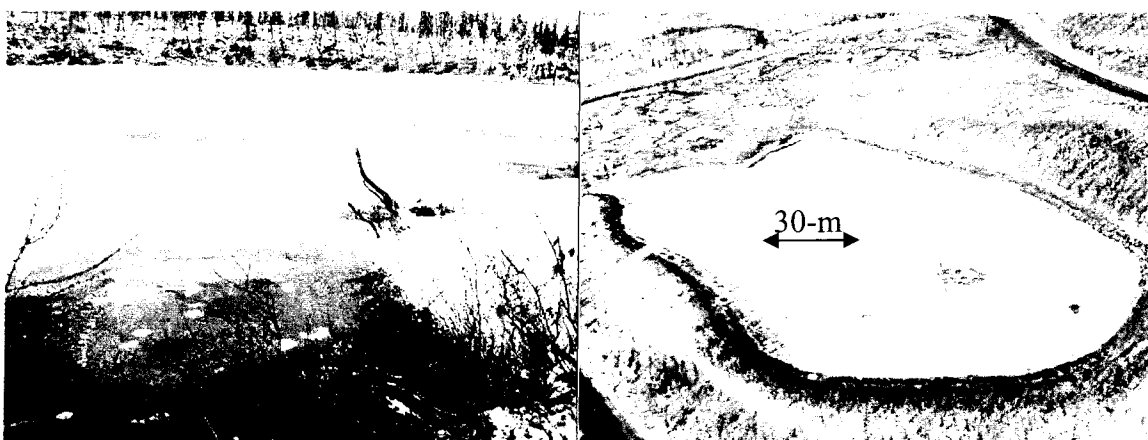
Figure 2-6. Hotspots of methane bubbling are visible from helicopter surveys as open holes in lake ice, through which lake water overflows due to the pressure of a recent snow fall in October 2003 (a). Hotspots were present in 59 of 60 lakes that we surveyed by helicopter, always located along active thermokarst margins of lakes (b).
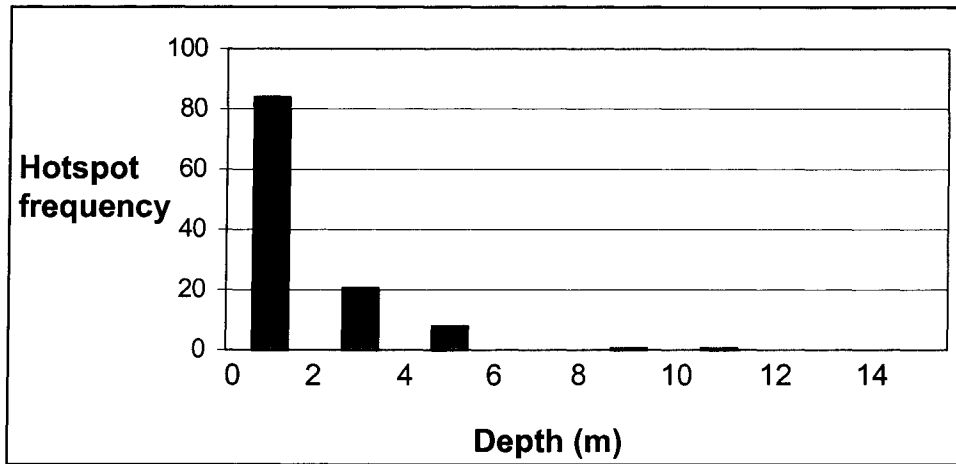
Figure 2-7. Frequency of hotspots in Siberian yedoma lakes. The number of hotspots (y-axis) increased exponentially towards the shallow thermokarst margins of lakes (x-axis = water depth beneath ice depth), according to our ground surveys of hotspots on two North Siberian lakes. We observed similar patterns in other yedoma thaw lakes during helicopter surveys for half of the regions lakes. Other lakes had wider bands of hotspots due to more active thermokarst erosion during recent decades.
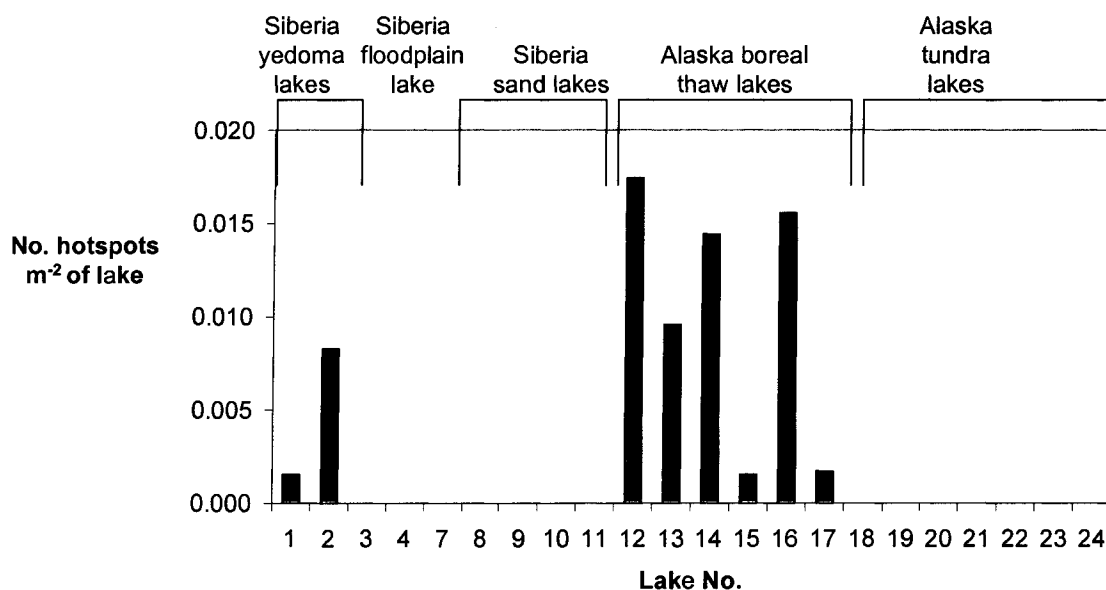
Figure 2-8. Density of hotspots in Siberian and Alaskan lakes. Lakes with visible thermokarst erosion along lake margins contained hotspots, though the number of hotspots varied among lakes. Lakes without thermokarst erosion did not contain hotspots. We speculate that the magnitude of hotspot emissions in a lake is related to the amount of labile organic substrate available to methanogens in thawed lake sediments

Zone	Reference	Object	Mode	Method†	% CH$_4$	min	max	seasonal averge
Tropics	Keller and Stallard 1994	Tropical man-made lake	D					12.4
	Keller and Stallard 1994	Tropical man-made lake	E	BT,C	67-77%	10	2000	47-1302
	Bartlett et al. 1988	Amazon floodplain	D	C				8.3
	Bartlett et al. 1988	Amazon floodplain	E	C	58-72%	0	2997	17-346
Temperate	Miller & Oremland 1988	Searsville L. (freshwater reservoir), CA	D + E	C				160
	Miller & Oremland 1988	Searsville L. (freshwater reservoir), CA	D	C		0.5	11.6	3.0
	Miller & Oremland 1988	Western USA meromictic saline lakes	D	C		0.2	77.1	10
	Barber & Ensign 1979	Lake Wingra (eutrophic)	E	BT	4-56%	8.0	3200	16-768
	Casper et al. 2000	Priest Pot (hypertrophic)	D			1.0	22.4	5.4
	Casper et al. 2000	Priest Pot (hypertrophic)	E	BT	44-88%	0	1734	198
	Mattson & Likens 1990	Mirror Lake (softwater)	E	BT	70	0.8	68.2	12.2
	Fallon et al. 1980	L. Mendota	D				132	42.1
	Baker-Blocker et al. 1977	Michigan ponds	E	BT		92	1100	
	Stayer and Tiedje 1978	Wintergreen Lake, Michigan	E	BT	73-107%			336
	Stayer and Tiedje 1978	Wintergreen Lake, Michigan	D					160-736
	Bastviken et al. 2004	Wisconsin lakes	D + E	C				2.7-70
	Smith & Lewis 1992	Colorado high altitude lakes	D + E	C		0	160	25.6
Arctic	Kling et al. 1992	N. Alaska Lakes	D			1.3	16.3	6.5
	Whalen and Reeburgh 1990	N. Alaska ponds	D	C		4.6	131	21
	Bastviken et al. 2004	Swedish lakes	D	HE				0.3-7.5
	Rudd & Hamilton 1978	Canadian Shield Lakes	D			0	960	544
	Rudd et al. 1993	Candian Shield Lakes (oligotrophic)	D			0.8	8.3	
	Rudd et al. 1993	Canadian reservoirs	D			10.2	20.0	
	Naiman et al. 1991	beaver pond	D + E	C		5.0	200	32-40
	Grant and Roulet 2002	beaver pond	E	BT,C,T				100
	Grant and Roulet 2002	beaver pond	D	C				91.5
	Roulet et al. 1994	Hudson Bay Lowland pools	D					100-163
	Roulet et al. 1997	beaver ponds	D + E	FG		-70	3240	109
	Hamilton et al. 1994	Hudson Bay Lowland ponds	D				770	110-180
	Hamilton et al. 1994	Hudson Bay Lowland ponds	E	BT			0	0
	Nakayama et al. 1994	Shallow Siberian alases near Yakutsk	E	SS	38-74%			231-528
	Zimov 2001	Siberian thermokarst lakes	D			0		7.6
	Zimov 2001	Siberian thermokarst lakes	E	BT	>80%			>70
	This study	**Siberia thermokarst lakes**	**D**	**HE**				**12.0**
	This study	**Alaska & Siberia thermokarst lakes**	**koshka & E**	**ICE,BT**	**53-80%**	**0**	**25,000**	**415**

Table 2-1. Summary of published methane emissions from tropical, temperate, and arctic lakes by diffusion (D) and ebullition (E). Minimum, maximum, and seasonal averages for measurements of methane flux are given in mg CH$_4$ m^{-2} d^{-1}. Methane concentrations (% CH$_4$) were measured in bubble samples.

Table 2-1 Cont.

[†]Methods are abbreviated as follows:

BT	Bubble trap
C	Floating chamber
HE	Headspace equilibration
T	Eddy flux tower
FG	Flux gradient technique measuring CH_4 concentration in air at different heights above lake
SS	Sediment stirring to release bubbles into inverted funnels
ICE	Surveys of bubble clusters on lake ice

Table 2-2. Location, size, biome, substrate type, level of thermokarst activity and survey dates for Siberian and Alaskan lakes studied with regards to point-source and hotspot distributions.

Region	Lake No.	Lake Name	Biome	Substrate†	Thermokarst	Date	Latitude	Longtitude	Area (m²)	Max Depth (m)
Northeast Siberia Kolyma R.	1	Shuchi Lake	Boreal	Yedoma	Moderate	May. 2003 Oct. 2002			58,051	11.0
	2	Tube Dispenser Lake	Boreal	Yedoma	Moderate	May. 2003 Oct. 2002			110,175	16.5
	3	Grass Lake	Boreal	Yedoma	Mature, inactive	May. 2003 Oct. 2002			5,363	12.5
	4	Meadow Lake	Boreal	HA-FD	Moderate	Oct. 2002				2.3
	5	Airport Lake 1	Boreal	HA-FD	Moderate	Oct. 2002				1.8
	6	Airport Lake 2	Boreal	HA-FD	Moderate	Oct. 2002				2.0
North Central Siberia Lena R.	7	Olba Lake	Boreal	Sand	Minimum	Oct. 2005	66°38'14"	123°18'39"		2.5
	8	Big Black Blood Lake	Boreal	Sand	Minimum	Oct. 2005	66°37'21"	123°20'42"		5.0
	9	Little Black Blood Lake	Boreal	Sand	Minimum	Oct. 2005	66°36'33"	123°20'31"		1.5
	10	Simple Lake	Boreal	Sand	Minimum	Oct. 2005	66°37'51"	123°17'30"		1.1
	11	Pope Lake	Boreal	Sand	Minimum	Oct. 2005	66°39'13"	123°17'45"		3.0
Interior Alaksa	12	Rosie Creek Beaver Pond	Boreal	HA-RPL	Active	Nov. 2004			6,324	1.5
	13	Goldstream Valley Lake	Boreal	RPL	Active	Nov. 2004			9,797	-
	14	Goldstream Valley Pond	Boreal	RPL		Nov. 2004			484	-
	15	Ballaine Lake	Boreal			Nov. 2004			8,638	-
	16	Sheep Creek Pond	Boreal		Active	Nov. 2004			1,348	-
	17	Parks Hwy. Gravel Pit	Boreal	RPL	Active	Nov. 2004				
North Slope Alaska	18	Toolik Lake	Tundra	GD	Minimum	Oct. 2005			1,470,000	24.0
	19	E1	Tundra	GD	Minimum	Oct. 2005			30,099	12.4
	20	E5	Tundra	GD	Minimum	Oct. 2005			113,172	11.9
	21	E6	Tundra	GD	Minimum	Oct. 2005			19,967	3.2
	22	NE1	Tundra	GD	Minimum	Oct. 2005			21,502	-
	23	N2	Tundra	GD	Minimum	Oct. 2005			13,663	10.7
	24	N3	Tundra	GD	Minimum	Oct. 2005			9,349	-

†Substrate types are abbreviated as follows:

Yedoma: Icy, Pleistocene-age, organic-rich loess

HA-FD: Holocene alluvium; floodplain deposits

HA-RPL: Holocene alluvium and reworked Pleistocene-age loess from Stage 3 at LGM

RPL: Reworked Pleistocene-age loess from Stage 3 at LGM

Sand: Organic-poor sand

GD: Glacial deposits

Table 2-3. Categorization of methane bubble clusters in lake ice. We removed snow from lake surfaces in replicated (1-m x 50-m) transects to count the number and type of bubble clusters in lake ice for scaling ebullition fluxes to the entire lake (a). We recognized four distinct categories of bubbling (b-e). Discrete ebullition points caused bubbles to stack-up in lake ice during winter (b. kotenok, c. koshka, d. kotara), while exceptionally high rates of continuous bubbling through hotspots (e) are identified as open holes in lake ice. Mean daily fluxes were measured during October 2003 for each ebullition category using 6-8 bubble traps per category (ANOVA, $F=16.23_{3,27}$ $p<.0001$). Error estimates (standard deviation) represent spatial differences in ebullition between individual bubble traps in each category. The lines on meter stick of panels b and c mark 10-cm wide intervals.
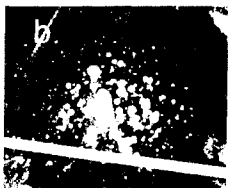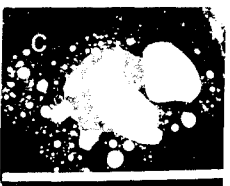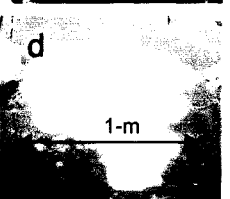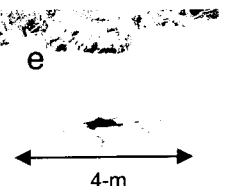
	Bubble category on ice transects	Description	Average flux (mg CH_4 d^{-1})
b	kotenok	stacks of small individual, unmerged bubbles	25 ± 12
c	koshka	merged bubbles clustered in multiple layers of ice	190 ± 172
d	kotara	single large pockets of merged bubbles in ice	825 ± 348
e	hotspot	open-hole in lake ice	2,175 ± 1,195

Table 2-4. Surveys of hotspots[†] and point sources as bubble clusters in ice of lakes in Siberia and Alaska. Point-source densities were measured along 50-m x 1-m transects, replicated across lake surfaces.

Region	Lake No.	Lake Name	Transect[Y]	Transect depth (m)	No. kotenok m^{-2}	No. koshka m^{-2}	No. kotara m^{-2}	No. hotspot m^{-2}
Northeast	1	Shuchi Lake						0.0015
Siberia			non-therm	1.9	0.100	0	0	
Kolyma R.			non-therm	3.9	0.160	0	0	
			non-therm	5.3	0.160	0	0	
			thermokarst	1.7	0.020	0.320	0.280	
			thermokarst	3.5	0.080	0.020	0	
			thermokarst	5.0	0.080	0.020	0	
	2	Tube Dispenser						0.0083
		Lake	non-therm	2.1	0.060	0	0	
			non-therm	4.4	0.080	0.020	0	
			non-therm	5.8	0	0.020	0	
			thermokarst	1.1	0	0.700	0.180	
			thermokarst	7.2	0.200	0.060	0	
	3	Grass Lake						0
			nearshore	7.6	0.330	0	0	
			center	9.1	0.356	0.067	0	
			offshore	11.4	0.195	0.112	0	
	4	Meadow Lake						0
			nearshore	1.4	0.020	0.020	0	
			thermokarst	0.8	0	0	0	
			center	2.1	0.200	0.080	0	
			center	2.3	0.240	0	0	
	5	Airport Lake 1						
			offshore	1.7	0.080	0.080	0.080	
			center	1.8	0.027	0.080	0.027	
	6	Airport Lake 2						
			nearshore	0.6	0.180	0	0	
			offshore	1.0	0.360	0.180	0.020	
			center	2.0	0.060	0.120	0.020	
North	7	Olba Lake						0
Central			nearshore	0.5	0	0	0	
Sibera			offshore	1.0	0	0	0	
Lena R.			center	1.5	0	0	0	
	8	Big Black Blood						0
		Lake	nearshore	2.3	0	0	0	
			center	3.3	0	0	0	
	9	Little Black						0
		Blood Lake	nearshore	1.3	0.150	0	0	
			center	1.4	0.350	0.150	0	
	10	Simple Lake						0
			nearshore	0.9	0	0	0	
			center	0.5	0	0	0	
	11	Pope Lake						0
			nearshore	1.6	0	0	0	
			center	2.6	0	0	0	

Table 2-4. Cont.

North Slope Alaska	18	Toolik Lake						0
			nearshore	2.2	0	0	0	
			offshore	6.9	0	0	0	
			center	7.4	0	0	0	
	19	E1						0
			center	2.4	0.043	0.283	0	
			nearshore	3.2	0.087	0	0	
			center	4.8	1.286	0.821	0	
	20	E5						0
			nearshore	4.3	0.028	0	0	
			center	7.1	0	0	0	
			center	10.3	0	0	0	
	21	E6						0
			nearshore	1.5	0.174	0.217	0	
			center	2.4	0.143	0.371	0	
	22	NE1						0
			center	3.7	0.718	0.154	0	
			offshore	1.8	0	0	0	
			nearshore	1.5	0.139	0.167	0	
	23	N2						0
			offshore	8.8	0.040	0.140	0	
			center	9.4	0.020	0.040	0	
			center	9.5	0	0.020	0	
	24	N3						0
			center	3.5	0.474	0.316	0	
			center	3.4	0.462	0.538	0	
			center	5.2	0.571	0.071	0	

[†]Due to the rarity of hotspots, we walked the perimeters of lakes and made wide transects across lake surfaces to count the total number of hotspots per lake.
[ɤ]Locations of transects are given as along non-thermokarst margins (non-therm), along thermokarst margins, and in the 'center', 'nearshore' or 'offshore' when there were no obvious thermokarst margins.
[ᴾ]Water flowed onto the lake surface and froze following a heavy snowfall creating white ice, through which it is not possible to see bubble clusters in lake ice beneath.

Table 2-5. Methane emissions from point sources and hotspots on Siberian and Alaskan lakes, presented separately for winter (244 days) and summer (121 days). Fluxes were calculated as the product of point source density and mean flux per point source, and reported as the mean of n transects ± SD. In lakes where n = 2 transects, the error symbol represents half of the absolute difference between two values. We subtracted 34% from the winter point source emissions to account for oxidation and diffusion of CH_4 from bubble clusters in ice during winter. Point-source and hotspot emissions were studied in detail for different zones of the two intensive study lakes on yedoma in North Siberia (Shuchi Lake and Tube Dispenser Lake). These zones are the shallow water area within 15-m of thermokarst margin (15.8 ± 2.2% of lake area), shallow water area adjacent to non-thermokarst margins (4.4 ± 1.4% of lake area) and lake center (79.8 ± 0.8% of lake area). Point-source and hotspot distributions on n transects averaged across entire lake surfaces for all other Siberian and Alaskan lakes.

Lake No.	Site	Zone	Transects n	Point sources				Hotspots		
				mg CH_4 m^{-2} d^{-1}	g CH_4 m^{-2} winter^{-1}	g CH_4 m^{-2} summer^{-1}	g CH_4 m^{-2} yr^{-1}	g CH_4 m^{-2} winter^{-1}	g CH_4 m^{-2} summer^{-1}	g CH_4 m^{-2} yr^{-1}
1	Shuchi Lake									
		non-therm	1	2.5	0.40	0.30	0.70	0.79	0.33	1.12
		thermokarst	1	292.3	47.07	35.37	82.44			
		center	4	4.9 ± 1.0	0.79 ± .17	0.59 ± .13	1.38 ± .3			
2	Tube Dispenser Lake							4.30	1.76	6.06
		non-therm	1	1.5	0.24	0.18	0.42			
		thermokarst	1	281.5	45.33	34.06	79.39			
		center	3	14.3 ± 12.6	2.30 ± 2.02	1.73 ± 1.52	4.03 ± 1.90			
3	Grass Lake		3	23.8 ± 3.2	3.00 ± 1.5	2.25 ± 1.12	5.24 ± 2.62	0	0	0
4	Meadow Lake		4	7.6 ± 8.7	1.22 ± 1.41	0.92 ± 1.06	2.14 ± 2.46	0	0	0
5	Airport Lake 1		2	60.5 ± 32.0	9.75 ± 5.16	7.32 ± 3.88	17.07 ± 6.39			
6	Airport Lake 2		3	46.2 ± 13.1	5.63 ± 4.52	4.23 ± 3.39	9.86 ± 7.91			
7	Olba Lake		3	0	0	0	0	0	0	0
8	Big Black Blood Lake		2	0	0	0	0	0	0	0
9	Little Black Blood Lake		2	20.5 ± 23.7	3.29 ± 3.81	2.47 ± 2.86	5.77 ± 4.72	0	0	0
10	Simple Lake		2	0	0	0	0	0	0	0
11	Pope Lake		2	0	0	0	0	0	0	0
12	Rosie Creek Beaver Pond		3	519.8 ± 7.3	85.8 ± 3.72	64.5 ± 2.79	150.3 ± 6.51	9.07	3.71	12.78
13	Goldstream Valley Lake[t]							4.97	2.03	7.00
14	Goldstream Valley Pond[t]							7.50	3.07	10.57
15	Ballaine Lake[t]							0.80	0.33	1.13
16	Sheep Creek Pond[t]							8.08	3.31	11.38
17	Parks Hwy. Gravel Pit[t]							0.90	0.37	1.26
18	Toolik Lake		3	0	0	0	0	0	0	0
19	E1		3	95.1 ± 131.4	13.15 ± 15.42	9.88 ± 11.59	23.02 ± 27.01	0	0	0
20	E5		3	0	0.04 ± 0.06	0.03 ± 0.05	0.07 ± 0.11	0	0	0
21	E6		2	59.9 ± 20.2	9.64 ± 3.25	7.24 ± 2.44	16.88 ± 4.02	0	0	0
22	NE1		3	37.8 ± 29.8	4.41 ± 3.94	3.31 ± 2.96	7.72 ± 6.9	0	0	0
23	N2		3	5.9 ± 3.0	2.12 ± 2.04	1.59 ± 1.53	3.71 ± 3.58	0	0	0
24	N3		3	70.7 ± 60.8	11.45 ± 6.93	8.60 ± 5.20	20.05 ± 12.13	0	0	0

[t] Water flowed onto the lake surface and froze following a heavy snowfall creating white ice, through which it is not possible to see bubble clusters in lake ice beneath.

CHAPTER 3

Thaw lakes as a source of atmospheric CH_4 during the last deglaciation.

Abstract

Methane (CH_4) is a potent greenhouse gas that exhibits large concentration changes through time. Though specific sources of late-Quaternary atmospheric CH_4 are poorly quantified, records of CH_4 concentration in ice cores from Greenland and Antarctica suggest that an arctic/boreal source was responsible for >30% of the abrupt increases of global atmospheric methane concentration (AMC) during deglacial climate warming. Based on 1) high rates of CH_4 bubbling from modern thaw lakes in the Arctic, 2) high CH_4 production potentials of organic matter from Pleistocene-aged frozen sediments, and 3) estimates of the changing extent of these deposits as thaw lakes developed during deglaciation, we advance a new hypothesis: CH_4 bubbling from newly forming thaw lakes comprised 32-70% of the high-latitude increases in AMC and, in turn, contributed to the climate warming at the Pleistocene-Holocene boundary.

During deglaciation in northern high latitudes, increasing temperatures and moisture levels were accompanied by increases in atmospheric methane (CH_4) concentrations (AMC) from 400 ppb at the Last Glacial Maximum (LGM, 21 ka B.P.; all ages given in cal yr B.P.) to >700ppb in the early Holocene (Stuiver *et al.* 1995, Severinghaus and Brook 1999, Brook *et al.* 2000, Raynaud 2000). After the abrupt (decadal-scale) increases in temperature and precipitation recorded in the GISP2 and Taylor Dome ice cores, AMC rose more slowly over 100-300 years. This has been interpreted to reflect the lag in terrestrial ecosystem response to rapid climate change (Severinghaus and Brooks 1999, Brook *et al.* 2000). Values of the interpolar methane gradient (IPG), an indicator of the latitudinal distribution of CH_4 sources computed from the difference in methane concentration between Greenland and Antarctic ice cores, suggest that a new arctic/boreal source accounted for >30% (30 to 40 Tg CH_4 yr^{-1}) of the rapid rise of CH_4 emissions (83 to 99 Tg CH_4 yr^{-1}) during the early Holocene (11.5 – 9.5 ka B.P.) (Severinghaus and Brook 1999, Dallenbach 2000, Chappellaz *et al.* 1997, Brook *et al.* 2000). Based on the IPG, this new source was absent during the Bolling warming (14.8 to 13.5 ka B.P.) and the Younger Dryas (12.5 to 11.5 ka B.P.) periods. Changes in the AMC are attributed to new sources of CH_4 because changes in the atmospheric methane sink strength are thought to have been small (Martinerie *et al.* 1995).

Two hypotheses have been advanced to explain millennial-scale variations in AMC: 1) CH_4 emission from northern wetlands increased in response to climate warming [wetland hypothesis (Chappellaz *et al.* 1993, Smith *et al.* 2004)], and 2) catastrophic release of methane hydrates in sea floor sediments caused rapid increases in AMC ['clathrate gun hypothesis' (Kennett *et al.* 2003)]. The wetlands hypothesis is poorly supported because of incomplete data on the extent of paleo-wetlands and by a discrepancy between the relatively fast AMC increase and the slower [centuries to millennia (Kennett *et al.* 2003)] process of wetland expansion. However, recent evidence for peatland formation in the West Siberian Lowlands during the Early Holocene suggests that Siberian peatlands probably contributed to the rise in AMC (Smith *et al.* 2004). Limitations of the clathrate gun hypothesis include uncertainties concerning the

magnitude and time course of CH_4 release. In particular, there were no exceptionally high CH_4 peaks in ice records that should have resulted from rapid releases of CH_4 upon catastrophic clathrate destabilization (Chappellaz *et al.* 1997, Thorpe *et al.* 1996, Brook *et al.* 2000).

Here we propose a new hypothesis—that CH_4 ebullition (bubbling) from newly formed thaw lakes occurred extensively across large unglaciated regions in northern high latitudes, particularly Siberia, as climate became warmer and wetter. We provide three lines of evidence: 1) A reconstruction of late-Quaternary paleogeography documenting the areal extent over which this process likely occurred, and a synthesis of ^{14}C-dated basal thaw-lake sediments indicating that many thaw lakes were initiated 11.5-10.0 ka B.P., coinciding with the CH_4 rise; 2) Laboratory incubations showing that Pleistocene-aged frozen sediments support high rates of CH_4 production; and 3) Thaw lakes currently expanding in areas of frozen Pleistocene sediments have high ebullition rates of Pleistocene-aged CH_4. We integrate the information on CH_4 production rates from sediments, carbon loss from drained thaw lakes that refroze, flux rates from modern thaw lakes, and the areal extent of Pleistocene sediments subject to thaw-lake development to estimate post-Pleistocene CH_4 emissions by lake ebullition. We show that these emissions could have contributed 32-70% of the arctic/boreal contribution to the AMC increases recorded in ice cores.

During the late Quaternary, extensive loess deposits formed throughout unglaciated regions of North Siberia, Europe and North America (Fig. 3-1). In Northeast Siberia, the ice-complex deposits, 'yedoma', have remained frozen throughout the Holocene; they currently occupy an area of $>1 \times 10^6$ km^2 and in many regions are tens of meters deep (Zimov *et al.* 1997, Romanovskii *et al.* 2000). Yedoma has a high ice content (50% by volume) (Romanovskii *et al.* 2000, Czudek and Demek 1970) because ice-wedge growth paralleled loess accumulation. Yedoma also has a relatively high organic carbon content (2-3% C), derived from the herbaceous Pleistocene vegetation (Zimov *et al.* 1997). Similar loess deposits covered significant areas of the exposed continental margins along northern coastal areas when sea level was 120-m lower than

today ($0.8 \times 10^6 \text{km}^2$) (Tomidiaro 1980, Romanovsky 1993, our calculation- note 1). The New Siberian Islands (Fig. 3-1) are relicts of this landscape, and similar but less extensive landscapes occur in Alaska and northwest Canada. Yedoma-type landscapes that extended into West Siberia, Europe and South of the Laurentide Ice Sheet during the Pleistocene are now ice-free and difficult to estimate. To be conservative, our calculations are based on the best defined extent of yedoma, which is its current distribution in North Siberia and the previously exposed continental shelf ($1.8 \times 10^6 \text{km}^2$ total at 16 ka B.P.) (note 1).

When yedoma thaws, the ice wedges melt, and the resulting loss of soil volume (note 2) creates depressions, a process called thermokarst erosion. Ponding of water in depressions creates lakes, known as thermokarst or thaw lakes. Permafrost continues to thaw at the lake margins due to thermal erosion, causing lakes to enlarge and migrate across the landscape over time scales of decades to centuries. In the process, organic-rich thawed yedoma sediments are deposited in anaerobic lake bottoms, where they fuel the production of CH_4. Once initiated, these lakes can persist for thousands of years (Czudek and Demek 1970, Tomidiaro 1982, Romanovsky *et al.* 2000) (note 3). These contrast with the more thoroughly studied short-lived (centuries, sometimes millennia) thaw lakes on the Alaskan arctic coastal plain that developed on relatively shallow unconsolidated deposits (Hinkel *et al.* 2003). In certain areas of Siberia and northern Alaska where thaw lakes are prominent, as much as 50% of the landscape is covered with lake scars (Czudek and Demek 1970, Hinkel *et al.* 2003). In several major Siberian lowlands the yedoma ice complex has been nearly 100% degraded by lakes (Czudek and Demek 1970, Romanovsky *et al.* 2000).

Until recently, lakes were not recognized as a globally significant source of atmospheric CH_4. Measurements of methane bubbling in tundra and boreal lakes of Alaska and Siberia showed that CH_4 bubbling in areas of active thermokarst exceeded CH_4 emissions from non-thermokarst lakes by several orders of magnitude (Chapters 1 and 2). Thermokarst lakes currently cover a large proportion (8.5-30%) of yedoma region in Siberia and have average CH_4 emissions of 25-44 g CH_4 m^{-2} of lake yr^{-1} (note

4). Thermokarst margins have particularly high fluxes (128 g CH_4 m^{-2} of lake yr^{-1}).

Regional extrapolation of year-round continuous flux measurements to Siberian yedoma

lakes (~3.8 Tg CH_4 yr^{-1}) significantly increases current estimates of northern wetland

emissions (<6-40 Tg CH_4 yr^{-1}) (Chapters 1 and 2). Radiocarbon ages of CH_4 from

bubbling hotspots (39-44 ka B.P.) indicate that Pleistocene-aged organic matter from

yedoma fuels methane production and emission from thermokarst lakes (Chapter 1).

Laboratory incubations independently confirmed the high CH_4-production potential of

Pleistocene-aged sediments (Zimov *et al.* 1997).

Basal thaw-lake sediments can be identified by their sediment properties and

often contain organic detritus from the initial surface collapse. A compilation of

published and new basal radiocarbon ages (Table 3-1) indicates that permafrost thaw and

degradation of yedoma began relatively early in deglaciation and continued throughout

the Holocene (14 ka B.P. onwards) in Siberia, Alaska, and western Canada, with a cluster

of ages occurring at 11-10 ka B.P. Thaw lake basal ages of 22 to 17 ka B.P. in N. Yukon

Territory and Siberia suggest that some permafrost thawing occurred in the last glacial

stage. Romanovskii *et al.* (2000) and Kaplina and Lozhkin (1979) linked thermokarst

lake appearance with the onset of post-glacial warming in eastern Siberia at 14.5 ka B.P.

The Younger Dryas climatic reversal (12.9-11.6 ka B.P.) is not prominently expressed in

eastern Siberia (Anderson and Lozhkin 2002). Few basal lake sediments date to this

period, but it is likely that lakes persisted, although rates of thermokarst erosion and CH_4

production may have slowed compared with the preceding period (Romanovskii *et al.*

2000). The largest clustering of basal ages 11-10 ka B.P. (Fig. 3-2) suggests a period of

maximal thermokarst lake expansion coincident with high temperatures (Sher 1997) and

northward migration of treeline (MacDonald *et al* 2000). Rates of thaw lake initiation

appear to have slowed after this early burst of activity. Czudek and Demek (1970)

describe another period of extensive thaw lake formation on Siberian yedoma territory 4-

5 ka B.P., which is supported by another cluster of dates during this interval in our

compilation of lake basal ages (Fig. 3-2). Remote sensing analyses of a yedoma study

area in North Siberia (Chapter 1) and non-yedoma area of the West Siberia Lowlands

(Smith *et al.* 2005) suggest thaw lakes have expanded (12-14% increase in lake area) during recent decades in zones of continuous permafrost.

Given the extensive degradation of yedoma permafrost since the LGM (Fig. 3-1), the observed CH_4 emissions associated with yedoma degradation today (Chapter 1), and the clear expansion of thermokarst lakes with CH_4 emissions at the onset of the Holocene (Fig. 3-2), we propose that CH_4 bubbling from thermokarst lakes contributed substantially to the rapid increases in AMC during deglaciation.

To assess this hypothesis, we applied rates of CH_4 emissions measured in modern thermokarst lakes to the pattern of post-LGM lake development implied by basal dates and the potential areal extent of these lakes as a function of exposed continental shelf in time steps during deglaciation (note 5). In our scenario, lakes appeared as a relatively small fraction of the landscape on the exposed yedoma land surface at 13.1 ka B.P, and emitted 1.9 to 1.7 Tg CH_4 yr^{-1} until 12.5 ka B.P., the start of the Younger Dryas climate reversal (Fig. 3-3). At 11.6 ka B.P., in response to abrupt increases in temperature and precipitation (Severinghuas and Brook 1999), thaw lakes 'flared-up' (Fig. 3-2), and in our scenario occupied 10% of the exposed yedoma surface (note 6), emitting 15.8 Tg CH_4 yr^{-1}. Sea-level rise, reducing the area of land surface that could support lakes, explains the decline in regional lake emissions to 14.2 Tg CH_4 yr^{-1} by 10 ka B.P. in the scenario. We did not include CH_4 that would have been released from lakes inundated by sea-level rise (Romanovskii *et al.* 2000). From 10-8 ka B.P. lake area and emission rates would have fluctuated in response to climate, but ice core CH_4 records show a decline in total source emissions (Fig. 3-3). Our scenario depicts a reduction in flux rates from lakes as lakes matured and thermokarst activity slowed. A progressive cooling in Siberia from 7.5-6 ka B.P. led to a reduction or extinction of thaw lakes (Romanovskii *et al.* 2000). The actual extent of lake area decline and response of CH_4 flux are unknown, but, in our scenario, low emission rates similar to those of modern yedoma lakes that are not currently enlarging (Chapter 1) resulted in a decline of regional lake emissions. From 5-4 ka B.P., a period when thaw lake formation and expansion began again (Czudek and Demek 1970, Romanovskii *et al.* 2000), emissions would have increased in association

with actively expanding, mature thaw lakes. During this period, anthropogenic sources, such as rice cultivation (Ruddiman 2003), and extensive peatlands (Smith *et al.* 2004) also would have been major contributors of atmospheric CH_4. From 4 ka B.P. onwards our scenario depicts maturing thaw lakes accompanied by reduction in thermokarst activity, leading to a decline in regional CH_4 emissions that approached emission levels measured in modern yedoma lakes (Chapter 1), which were 3.8 Tg CH_4 yr^{-1}.

We provide a second, independent estimate of CH_4 emissions by calculating the carbon lost from yedoma beneath former thermokarst lakes (note 2). Thaw lakes that formed in the Holocene and subsequently drained and refroze had 30% less soil C (29.4 kg C m^{-3}) than yedoma that never thawed (42 kg C m^{-3}) (Zimov *et al. in review*). Based on the stoichiometry of CH_4 production from cellulose (Conrad *et al.* 2002), if half of the carbon was lost as CH_4 from anaerobic sediments (6.3 kg C m^{-3}, or 8.4 kg CH_4 m^{-3}) over the lifespan of lakes, which is estimated at 1,000 to 3,000 years (Tomidiaro 1982, note 3), the average flux would be 2.8 to 8.4 g CH_4 m^{-3} yr^{-1}. Applying this flux to lakes occupying 10% of the land surface area of the North Siberian ice complex during the early Holocene (note 6) yields annual emissions from lakes of 4.2 to 12.6 Tg CH_4. This estimate is conservative because it ignores Holocene organic detritus accumulating on lake bottoms (Hopkins and Kidd 1988) that would also produce CH_4. Pleistocene organic carbon fuels ~57% of the CH_4 emitted from modern yedoma thaw lakes in North Siberia (Chapter 1), suggesting that contributions of Holocene substrates for methanogenesis could also have been large in the early Holocene.

Finally, we used CH_4 production potentials (140 g CH_4 m^{-3} yr^{-1}) of thawed North Siberian yedoma in laboratory incubations to provide a third independent estimate of pond and lake contributions to the AMC rise at the onset of this interglacial period (note 8). Assuming that abrupt warming and wetting transformed the dry-unglaciated landscape (1.5x10^6 km^2) into a ponded surface regime dominated by low-center polygonal pools (assuming 10% of land surface), then anaerobic decomposition in the surface 1-m of the newly forming thaw bulbs might have produced CH_4 on the order of 21 Tg yr^{-1}. Although microbial oxidation in the shallow pools might have reduced total

CH_4 emissions during early stages of pond formation, our incubation-based calculation demonstrates that the CH_4 production potential of yedoma soils was high enough to contribute significantly to the abrupt rise in AMC.

Our three estimates (14.2-15.8 Tg CH_4 yr^{-1}, up to 12.6 Tg CH_4 yr^{-1}, and 21 Tg CH_4 yr^{-1}) of thaw lake contributions to the rise in AMC are similar to one another and to the ~30 to 40 Tg yr^{-1} boreal source constraint from the interpolar methane gradient recorded in ice cores (Dallenbach et al. 2000). This evidence suggests that formation and expansion of thaw lakes at the onset of Holocene warming led to a large new AMC source: bubble emissions from lakes. Our estimate of CH_4 derived from the Pleistocene-aged carbon reservoir can account for 32-70% of the AMC rise at a time when extensive mires had not yet appeared. If our estimate is approximately correct, other boreal sources, such as clathrate destabilization (Kennett et al. 2003) and/or the West Siberian peatlands (Smith et al. 2004), are also required to account for some inputs in AMC during deglaciation.

About 425 Gt C remain preserved in the yedoma ice complex in North Siberia (Zimov 2005). If the yedoma territory with its high-ice-content permafrost warms more rapidly in the future, as projected (Sazonova et al. 2004), ebullition from thaw lakes could again become a powerful positive feedback to high-latitude warming, as it appears to have been during deglacial climate warming at the onset of the Holocene. Expansion of yedoma thaw lakes during the era of satellite observations in North Siberia suggests that this positive feedback (Chapter 1) is already underway. This important source of atmospheric CH_4 has not been previously considered in climate-change projections.

Notes:

1.   All calculations are based on the derived area (1.8×10^6 km^2) of the North Siberian yedoma ice complex at the LGM that includes the yedoma still present today and the exposed continental margins calculated from the modern 120-m

isobath. To estimate the area of the exposed shelf, we used bathymetric contours to represent the coastline at time steps from 16-8 ka B.P., guided by the late-Quaternary sea-level estimates of Bard *et al* (1990). We postulated that yedoma occupied most of the exposed shelf east of170-110 °E, as this region is adjacent to the yedoma-dominated Yana-Indigirka-Kolyma lowland. Although thermokarst likely produced lakes on some shelf deposits eastwards in the Chukchi, Bering, and Beaufort Seas, we omitted these areas from our calculation in order to keep the estimate conservative. Areas lying within successive contours were approximated using a 1.0 ° (lat) x 0.5° (long) gridded map (Supplementary Online Material), with grid areas calculated trigonometrically; this allowed us to estimate the reduction in exposed shelf during deglacial sea-level rise (Fig. 3-3). At 16 k cal yr. B.P. the estimated shelf area was ~0.8×10^6 km^2, at 8 k cal yr B.P. it was ~65×10^3 km^2. The current extent of continental yedoma is 1×10^6 km^2 (Zimov *et al*. 1997). Our measurement of yedoma area at 16 ka B.P. is similar to estimates based on less rigorous map analysis (Zimov *et al. in review*).

2. To determine the total volume of yedoma degraded by lakes in our mass balance calculation we used the following soil thickness parameters based on published values from the literature: Without ice, loess consolidated to an average thickness of 12.5 m in areas of active loess deposition in North Siberia and 5-m in the extremely ice-rich area of the exposed East Siberian continental shelf (Tomidiaro, 1980, Romanovsky 1993, Zimov *et al. in review*).

3. We sampled basal and surface age dates of lake deposits in cross sections of paleolakes cut by the Kolyma River to estimate longevities of lakes that formed in the North Siberia yedoma ice complex. Five lakes persisted 867 years, 1051 years, 1114 years, 2215 years, and 2937 years. In addition we cored four modern thermokarst lakes near Cherskii, Siberia, and determined radiocarbon ages on lake sediments at >2 m of 941 ± 11 (Airport Lake; 3,165 ± 46 (Grass Lake); 3,305 ± 35 (Tube Dispenser Lake); and 4,476 ± 34 yr B.P. (Shuchi Lake), suggesting that the lakes have persisted for at least this long. We are not certain that our cores

reached the base of the lake sediments. The basal sediments of a lake cored in loess terrain in northern Alaska date to >11,000 yr B.P.; a second lake was >5,000 yr B.P. (base not reached).

4. We quantified CH_4 bubbling from modern thermokarst lakes on the North Siberian yedoma ice complex using daily measurements of CH_4 bubbles collected continuously in underwater bubble traps (n= 11-25 traps per lake) for one year, and by measuring the distributions of bubble clusters trapped in lake ice in winter (Chapters 1 and 2). This technique accounted for patchiness of bubbling, and improved whole lake and regional estimates of bubbling from lakes (25 g CH_4 m^{-2} yr^{-1}; Zimov et al. 1997). This is a conservative estimate because measurements were made in mature thermokarst lakes with moderate thermokarst erosion, marked by banks covered with vegetation and minimal exposure of mud and ground ice (Chapter 1). Other North Siberian thaw lakes have more active thermokarst erosion with unvegetated banks, exposed mud and ice wedges, and higher whole-lake emissions (44 g CH_4 m^{-2} yr^{-1}) (Chapter 1).

5. Actual thaw lake area and emission rates during the early Holocene are unknown. We provide a plausible scenario (Fig. 3-3) based on assumptions of the time course of total yedoma area (note 1), lake area (note 3), and CH_4 fluxes measurements of modern yedoma lakes, which varied depending on the level of thermokarst activity (note 4). Given the paucity of basal ages prior to 13.1 ka B.P., lakes appeared on 1% (note 6) of the exposed Siberian shelf and continental yedoma ($\sim1.45\times10^6$ km^2, measured) at 13.1 ka, emitting CH_4 at the rate measured along thaw margins in modern yedoma lakes (128 g CH_4 m^{-2} yr^{-1}) because active thermokarst would have dominated when the landscape was transformed by climate warming and wetting into a ponded surface in lowland environments, and eventually to a landscape covered by deep thaw lakes as thermokarst lake formation progressed (note 7). At the start of the cold Younger Dryas (12.5 ka. B.P.), we reduced fluxes from lakes to that of modern lakes that are not expanding (25 g CH_4 m^{-2} of lake yr^{-1}). At 11.6 ka, a flare-up (widespread appearance) of

lakes (based on time course of basal ages of lakes; Fig. 3-2) occupying 10% of the exposed land surface (i.e., the current lake area of yedoma; note 6) would have resulted in high fluxes (128 g CH_4 m^{-2} of lake yr^{-1}) until 10 ka B.P. In the scenario, lake area remained at 10% throughout the rest of the Holocene, but lake emissions fluctuated in response to climate events and declined over time as lakes matured, as thermokarst erosion slowed, and as organic matter sources beneath lakes became depleted. By 3 ka B.P. whole-lake fluxes approached those of modern lakes (25-44 g CH_4 m^{-2} yr^{-1}) (Chapter 1), yielding regional emissions of 3.7 Tg CH_4 yr^{-1} during recent millennia.

6. To be conservative, we assume lakes occupied 1% of the exposed shelf and continent yedoma when they first appeared at 13.1 k cal yr. B.P. On average, we assumed lakes covered 10% of the territory throughout the Holocene, following their flare-up at 11.5 k cal yr. B.P. (Fig. 3-2) The 1-10% lake-area parameter is conservative because in some lowland areas lakes are thought to have occupied up to 35% during the Holocene (Romanovsky 2000) and current lake coverage is 8.5-30% (Mostakhov et al. 1970, Zimov et al. 1997, Chapter 1). Our model calculations are also conservative because they do not include lakes that might have formed in other loess regions south of the Laurentide Ice Sheet and in West Siberia and Europe, where there is little evidence from which to estimate the formation and distribution of thaw lakes.

7. The ice complex of the North Siberian landscape was readily transformed to a wet surface with shallow ponds when precipitation increased at times of rapid climate change. During cold, arid periods, growing ice wedges elevated the soil surface, creating low-centered polygons, which turned into shallow ponds with methane bubbling as the permafrost began to thaw. Over time, ponds either filled in with wetland vegetation becoming bogs, drained altogether, or grew in size by melting into deeper permafrost horizons to form large thermokarst lakes.

8. To evaluate the initial (maximum) CH_4 production by yedoma we incubated 24 samples of soils collected frozen from permafrost wall exposures in three

different areas of the Kolyma lowlands [Duvanny Yar (n=15) and Zeleni Mys (n=3) (forest-tundra) and Mys Chukochy (n=6) (Arctic coast) under anaerobic conditions at 4° C. Samples of ~1 kg wet mass were placed in 1.5 L polycarbonate bottles and filled with water (~300ml). Additionally, ~1g of lake sediment was placed in each bottle as innoculum. Each bottle was squeezed to remove all air, and closed immediately. After 544 days, when the bottles stopped swelling, we released the gas, measuring its volume and CH_4 concentration by gas chromatography using a flame ionization detector (FID Shimadzu 6A). Average CH_4 production was 140 g CH_4 m^{-3} yr^{-1}, a rate several times higher than the average flux for hundreds of years owing to the high content of labile organic matter in freshly thawed yedoma.

References:

Anderson, P.M. and A.V. Lozhkin, *Late Quaternary vegetation and climate of Siberia and the Russian Far East* (NOAA and the Russian Academy of Sciences, Magadan, 2002).

Bard, E., B. Hamelin, R.G. Fairbanks, Nature **346**, 456 (1990).

Brook, E.J., T. Sowers, and J. Orchardo, Science **273**, 1091 (1996).

Brook, E. J., S. Harder, J. Severinghaus, E. J. Steig, and C. M. Sucher, Global *Biogeochem. Cycles* **14**, 559 (2000).

Conrad, R., M. Klose, and P. Clause, *Chemosphere* **47**, 797 (2002).

Chappellaz, T., T. Blunier, D. Raynaud, J. M. Barnola, J. Schwander, B. Stauffert, Nature **366**, 443 (1993).

Chappellaz T. *et al.*, J. *Geophys. Res.* **102**, 15,987 (1997).

Czudek, T. and J. Demek. *Quat. Res.* **1**, 103 (1970).

Dallenbach, A., T. Blunier, J. Fluckiger, and B. Stauffer, *Geophys. Res. Letters* **27**, 1005 (2000).

Hinkel, K. M., W. R. Eisner, J. G. Bockheim, F. E. Nelson, K. M. Peterson, and X. Dai, *Arctic, Antarctic and Alpine Research* **35**, 291 (2003).

Hopkins, D. M., J. G. Kidd, *Thaw lake sediments and sedimentary environments.* (Permafrost 5th International Conference, Trondheim, Tapir Publishers, 1988).

Kaplina, T. N., A. I. Lozhkin., *Izv. AN SSSR, Ser. Geol.* **2**, 69 (1979).

Kennett, J. P., K. G. Cannariato, I. L. Hendy, R. J. Behl. *Methane Hydrates in Quaternary Climate Change* (American Geophysical Union, Washington DC, 2003).

MacDonald, G. *et al.*, *Quat. Res.* 53, 302 (2000).

Martinerie, P., G. P. Brasseur, and C. Granier, *J. Geophys. Res.* **100**, 14,291 (1995).

Mostakhov, S. E., *Mezhdunarodnaia conferentsiia po merzlotovedeniiu, Podzemnye vody kriolitosfery* (ed. Tolstikhin, N. I., Iakustkoe Knizhnoe Izdeatel'stvo, Iakutsk, Russia, 1973).

Raynaud, D., J. M. Barnola, J. Chappellaz, T. Blunier, A. Indermuhle, and B. Stauffer, *Quat. Sci. Reviews* **19**, 9 (2000).

Romanovsky, N. N., *Osnovy Kriogeneza Litosfery* (Izdatelstvo Moscow State University, Moscow, 1993).

Romanovskii, N. N., H.-W. Hubbertten, A. V. Gavrilov, V. E. Tumskoy, G. S. Tipenko, M. N. Grigoriev, and Ch. Siergert, *Perm. Periglac. Process.* **11**, 137 (2000).

Ruddiman, W. *Climatic Change* **61**, 261 (2003).

Sazonova, T. S., V. E. Romanovsky, J. E. Walsh, D. O. Sergueev, *J. Geophys. Res.* 109, doi:10.1029/2003JD003680 (2004).

Severinghaus, J. P and E. J. Brook. *Science* **286**, 930 (1999).

Sher, A, *Cryosphere of Earth* **1**, 3 (1997).

Smith, L. C., G. M. MacDonald, A. A. Velichko, D. W. Beilman, O. K. Borisova, K. E. Frey, K. V. Kremenetski, Y. Sheng, *Science* **303**, 353 (2004).

Smith, L. C., Y. Sheng, G. M. MacDonald, & L. D. Hinzman, *Science* **308**, 1429 (2005).

Stuiver M, P. M. Grootes, T. F. Braziunas, *Quat. Res.* **44**, 341 (1995)

Thorpe, R. B., K. S. Law, S. Bekki, and J. A. Pyle, *J. Geophys. Res.* **101**, 28,672 (1996).

Tomidiaro, S.V., *Lessovo-ledovaya formatsia Vostochnoi Sibiri v pozdnem pliestotsene I golotsene* (Nauka, Moscow, 1980)

Tomirdiaro, S.V., *In: Paleoecology of Beringia* (Ed. by D.M. Hopkins, J.V. Matthews Jr., C.E. Schweger and S.B. Young, pp. 29-37, Academic Press, New York 1982).

Zimov, S. A., Y. V. Voropaev, I. P. Semiletov, S. P. Davidov, S. F. Prosiannikov, F. S. Chapin III, M. C. Chapin, S. Trumbore, and S. Tyler, *Science* **277**, 800 (1997).

Zimov, S. A., E. A. G. Schuur, and F. S. Chapin, *In review.* Mammoth Steppe-Tundra: A globally significant carbon sink in glacial times. *Science.*
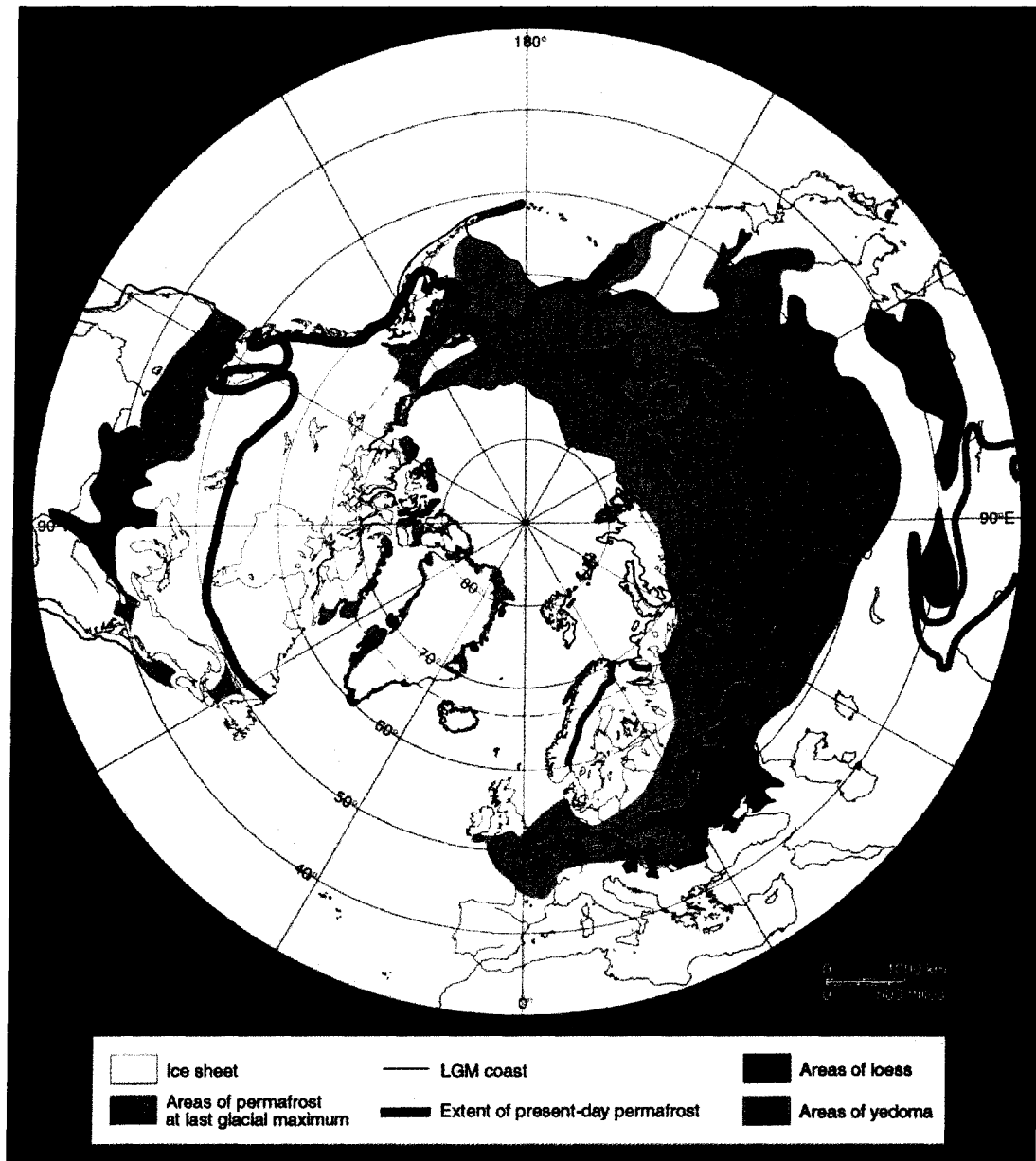
Figure 3-1. Current regions of loess and yedoma mapped in relation to the modern and LGM distribution of permafrost. Modern and LGM coasts are shown, the latter approximated from the modern 120 m isobath (note 1). The modern and LGM limits of permafrost in central Asia are likely inaccurate, but in other regions, which are more critical to this study, we consider the information sources to be fairly reliable (Supplementary Online Material). The map indicates that considerable areas of loess would have been frozen at the LGM and subsequently thawed, and yedoma would have extended northward on the exposed Siberian shelf.
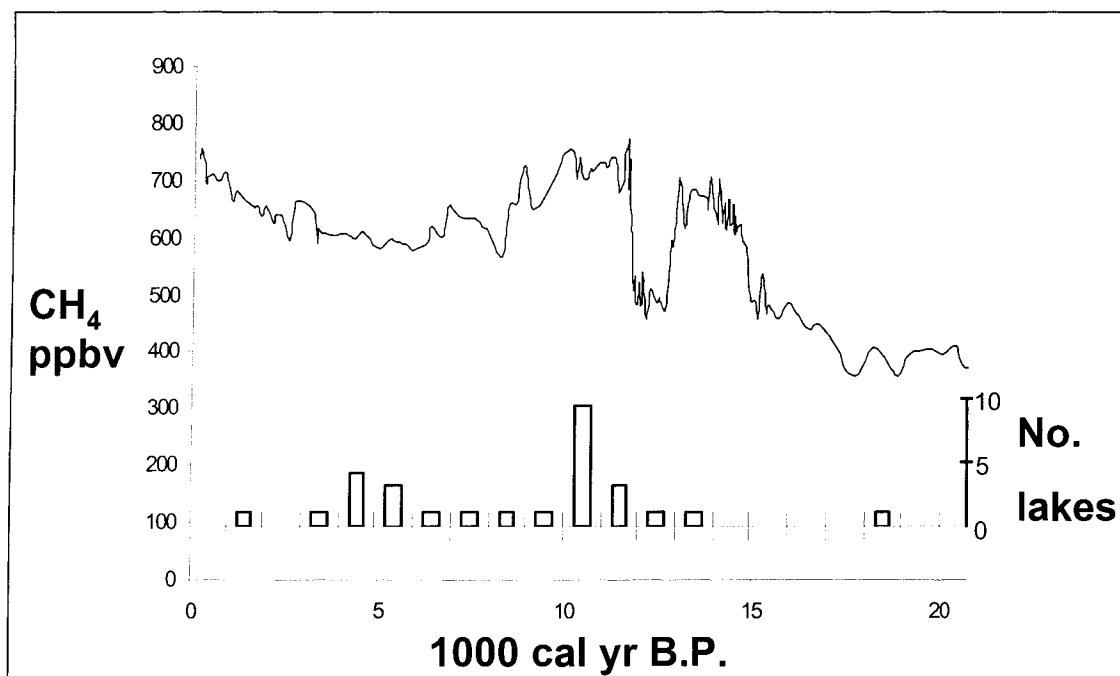
Figure 3-2. Thaw lake development during deglaciation as a source of atmospheric methane. The frequency of basal ages of Siberian yedoma lakes (y-axis, number of documented lakes per 1000 calendar years; from Table 3-1) plotted against the methane concentration in the GISP2 ice core (Brook *et al.* 1996) shows a cluster of lakes initiated between 11,500-10,000 cal yr B.P following abrupt warming.
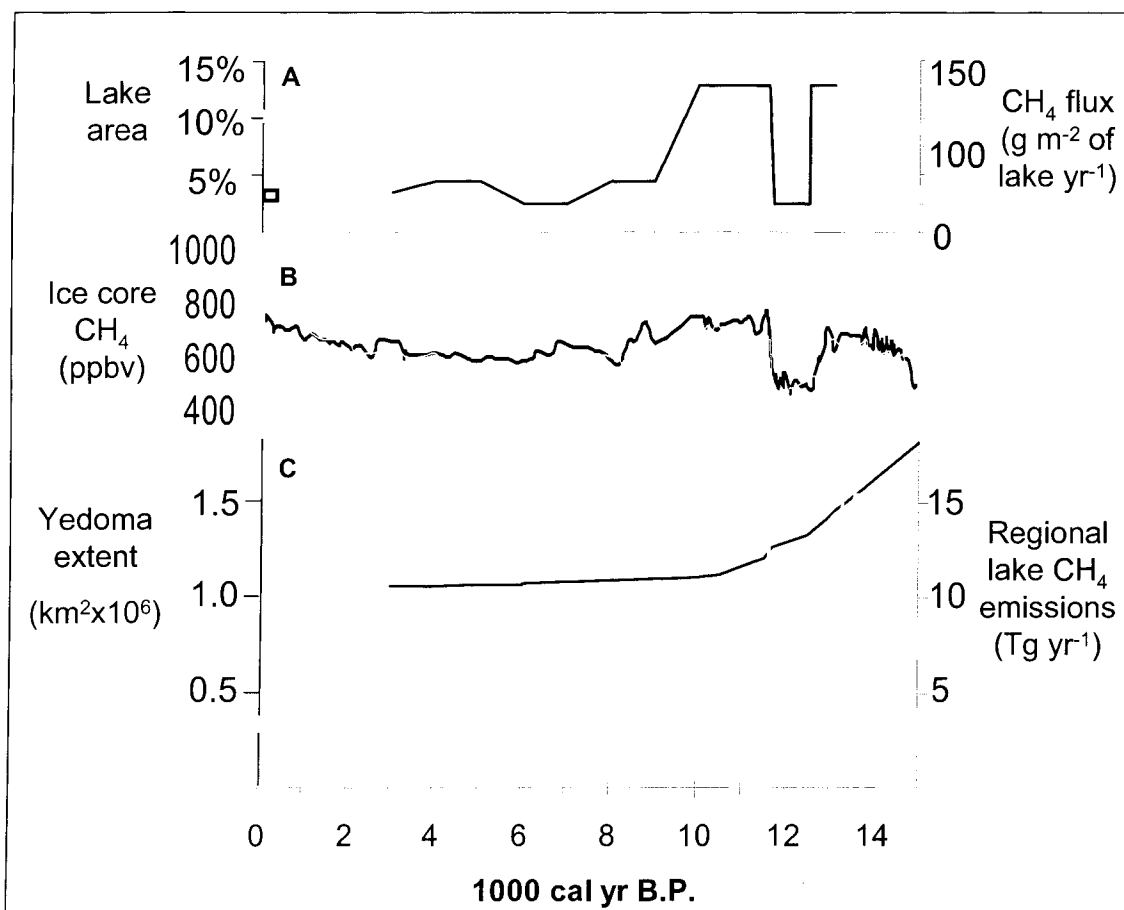
Figure 3-3. Estimates of CH₄ emissions from Siberian thaw lakes during deglaciation. Methane emissions from yedoma thaw lakes modeled from assumptions of paleolake area and ebullition flux in response to climate change (note 5) are shown as solid squares connected by the pink dotted line (C). The empty square shows the emission estimate from modern yedoma lakes (Chapter 1). The potential extent of yedoma on which lakes could have formed decreased as sea level rose from 16 to 8 cal ka B.P. (solid line, C) (note 1). The model suggests that a 'flare up' yedoma thaw lakes could have released as much as 15.8 Tg CH₄ yr⁻¹ following abrupt warming at the end of the Younger Dryas at 11.5 ka B.P., which would have been a significant contribution to the new boreal CH₄ source (~30 to 40 Tg yr⁻¹) observed in ice core records (B) from Greenland (GISP2, solid black line) and Antarctica (Taylor Dome, solid grey line) (Brook et al. 1996). The fractions of exposed yedoma surface covered in lakes and CH₄ flux rates from lakes for times steps in the scenario are shown in (A).

Table 3-1. Basal ages of thaw lakes (^{14}C age and calendar years) in Siberia (yedoma) and East Beringia (yedoma and non-yedoma) compiled from the literature and from our age measurements of macrofossils exposed at the base of lake cross sections along cut banks of the Kolyma River in Northeast Siberia. Error terms are standard deviation. References are available as Supplementary Online Material.

Region	Location	Reference	^{14}C age (BP)	±	CAL YR	±
Northeast	Kolyma Lowland	This study	290	25	368	54
Siberia	Kolyma Lowland	This study	2,815	20	2,918	28
(yedoma)	Kolyma Lowland	This study	2,885	20	3,018	36
	Kolyma Lowland	This study	3,300	20	3,523	32
	Kolyma Lowland	This study	4,445	25	5,111	116
	Kolyma Lowland	This study	5,970	35	6,182	49
	Kolyma Lowland	This study	7,320	25	8,119	49
	Kolyma Lowland	This study	8,085	35	9,036	33
	Kolyma MLC[†]	This study	2,885	20	3,018	36
	Kolyma MLC[†]	This study	2,890	20	3,164	45
	Kolyma MLC[†]	This study	3,070	20	3,305	33
	Kolyma MLC[†]	This study	4,000	25	4,476	34
	Kolyma MLC[†]	This study	4,445	25	5,111	116
	Siberia	Tomidiaro 1982	8,670	±	9,600	
	NW Chukotka	Anderson and Lozhkin 2002	8,400	40	9,422	52
	S Chukotka	Anderson and Lozhkin 2002	8,450	490	9,464	626
	S Chukotka	Anderson and Lozhkin 2002	9,300	200	10,580	285
	S Chukotka	Anderson and Lozhkin 2002	14,045	180	17,460	218
	Coast, Yana-Kolyma Lowland	Anderson and Lozhkin 2002	3,885	60	4,310	88
	Coast, Yana-Kolyma Lowland	Anderson and Lozhkin 2002	8,450	160	9,411	184
	Coast, Yana-Kolyma Lowland	Anderson and Lozhkin 2002	9,315	50	10,514	71
	Coast, Yana-Kolyma Lowland	Anderson and Lozhkin 2002	9,910	50	11,330	65
	Coast, Yana-Kolyma Lowland	Anderson and Lozhkin 2002	10,730	230	12,573	321
	Yana-Kolyma Lowland	Anderson and Lozhkin 2002	8,620	200	9,721	265
	Yana-Kolyma Lowland	Anderson and Lozhkin 2002	8,650	650	9,766	834
	Kolyma Lowland	Anderson and Lozhkin 2002	3,955	80	4,402	116
	Kolyma Lowland	Anderson and Lozhkin 2002	6,300	60	7,233	59
	Kolyma Lowland	Anderson and Lozhkin 2002	8,370	100	9,344	121
	Kolyma Lowland	Anderson and Lozhkin 2002	8,450	100	9,423	96
	Kolyma Lowland	Anderson and Lozhkin 2002	9,200	150	10,427	170
East Beringia	Mackenzie-Beaufort	Rampton 1974	22,400	240	26,943	536
(yedoma)	Mackenzie-Beaufort	Rampton 1974	17,860	240	21,328	508
	Sabine Point Yukon Territories	Harry 1988	11,000	100	12,923	117
	Sabine Point Yukon Territories	Harry 1988	14,400	180	17,730	260
	Tuktoyaktuk Coastlands	Murton 2001	9,620	100	10,964	163
	Mayo, Yukon Territory	Burn and Smith 1990	8,560	130		
	Mayo, Yukon Territory	Burn and Smith 1990	8,520	120		
	Mayo, Yukon Territory	Burn and Smith 1990	3,890	80		
	Mayo, Yukon Territory	Burn and Smith 1990	2,340	100		

Table 3-1. *Cont.*

East Beringia	Coastal Plain	Brigham-Grette and Edwards 1990			7,200-11,000
(not yedoma)	Coastal Plain	Hinkel et al. 2003	80	90	
	Coastal Plain	Hinkel et al. 2003	230	50	
	Coastal Plain	Hinkel et al. 2003	>modern		
	Coastal Plain	Hinkel et al. 2003	1,150	50	
	Coastal Plain	Hinkel et al. 2003	4,770	50	
	Coastal Plain	Hinkel et al. 2003	3,660	60	
	Coastal Plain	Hinkel et al. 2003	2,260	60	
	Coastal Plain	Hinkel et al. 2003	>modern		
	Coastal Plain	Hinkel et al. 2003	590	50	
	Coastal Plain	Hinkel et al. 2003	>modern		
	Coastal Plain	Hinkel et al. 2003	80	40	
	Coastal Plain	Hinkel et al. 2003	4,520	50	
	Coastal Plain	Hinkel et al. 2003	5,370	100	
	Coastal Plain	Hinkel et al. 2003	4,090	40	
	Coastal Plain	Hinkel et al. 2003	2,970	40	
	Coastal Plain	Hinkel et al. 2003	4,970	160	
	Coastal Plain	Hinkel et al. 2003	>modern		
	Coastal Plain	Hinkel et al. 2003	3,760	40	
	Coastal Plain	Hinkel et al. 2003	3,230	190	
	Coastal Plain	Hinkel et al. 2003	1,420	40	
	Coastal Plain	Hinkel et al. 2003	2,075	40	
	Coastal Plain	Ritchie 1983	~10,000		
	Coastal Plain	Hopkins and Kidd 1988	~10,000		
	Coastal Plain	Rampton 1988	~10,000		
	Coastal Plain	Cote and Burn 2002	~10,000		

[†] Macrofossils dated at the bottom of cores extracted from modern yedoma lakes. This is not necessarily the base of the lake, but indicates a minimum bound of how long the lake has been in existence.
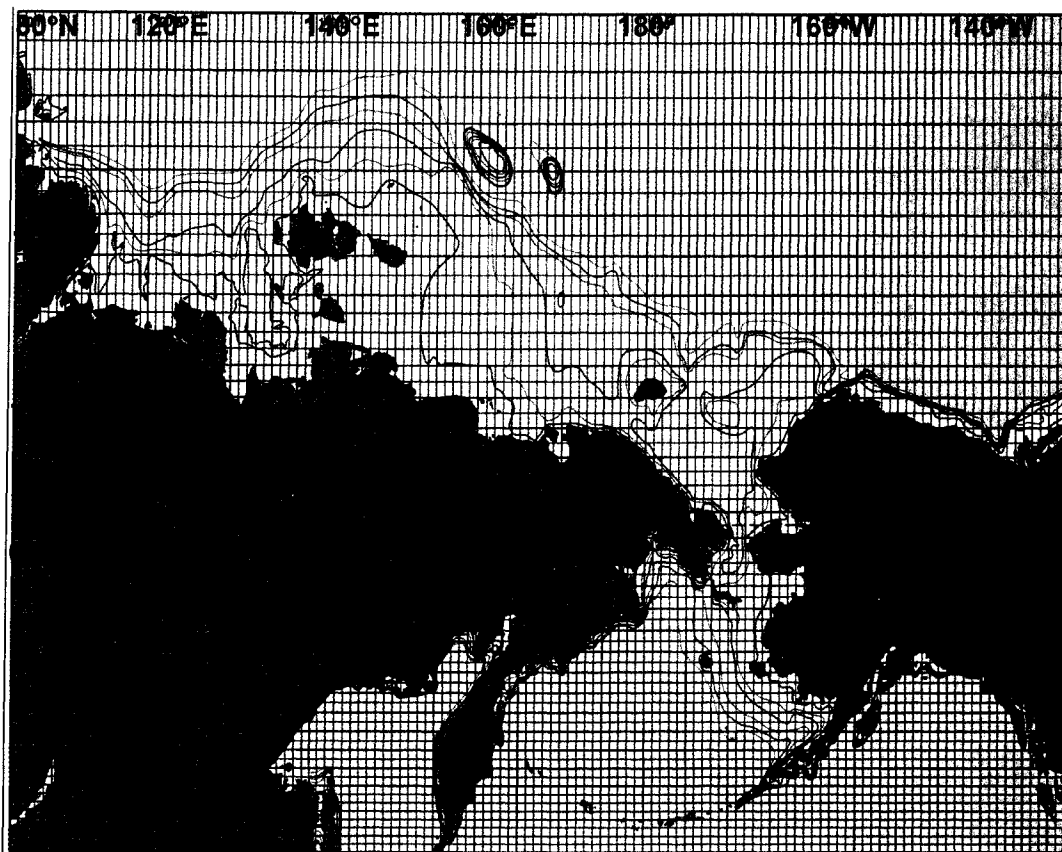
Supplementary Figure 3-1. Gridded map of exposed continental shelf showing bathymetric contours. Contours were used to represent the coastline at time steps from 16-8 ka B.P., guided by the late-Quaternary sea-level estimates of Bard *et al* (1990) to calculate the potential aerial extent of yedoma on which thaw likes could have formed during deglaciation.

Supplementary Material 3-1. Sources of information for the permafrost map in Fig. 3-1.

1. The base map for modern circumpolar permafrost distribution was derived from the UNEP-GRID Arendal information center, accessed on line, December 2004, at http://vitalgraphics.grida.no/arctic/go/showgraphic/graphicid/23658/chapterid/43

2. The current distribution of *yedoma* in Siberia was taken from the map published in Russian (Barachkov).

3. Loess cover in Europe and Asia was derived from maps in Dawson (1992, p. 166 and p. 169), based on information from Flint (1971).

4. Loess cover, inferred LGM permafrost limits, and the extent of the Wisconsin ice sheet in North America (excluding Alaska) was from Dawson (p. 118), after Washburn (1979) and Péwé (1983).

5. LGM permafrost extent in Europe was from Dawson, p. 123, after Washburn (1979).

6. LGM permafrost extent in Asia was from Dawson, p. 112, after Baulin and Danilova (1984).

7. LGM ice extent in Eurasia from Siegert (2001), p. 132, after Svendsen *et al.* (1999) and Siegert *et al* (1999).

8. Cordilleran and Alaskan LGM Ice from Dawson p. 57, after Flint (1971).

9. Alaskan loess distribution from Muhs *et al.* (2004).

10. Yedoma on the coast of NW Canada was from Burn (2002).

Supplementary Material 3-2. References supporting basal ages of lakes in Table 3-1 and the map of loess and permafrost distribution since the Last Glacial Maximum in Figure 3-1.

Baulin, V.V., N.S. Danilova. Dynamics of late-Quaternary permafrost in Siberia. (In A.A. Velichko (Ed.) *Late Quaternary Environments of the Soviet Union*, pp 69-78. London. Longman. 1984).

Burn, C. R., M. W. Smith, *Perm. Periglac. Process*. **1**: 161 (1990).

Burn, C. R., *Can. J. Earth Sci*. **39**: 1281 (2002).

Cote, M. M., C. R. Burn, *Perm. Periglac. Process* **13**, 61 (2002).

Edwards, M. E, J. Brigham-Grette, Climatic change and thaw lake formation in Alaska, In Proceedings from AMQUA, University of Waterloo, June 4-6: 17 (1990).

Dawson, A. G. *Ice Age Earth* (Routledge, London, 1992).

Flint, R. F. *Glacial and Quaternary Geology* (Wiley, New York, 1971).

Harry, D. G., French, H. M. and Pollard, W. H., Can. J. Earth Sci. **25**, 1846 (1988)

Hopkins, D. M. *Aspects of the paleogeography of Beringia during the late Pleistocene.* (In: "Paleoecology of Beringia", Eds. D. M. Hopkins, J. V. Matthews, C. E. Schweger, S. B. Young, Academic Press, New York, 1982).

Muhs, D. R., J. P. McGeehin, J. Beann, and E. Fishera, *Quat. Res*. **61**, 265 (2004).

Murton, J. B., *Global and Planetary Change* **28**, 175 (2001).

Péwé, T.L. The periglacial environment in North America during Wisconsin time. (In S. C. Porter, Ed. *Late Quaternary Environments of the United States, Volume I: The Late Pleistocene*, pp 157-189. London. Longman, 1983).

Rampton, V.N. *The influence of ground ice and thermokarst upon the geomorphology of the Mackenzie-Beaufort region.* (In: Research in Polar and Alpine Geomorphology, Eds. B. D. Fahey, R.D. Thompson), pp. 43-59. Proceedings of the Third Guelph Symposium on Geomorphology, Geo-Abstracts, Norwich, 1974).

Rampton, V. N. *Quaternary Geology of the Tuktoyaktuk Coastlands, Northwest Territories.* (Geological Survey of Canada, Memoir 423, 1988).

Ritchie, J. C., L. C. Cwynar, R. W. Spear, Nature **305**, 126 (1983).

Siegert, M. J. Ice *Sheets and Late Quaternary Environmental Change.* (Chichester, 2001).

Seigert, M. J., J. A. Dowdeswell, M. Melles. *Quat. Res.* **52**, 273 (1999).

Svendsen, J.I., V.I. Astakov, D.Y. Bolshiyanov, J.A. Dowdeswell, V. Gataullin, C. Hjort, H. Hubberten, E. Larsen, J. Mangerud, P. Möller, M. Saarnisto, and M.J. Siegert. *Boreas* **28**, 234 (1999).

Washburn, A.L., *Geocryology,* (Arnold, London, 1979).

CHAPTER 4

Methane production and bubble emissions from arctic lakes: Isotopic implications for source pathways and ages†

Abstract

Methane (CH_4) production and emission from a variety of arctic and boreal lakes in Siberia and Alaska were characterized using stable isotopes (^{13}C and D) and radiocarbon (^{14}C) analyses. We classified ebullition (bubbling) into three categories based on concentrations of major gases and isotopic composition: 1) background (low flux sampled from randomly placed bubble traps), 2) point sources (moderate flux from fixed points, which produced stacks of bubbles in lake ice during winter), and 3) hotspots (high flux from fixed bubbling points sufficient to maintain open holes in lake ice throughout winter). The occurrence of point sources and hotspots had a strong association with thermokarst (thaw) erosion because thawing permafrost along lake margins releases organic matter into anaerobic lake bottoms, enhancing methanogenesis. As CH_4 ebullition rate increased, we observed an increase in the concentration and radiocarbon age of CH_4, depletion of $^{13}C_{CH4}$ and δD_{CH4}, and enrichment of $^{13}C_{CO2}$. Methanogenic pathways also differed among the bubble sources. Background bubbles exhibited roughly equal contributions from CO_2 reduction and acetate fermentation pathways, whereas CH_4 from point sources and hotspots was produced predominately *via* CO_2 reduction. We combined maps of bubble-source distributions in lakes with long-term, continuous flux measurements and isotopic composition of bubbles to provide annual whole-lake and regional CH_4 isofluxes (flux-weighted isotope signatures). Bubbling from lakes has yet to be included in established biogeochemical and inverse models of CH_4 sources. In contrast to typical values used in inverse models of atmospheric CH_4 for northern wetland sources ($\delta^{13}C_{CH4}$ = -58‰, ^{14}C age modern), we show that this large, new source of high-latitude CH_4 from lakes is isotopically distinct

$(\delta^{13}C_{CH4} = -70‰, \delta D_{CH4} -428‰, {}^{14}C$ age 16,500 yrs in North Siberian thaw lakes). This study reports an atmospheric source term previously uncharacterized in terms of strength and isotopic composition.

Introduction

The atmospheric concentration of methane (CH_4), a greenhouse gas responsible for ~20% of the direct radiative forcing from all long-lived green-house gases (IPCC, 2001), has been rising during recent decades (Dlugokencky et al., 1998). The increase in global atmospheric CH_4 results from an imbalance between sources and sinks. While new large sources are still being identified (Keppler et al., 2006), several known sources are poorly quantified due to difficulties in assessing high variability in emission rates (Fung et al., 1991; IPCC, 2001, Mikaloff Fletcher, 2004). Wetlands play a major role in global atmospheric CH_4 dynamics, representing ~10-30% (50-150 Tg CH_4 yr^{-1}) of known sources (Mathews and Fung, 1989; Fung et al., 1991), with northern wetlands contributing substantially to the total (<6 -40 Tg CH_4 yr^{-1}) (Roulet et al. 1994; Reeburgh et al. 1998; Worthy et al., 2000; IPCC 2001). This wide range in wetland emission estimates results primarily from uncertainties in the areal extent of wetlands and from the large spatial and temporal variability of short-term local CH_4 emission measurements (Reeburgh et al., 1998; Mikaloff Fletcher et al., 2004a,b).

Local CH_4 emissions from most lakes and wetlands can vary by several orders of magnitude on the scale of a few meters or over several hours. Heterogeneity in ebullition (bubbling) is a major contributor to this variability, and the spatial and temporal patchiness of ebullition challenges efforts to quantify this mode of emission. As a result, many studies of CH_4 emissions from lakes and wetlands report only emissions via molecular diffusion and aquatic plant transport (Kling et al., 1992; Chapter 2). Studies that aimed to assess ebullition with greater accuracy showed that in lakes ebullition is a dominant, yet inadequately quantified mode of CH_4 emission

leading to a systematic underestimation from lakes globally (Casper *et al.*, 2000; Bastviken 2004; Chapters 1 and 2).

Model estimates of northern wetland emissions have yet to include ebullition from lakes (Zhaung *et al.*, 2004; Mikaloff Fletcher *et al.*, 2004a,b). Recent studies that quantified the patchiness of ebullition showed that adding emission estimates of CH_4 from North Siberian yedoma (Pleistocene-aged organic-rich loess permafrost) lakes alone increases current estimates of total northern wetland emission by 10-63% (Chapter 1). Thermokarst (thaw) erosion resulting from permafrost degradation along lake margins drives CH_4 emissions from North Siberian lakes by depositing thawed Pleistocene-aged organic matter into anaerobic lake bottoms. Expansion of thermokarst lakes in continuous permafrost regions of Siberia during recent decades constitutes a positive feedback to climate warming (Smith *et al.*, 2005; Chapter 1). Global circulation models predict the greatest warming at high latitudes (IPCC, 2001) with significant permafrost degradation during the 21st century (Lawrence and Slater, 2005), raising concerns about the increase of CH_4 emissions from northern lakes and wetlands to future climate change.

Isotopic signatures of atmospheric CH_4 and its sources can be used in isotope mass balance models to define the magnitudes of different sources and sinks (Hein *et al.*, 1997; Houweling *et al.* 1999; Mikaloff Fletcher *et al.* 2004a,b). For instance, inverse modeling of high-resolution spatiotemporal atmospheric CH_4 concentrations and its ^{13}C isotope ratio determined the relative contributions of northern wetland emissions and biomass burning in the tropics (Lowe *et al.*, 1994; Mikaloff Fletcher *et al.*, 2004a,b). Similarly, the ^{14}C isotope ratio of CH_4 has been used to estimate the contribution of fossil carbon (^{14}C-free) attributed to natural gas seepage and coal mining (Lowe *et al.*, 1994; Wahlen *et al.*, 1989). Stable hydrogen isotopes can be combined with stable carbon isotopes and used to distinguish sources of CH_4 including bacterial formation, thermogenic formation and biomass burning (Whiticar *et al.* 1986), as well as to determine the effect of microbial oxidation in lake and wetland environments (Coleman *et al.*, 1981; Happell *et al.*, 1994). In aquatic environments, variations in the $\delta^{13}C$ of CH_4

and CO_2 can reveal the importance of different biochemical pathways of methanogenesis including CO_2 reduction and acetate fermentation (Whiticar *et al.*, 1986; Chasar *et al.*, 2000a,b; Chanton *et al.*, 2005), while differences in δD_{CH4} are primarily linked to δD of the source water (Sugimoto and Wada, 1995; Chanton et al, 2006). However, careful bottom-up studies of processes driving CH_4 emissions and isotope signatures are necessary to help define source estimates in models, as has been demonstrated by the recent discovery of a potentially large new source of atmospheric CH_4: emissions from terrestrial plants under aerobic conditions (Keppler *et al.* 2006).

The purpose of this study is to characterize CH_4 production and emission from a variety of arctic and boreal lakes in Siberia and Alaska and to use ^{13}C, D and ^{14}C isotopic ratios to help elucidate the role of lake ebullition in global atmospheric CH_4 dynamics. Specific objectives include (1) identifying CH_4 production pathways in Siberian thaw lakes, (2) characterizing the isotopic composition of different CH_4 bubble sources with particular attention to ebullition hotspots associated with thermokarst erosion, (3) combining detailed flux measurements of ebullition patchiness in Siberian lakes with isotopic signatures of bubbles to show that whole-lake and regional CH_4 isofluxes (flux-weighted average isotopic signatures) differ from previous estimates based on methods that ignored point-source and hotspot ebullition, and (4) surveying Alaskan lakes to determine whether results from Siberia could be extrapolated more broadly.

Methods

Location of study lakes

Most isotopic studies in northern lakes have been conducted in North America and Europe (Whalen, 1989, Quay *et al.* 1988, Martens *et al.* 1992), with little attention to Russian lakes (Nakagawa *et al.* 2002), which comprise ~70% of arctic lakes *(Robert Holmes, in prep.)*. We studied a variety of lakes in the boreal forest and tundra of Siberia

and Alaska situated on permafrost substrates of various types including: 1) Pleistocene-aged, organic-rich, silty ice-complex "yedoma" near Cherskii in northeast Siberia (68°45' N, 161°20' E) (Zimov *et al.*, 1997; Zimov, 2005), 2) Holocene organic soil on top of organic-rich, Pleistocene-aged retransported silt near Fairbanks in Interior Alaska (64°49' N, 147°52' E), and 3) organic-poor glacial deposits near Toolik Lake in northern Alaska (68°28'N, 149°34' W) (Table 4-1, Fig. 4-1). Siberian and Interior Alaskan lakes that we studied were formed by thermokarst, i.e., ground subsidence resulting from the thawing of ground ice (Davis 2001). Thermokarst along lake margins releases terrestrial organic matter from thawing permafrost into lake bottoms. Study lakes in northern Alaska were kettle lakes that formed when ice blocks deposited in glacial drift and outwash plains of late Pleistocene glaciation thawed (Hamilton 2003). These kettle lakes had organic-poor sediments and lacked thermokarst margins.

Sample collection and CH_4 flux measurements

We collected bubbles from Siberian lakes during the 2001 and 2003-04 field campaigns and from Alaskan lakes in 2005. In 2001 we stirred surface sediments with a long pole in a variety of tundra and boreal thermokarst lakes and collected bubbles through a hand-held funnel into glass serum vials which were sealed with butyl rubber stoppers. Samples were stored in a refrigeror at 4°C in the dark. There were no flux values measured in conjunction with bubble samples collected by stirring lake sediments. In 2003-04, all bubble samples were collected from natural ebullition events into floating traps without disturbing sediments. The majority of 2003-04 samples was collected from bubble traps (~1-m diameter) permanently placed under the surface of lakes and beneath winter ice.

Bubble traps were either freely floating to capture the average 'background' ebullition, or they were fixed in place over discrete points of bubbling, called 'point sources' and 'hotspots'. Freely floating bubble traps covered <0.03% of lake area.

Summed together point sources and hotspots covered 0.05% of the lake surface throughout the lake center (80% of total lake area), 0.9% of the lake surface along shallow, non-thermokarst margins (4% of total lake area), and 23% of lake area along margins with active thermokarst erosion (16% of total lake area) (Chapter 1), yielding an average area-weighted coverage of 3.7% for point sources and hotspots. Given the low probability of overlap between background bubble trap placement over point sources or hotspots (0.03%*3.7% = 0.001%), we assumed that ebullition captured in background traps was independent of point-source and hotspot ebullition. In addition, there was no overlap in the values of fluxes between background and point source/hot spots. Together, point-source and hotspot ebullition accounted for ~70% of annual emissions (Chapter 1).

In general, bubble samples were collected into serum vials within 2 hours of release from the lake bottom and are labeled as 'fresh' hereafter. Samples collected from background traps accumulated slowly and therefore sat up to a few days in the traps before collection.

In the spring of 2003, we collected bubbles trapped in lake ice by carefully tapping into frozen gas pockets from the ice surface and capturing trapped gases into serum vials as the bubbles streamed up from inside the ice. These samples, which represented wintertime point-source bubbling, are referred to as ice koshkas hereafter (Fig. 4-2). In autumn 2005, ice koshka samples were collected from tundra lakes in northern Alaska, and fresh bubbling from hotspots was captured from two boreal thaw lakes near Fairbanks.

The dynamics of annual emissions for background, point source and hotspot bubbling from Siberian and Alaskan lakes were presented in detail in Chapters 1 and 2. To show the relationship between CH_4 isotope values and bubbling rates in this study, we used the 10-day average ebullition flux surrounding each sample date for the bubbles collected for isotopic analyses in our regressions. To calculate the whole-lake and regional isofluxes, we applied seasonal rates of ebullition to the range of isotope values determined for methane bubbling from these arctic lakes.

Lake water samples were collected from the lake bottom with a Van Dorne bottle from June 14, 2003 through August 11, 2003 just above the sediment surface for determination of δD_{H2O}. Water was poured into glass vials avoiding air bubbles. Vials were capped and stored at 4°C in the dark until analysis in August 2005.

Gas concentration and isotope procedures

Concentrations of CO_2, O_2, N_2 and CH_4 in lake bubble samples were measured by gas chromatography using a thermal conductivity detector (TCD Shimadzu 8A). We measured $^{13}C/^{12}C$ of CH_4 by direct syringe injection using gas chromatography/mass spectrometry (Hewlet-Packard 5890 Series II GC coupled to a Finnigan MAT Delta S). A subsample of gas was combusted to CO_2, purified, and catalytically reduced to graphite (Stuiver and Polach, 1977), and the $^{14}C/^{12}C$ isotopic ratios were measured by accelerator mass spectrometry at the Keck Carbon Cycle AMS Facility at the University of California, Irvine. We determined D/H of CH_4 on a Finnigan MT delta +XP using a Trace GC with a poroplot column and the reduction column set at 1450°C. Lake water samples were analyzed for δD-H_2O by the zinc reduction method (Coleman et al. 1982).

Stable isotope compositions are expressed in δ (‰) = 10^3 (($R_{sample}/R_{standard}$)-1), where R is $^{13}C/^{12}C$ or D/H and standards refer to the Vienna Peedee belemnite (VPDB) and Vienna standard mean ocean water (VSMOW), respectively. The analytical errors of the stable isotopic analyses are ± 0.1 ‰ $\delta^{13}C$ and ± 0.1 ‰ δD. We express radiocarbon data as percent modern carbon, pmC (%) = (($^{14}C/^{12}C$)$_{sample}$/($^{14}C/^{12}C$)$_{standard}$) x 100, which is the percentage of $^{14}C/^{12}C$ ratio normalized to $\delta^{13}C$ = -25‰ and decay corrected relative to that of an oxalic standard in 1950 (Stuiver and Polach, 1977).

Methane production pathway

Methanogenesis is an ancient process that relies on relatively simple substrates (carbon monoxide, carbon dioxide, acetate (CH_3COOH), formate, methylamine, methanol, and dimethylsufide) produced by other metabolic processes (Conrad, 1989). The two main pathways of bacterial methane production in anaerobic sediments are carbon dioxide reduction and acetate fermentation:

$$CO_2 + 4H_2 \rightarrow CH_4 + H_2O \qquad \text{(CO}_2 \text{ reduction)}$$

$$CH_3COOH \rightarrow CH_4 + CO_2 \qquad \text{(acetate fermentation)}$$

We used two approaches to estimate the relative proportion of the two major pathways of methanogenesis (CO_2 reduction and acetate fermentation) (Whiticar *et al.*, 1986; Hornibrook *et al.* 2000). The carbon isotopic fractionation (α_C) between CH_4 and CO_2 is defined:

$$\alpha_c = \frac{(\delta^{13}C_{CO2} + 10^3)}{(\delta^{13}C_{CH4} + 10^3)} \qquad (1)$$

We also used a simple mixing model to estimate the relative proportion of the acetate fermentation and CO_2 reduction pathways (ref):

$$(f_{CO2} + f_{ace})(\delta^{13}C_{CH4}) = f_{CO2}(\delta^{13}CH_{4(CO2)}) + f_{ace}(\delta^{13}CH_{4(ace)}) \qquad (2)$$

where

f_{CO2} = the proportion of CH_4 produced by CO_2 fermentation

f_{ace} = the proportion of CH_4 produced by acetate fermentation

$\delta^{13}C_{CH4}$ = isotope ratio of measured CH_4, the mixture of both pathways

$\delta^{13}CH_{4(CO2)}$ = the isotope ratio of CH_4 produced by the CO_2 reduction pathway, and calculated using the isotope fractionation factor α_{CO2} of 1.079, which was determined in a study where CO_2 reduction was the sole pathway of CH_4 in natural wetlands (Lansdowne, 1992) and used in other studies to determine the pathway of CH_4 production in lake sediments (Nakagawa *et al.* 2002). $\delta^{13}CH_{4(CO2)}$ is calculated:

$$\delta^{13}CH_{4(CO2)} = \frac{\delta^{13}CO_2 + 10^3}{\alpha_{CO2}} - 10^3 \tag{3}$$

$\delta^{13}CH_{4(ace)}$ = the isotope ratio of CH_4 produced by the acetate fermentation pathway, and assumed to be -43‰ when acetate fermentation occurs in sediments with a sufficient supply of fresh organic material (Case 1), and - 27‰ when sediments are extremely depleted in fresh organic material (Case 2) (Nakagawa *et al.* 2002).

Results

Concentration and stable isotopes of gases in bubbles

Concentrations of the major gas constituents of bubbles varied by lake and bubble source (Table 4-2). A negative linear relationship between the concentration of CH_4 and N_2 in bubbles (Fig. 4-3) indicates that CH_4 is the gas predominately produced in sediments (Nakagawa *et al.* 2002). Bubble N_2 content may also be a sensitive indicator of ebullition rates because there is a strong inverse relationship between the N_2 concentrations in bubbles and the rate of ebullition (Chanton *et al.* 1989, Fig. 4-4). Nitrogen is present in pore waters when sediments

are deposited and, when depleted, it is resupplied by diffusion from overlying waters. High rates of bubbling strip N_2 from the pore waters, depleting the N_2 pool in sediments (Kipphut and Martens, 1982; Chanton et al. 1989). Bubbles collected from hotspots and point sources had the highest CH_4/N_2 ratios, while bubbles released from shallow surface sediments (background, stirred), where lower ebullition rates were observed, had lower CH_4/N_2 ratios. Gas from ice koshkas had lower CH_4/N_2 ratio than gas collected from fresh point source and hotspot bubbling streams, probably due to diffusion during long periods (weeks to months) when gases were trapped in lake ice at the surface of lakes.

Oxygen (O_2) concentration in gas bubbles ranged from 1.2 to 30% (Table 4-2), and was negatively related to CH_4 concentration ($[O_2] = -0.08[CH_4]+10.0$, $F=29.05_{146}$ $p<0.0001$). Some of this O_2 is likely an artifact of sampling oxygen-free bubbles in an oxygen-rich atmosphere. The background artifact O_2 values are those in the range of 1-2% as reported for stirred bubbles (Table 1). Bubbles from small, stagnant Siberian ponds had the lowest O_2 concentrations, possibly because wind-driven currents that operate on larger lakes were less apt to supply O_2 to lake bottoms in small ponds. Higher O_2 (11% and 30%) corresponding to very low CH_4 (5.2% and 2.7%) in two individual outlier bubble samples (individual data points not shown) collected from the non-thermokarst margin of Shuchi Lake and from Grass Lake are best explained by the active photosynthesis of productive macrophytes, benthic algae and moss, which characterize those specific sites. Higher O_2 concentrations in ice koshkas (4.4-12.8%) relative to fresh point-source bubbling (3.9 ± 1.4%) suggests O_2 diffusion into bubbles during entrapment in lake ice. The concentration of CO_2 was low (0-2%) in samples collected from fresh bubbling in Siberia and Alaska in 2003-05.

Stable isotopes in bubbles and lake water

The stable isotope signatures ($\delta^{13}C_{CO2}$, $\delta^{13}C_{CH4}$, δD_{CH4}) of bubbles and δD of Siberian and Alaskan lake water varied by lake and bubble source (Table 4-2). Siberian point sources and hotspot bubbles had less enriched $\delta^{13}C_{CH4}$ values (-79.5 ± 2.3‰, n=34) than bubbles collected from background traps or by stirring surface sediments (-61.6 ± 5.7‰, n=60) (t-value = 21.4$_{85}$ p<0.0001; Fig. 4-5), the latter being similar to typical values reported in the literature for northern lakes and wetlands [-64‰ Quay et al., 1988; -61‰ Martens et al., 1992; -58‰ Lansdowne et al., 1992)], including Siberian alasses (typical round landforms in permafrost terrain, consisting of a shallow lakes surrounded by wetlands; -61.1 ± 4.4‰, Nakagawa et al. 2002). Point-source CH_4 trapped in lake ice as ice koshkas (-69.3 ± 4.3‰, n=4) during the entire winter was more enriched in $\delta^{13}C_{CH4}$ than fresh point-source bubbles (-79.7 ± 3.0‰, n=13) (t-value = 5.43$_{15}$, p<0.0001). The $\delta^{13}C_{CO2}$ of point sources (-12.2 ± 7.5‰, n=12) and hotspots (-14.2 ± 4.1‰, n=27) was enriched relative to background bubbles (-18.7 ± 4.1‰, n=27), which was slightly more enriched than the $\delta^{13}C$ of photosynthetic organic C fixed from atmospheric CO_2 (C_3 plants). As CH_4 is produced with its ^{13}C depleted signature, the remaining organic matter and CO_2 derived from it becomes enriched due to mass balance (Nakagawa et al. 2002). The observed $\delta^{13}C_{CO2}$ variation is consistent with N_2 data and may be explained by variations in CH_4 production rate.

The CO_2 reduction pathway has a larger isotopic fractionation (α_C = 1.055-1.090) than acetate fermentation (α_C = 1.040-1.055) (Whiticar et al. 1986). In Siberian lakes and ponds, the CO_2 reduction pathway appears more prevalent in hotspot (α_C= 1.071 ± 0.006, n=21) and point-source bubbling (α_C= 1.073 ± 0.011, n=12), while the lower α_C of background bubbling (α_C= 1.048 ± 0.005, n=20) suggests acetate fermentation pathway is relatively more important in the sediment zone where these bubbles were produced (Fig. 4-5).

Using both $\delta^{13}CH_{4(ace)}$ values as two extreme cases, we calculated the amount of CH_4 produced from Siberian lake sediments as two cases: Case 1 (fermentation occurs

with labile organic substrates) and Case 2 (fermentation occurs with recalcitrant organic substrates) (Table 4-4). This yielded a range of likely proportions of CO_2 reduction and acetate fermentation pathways under different sediment organic matter conditions. The CO_2 reduction pathway dominated CH_4 production for point-source and hotspot bubbling, while background ebullition appeared to have a higher contribution from the acetate fermentation pathway (Fig. 4-8). These results agreed with the distribution of methane production pathways determined by the carbon isotopic fractionation (α_C) of CH_4 from Table 4-4.

Stable hydrogen isotopic composition in methane and water

Using the mean precipitation $\delta^{18}O$ inputs of -21‰ to the Kolyma River Basin (Welp et al. 2005) with the Local Meteorological Water Line ($\delta D = 7.0 * \delta^{18}O - 11.7$, $R^2 = 0.99$), we estimated the mean δD of precipitation in our study sites in the Kolyma River Basin to be -158‰. This value is similar to the weighted average of monthly data of δD in rainwater (-156‰) from 1997-1999 in Yakutsk (Nakagawa et al. 2002), to the southeast of our Siberian study region, and to the mean annual δD of all precipitation for interior Yukon Territory, Canada (-160‰; Anderson et al. 2005), which is again similar to the region of our boreal study lakes (Bruce Finney, pers. comm.). The semi-arid climates of the interior boreal regions of Alaska and Siberia promote lake water evaporation, resulting in a slight deuterium enrichment of water in some lakes [note that 2 of the values you cite are not enriched] (-154.0 ± 2.6‰ at 1-m, -158.7 ± 2.1‰ at 10-m, Shuchi Lake (Table 4-2)). The δD of lake water in other boreal lakes was -128.8 ± 0.7‰ (Smith Lake, interior Alaska, Chanton et al. 2006), -159 ± 2‰ (interior Yukon Lake Jellybean, Anderson et al. 2005), and -136 to -117 ‰ (East Siberian alasses, Nakagawa et al., 2002).

The δD in CH_4, which ranged widely in this study (-375‰ to -480‰), differed by study region and bubble type (Fig. 4-6). The most striking result was that the δD in CH_4 from thaw lakes in Siberia and Alaska, particularly for hotspots, was strongly δD

depleted relative to either lake water or precipitation in both Siberia and Alaska. One possible explanation is that CH_4 was produced in an environment with a very different water source than modern lake water, that is, frozen water from glacial periods (discussed below). The mean δD of Siberian CH_4 in bubbles stirred from shallow sediments in Fig. 4-6 was -433 ± 23‰, n=27. The δD of Siberian CH_4 of point sources and hotspots (-452 ± 8‰, n=40) was δD depleted compared to Alaskan hotspots (-411 ± 5‰, n=7) (t-value = 12.7$_{45}$, p<0.0001). Ice koshkas were enriched by 46‰ in Siberia and 23‰ in Alaska relative to the fresh point-source counterparts in both regions (Siberia -406 ± 13‰, n=4; Alaska -388 ± 5‰, n=22). Gases from trapped in lake ice would have been subject to diffusion and oxidation, processes that lead to isotopic enrichment of CH_4. The observed enrichment of both $\delta^{13}C$ and δD of CH_4 in ice koshkas relative to hotspots and fresh point sources indicates diffusion of CH_4 out of ice or CH_4 oxidation in bubbles trapped in ice (Fig. 4-6).

Radiocarbon of bubbles

Despite the wide range in ^{14}C age dates of CH_4 from Siberia and Alaska (Table 4-3), the large number of samples depleted in ^{14}C indicate the influence of ancient organic matter substrates in methanogenesis that gives rise to ebullition. These results differ from most ^{14}C data reported from other lakes and wetlands whose modern ^{14}C age indicates that CH_4 was produced from fresh organic matter that was recently fixed by photosynthesis (Whalen et al. 1989, Quay et al. 1991, Chanton et al., 1995; Chasar et al., 2000b; Nakagawa et al. 2002). Only Zimov et al. 1997 reported ^{14}C ages of CH_4 as old as 27,000 years, and these were measured from two of the same lakes used in this study. The ^{14}C age of CH_4 was positively correlated with the magnitude of CH_4 ebullition flux (Fig. 4-7). High-emission point sources and hotspots of CH_4 bubbling were older (11,355 to 42,900 yrs), while the younger ages of low-emission background bubbling (1,345 to 8,845 yrs) and stirred bubbles from surface sediments (>modern to 3,695 yrs) suggested

younger organic substrates fueling methanogenesis. Similar ancient radiocarbon ages of CH_4 bubbles (14,760 to 26,020 years, Table 4-3) from thaw lakes in interior Alaska suggest that this pattern is not unique to Siberia and may occur broadly.

Discussion

The stable isotope signature of CH_4 bubbles is influenced by multiple factors, including the degree of CH_4 oxidation, the isotopic composition of CH_4 precursors, and biochemical pathways of methanogenesis (Whiticar *et al.* 1986, Alperin *et al.* 1992, Sugimoto and Wada, 1993).

Methane oxidation and diffusion

Biological CH_4 oxidation results in the enrichment of the remaining δD_{CH4} and $\delta^{13}C_{CH4}$ with no additional fractionation to the reported $^{14}C_{CH4}$ values because they are corrected by any potential fractionation with the ^{13}C values. In the literature, a positive correlation between δD_{CH4} and $\delta^{13}C_{CH4}$ with a slope of 5-13.5 suggests the occurrence of aerobic oxidation (Coleman *et al.*, 1981; Happell *et al.* 1994), while some evidence suggests that the slope may be somewhat greater in anaerobic oxidation (Alperin *et al.*, 1988). We concluded that biological oxidation did not cause the variation observed in the stable isotope signature of CH_4 bubbles because we did not find a correlation between δD_{CH4} and $\delta^{13}C_{CH4}$ in bubbles collected freshly from sediments (Fig. 4-6). The lower slope (2.5, $R^2 = 0.6$) for fresh Siberian point sources plotted with ice-koshka CH_4 suggests that some isotopic enrichment occurred in CH_4 trapped in ice during the long winter months. This enrichment is likely due to the more rapid diffusion of the lighter isotopes of C and D from the ice than due to oxidation. Diffusion should affect both isotopes similarly since their mass difference is 1 unit in both cases (Mason and Marrero

1970) while oxidation has a greater effect on δD which would have resulted in a greater slope (Fig 4-6). We conclude that the isotopic enrichment in ice-koshkas was due to gas diffusion through the ice bubble enclosures rather than oxidation since concentrations in ice bubbles shifted in the direction of atmospheric composition during long winter entrapment (fresh point sources CH_4 80%, CO_2 0.9%, N_2 16.6% and O_2 3.9%; ice koshkas CH_4 54%, CO_2 0.3%, N_2 43.7%, O_2 4.4%).

Methane production pathways

Both the isotopic fractionation and the mixing models showed that the CO_2 reduction pathway dominated in hotspot and point-source bubbling, whereas the acetate fermentation and CO_2 reduction pathways both contributed to the background bubbling. Variations in availability of labile organic matter was likely an important contributing factor. In other lakes, high availability of labile organic substrates in lake and wetland sediments, particularly in sediments containing live plants, can support acetate production (Duddleston et al., 2002), leading to methanogenesis by acetate fermentation, whereas environments with less labile organic substrates, or the absence of particular compounds exuded by living plants, can be dominated by the CO_2-reduction pathway (Nakagawa et al., 2002). Sediment cores from our Siberian thaw lakes showed organic-rich layers of lacustrine peat in the shallow sediment zone (0.25 to >3-m thick, up to 51% organic C; Walter et al. in prep.), whereas deeper sediments were primarily mineral material derived from thermokarst erosion of the surrounding yedoma, with occasional peat layers. During the lifespan of lakes the organic content of yedoma in anaerobic lake sediments is decreased by ~30% from ~2% (42 kg C m^{-3}) to 29 kg C m^{-3} as CH_4 is produced (Zimov et al., 1997), suggesting a loss of labile C. It is therefore likely that organic matter availability influences the CH_4 production pathway in Siberian lakes, as in other studies, with acetate fermentation occurring in the organic-rich shallow peat layers and CO_2-

reduction in the relatively more organic-poor (by volume) deeper Pleistocene-loess horizons.

Other potentially contributing factors to the pattern of methanogenic pathways include temperature and iron (Fe) content in the deep and shallow sediments. Temperature decreases with depth in the North Siberian thaw lakes, and the CO_2-reduction pathway is favored at low temperatures (Nozhevnikova *et al.* 1994). We also observed high Fe III contents in the Pleistocene loess, and anaerobic utilization of acetate by Fe-reducing bacteria may also prevent CH_4 production by acetate fermentation in those deep horizons. Oligotrophic (nutrient-poor) conditions in wetlands have also been shown to favor the CO_2 reduction pathway, but this seems unlikely in the loess horizons of Siberian lakes, where yedoma nitrogen and phosphorus concentrations are exceptionally high (Dutta *et al. in prep*).

Depletion of carbon sources in methanogenesis

The availability of methanogenic precursors in natural ecosystems can fluctuate widely in time and space in response to dynamic environmental conditions. Some studies of lake and wetland CH_4 production show a positive linear relationship between the concentration of CH_4 and the $\delta^{13}C$ of CO_2, in which CH_4 production corresponds to the enrichment of $\delta^{13}C_{CO2}$ as the lighter CO_2 is preferentially reduced, leaving behind ^{13}C-enriched organic matter that produces CO_2 (Nakagawa *et al.* 2002). This relationship has been particularly evident in ecosystems where the CO_2-reduction pathway dominates over acetate fermentation (Wassmann *et al.* 1992, Waldron *et al.* 1999). We observed a weak linear relationship between CH_4 concentration and the $\delta^{13}C_{CO2}$ only in bubbles from ebullition hotspots (Fig. 4-9, $R^2 = 0.43$), the bubble source where both high CH_4 emission rates and low N_2 concentration indicated high CH_4 production rates (Chanton *et al.* 1989). We found no significant relationship for point-source bubbles or bubbles

collected in background traps (Fig. 4-9). Thus CH_4 production led to detectable ^{13}C enrichment only in zones of exceptionally high CH_4 production.

Nakagawa *et al.* (2002) suggested that oldest $^{14}C_{CH4}$ ages that they measured (up to 93.1 pmC, or 500 years B.P.), which came from deeper lakes, indicate the contribution of older CH_4 that was produced from recalcitrant material. Although our slight $\delta^{13}C_{CO2}$ enrichment in hotspots is consistent with this pattern, the exceedingly high rates of hotspot ebullition (up to >30 L CH_4 spot^{-1} d^{-1} ; Chapter 1) with exceptionally old radiocarbon ages ($^{14}CH_4$ 0.5 to 1.2 pmC, or 39,000 to 43,000 years B.P.) suggests that a large amount of CH_4 is produced at depth in our Siberian lakes, and that the organic matter source in Pleistocene loess may be labile, rather than recalcitrant. Laboratory incubation experiments of CH_4 produced from Pleistocene organic matter extracted from undisturbed yedoma permafrost confirmed the high quality of organic substrates contained in the deep lake horizons of North Siberia (Zimov *et al.* 1997; Chapter 3).

Radiocarbon-depleted peat accumulates over long time periods in anaerobic lake and wetland environments due to slow decomposition of poor-quality organic matter, particularly under cold conditions (Smith *et al.*, 2005). Due to the recalcitrant nature of peat, CH_4 emitted from peatlands largely results from decomposition of fresh, labile terrestrial substrates such as root exudates that were fixed during recent photosynthesis (King *et al.*, 2002). Thermokarst lakes represent a different situation because the labile properties of ^{14}C-depleted organic matter can be preserved for centuries to millennia because organic matter is frozen in permafrost. Upon thaw in deep, anaerobic lake bottoms, this Pleistocene-age organic matter is readily converted to CH_4 at greater depths and emitted through hotspots. These hot spots appear to represent conduits that funnel or integrate methane production over large volumes at depth (Fig. 4-10). Relatively younger radiocarbon ages of CH_4 emitted through point sources and particularly from background bubbling indicate that Holocene-age organic matter also contributes in part to methanogenesis (Table 4-3, Fig. 4-7).

We propose that the relationships between CH_4 emission rates and $^{14}C_{CH4}$ age (Fig. 4-7) and percent CO_2 reduction pathway (Fig. 4-8) demonstrate that CH_4 production

at depth differs from CH_4 production in shallow lake sediments (Fig. 4-10). At depth, despite the lower concentration of organic matter in Pleistocene loess, the large volume of the thaw bulb beneath lakes contains a large, labile pool of ^{14}C-depleted organic matter deposited in lakes by thermokarst erosion, which enhances CH_4 produced in microsites primarily through CO_2 reduction, resulting in turn in high emission rates as bubbles from microsites are channeled out of sediments through bubble pathways. In shallower surface sediments, more Holocene-age organic matter, which represents terrestrial and aquatic detritus that accumulate on lake bottoms during the lake's lifetime, produces CH_4 under a combination of CH_4 production pathways. Similar to other lake and wetland environments, fresh organic substrates associated with modern aquatic plant and algae production in our Siberian lakes are likely the fuel for methanogenesis *via* the acetate fermentation pathway. We observed submerged macrophytes, aquatic mosses, benthic algae and phytoplankton growing in our Siberian study lakes.

Possible sources of δD-depleted CH_4 in lake bubbles

Compared to isotopic separations between the δD of environmental water and CH_4 in other studies of arctic lakes and wetlands (Chanton *et al.*, 2006; Nakagawa *et al.*, 2002), the δD in most CH_4 bubbles from Siberian and Alaskan thaw lakes in this study was strongly depleted relative to lake water and precipitation. Methane is usually D-depleted relative to ambient water due to fractionation during methanogenesis (δD_{CH4}= 1.55 δD_{H2O} – 145.4, r^2 = 0.69 in Alaskan samples; Chanton et al. 2006). Based on this relationship, the δD of CH_4 of our Siberian lakes, whose δD_{H2O} was -160 ± 1‰, should be -393‰, much higher than our measured values of -454‰ to -476‰. Assuming a similar evaporative enrichment between δD_{H2O} of precipitation and δD_{H2O} of lake water in interior Alaska to that of Siberia (~2‰), and using the equation of Chanton *et al.* (2006), we would expect δD_{CH4} of -397‰. In fact, our measured δD_{CH4} from hotspots of interior Alaska thaw lakes was -406 to -413‰. This unexpectedly large separation between the

δD of lake water and hotspot CH_4 suggests that the hotspot CH_4 emitted from these thaw lakes was produced in an environment with a very different water source than modern lake water.

Thermokarst lakes expand by thawing permafrost along their margins. In the yedoma region of North Siberia, Pleistocene-age, massive ice wedges are up to 80-m deep and occupy 50-90% of the permafrost by volume. Here the isotopic signature of water released from thawing ice-wedges should contribute to the signature of environmental water where CH_4 is produced. Cross sections of yedoma ice wedges measured near our boreal lake study sites in Siberia had hydrogen isotopes ranging from δD -260 to -235 ‰ (Vasil'chuk 2001). The highly depleted δD_{H2O} reflects precipitation under cold Pleistocene climate conditions. Ice wedge δD_{H2O} mostly likely recorded the signature of winter precipitation since it is the snowmelt in spring that flows into frost cracks to grow ice wedges. The δD for Pleistocene ice wedges is much less enriched (-260 to -235‰) than modern Siberian precipitation (-158‰), so it seems likely that hotspot CH_4 formed deep in the sediments is drawing, in part, on a δD-depleted water source, resulting in the extremely depleted δD_{CH4} signature (-454‰). We do not know the δD of ice wedges along the thaw fronts of Alaskan thermokarst lakes, but ice wedges in the region of our boreal study lakes derive from a combination of Pleistocene and Holocene precipitation (Kenji Yoshikawa, *pers. comm.*).

Although δD of CH_4 is strongly dependent on the δD of environmental water, there are several other possible explanations for δD-depletion of CH_4. The CH_4 production pathway can influence δD_{CH4}. Greater δD depletion occurs by the acetate fermentation pathway than CO_2 reduction pathway because all the hydrogen in CO_2 reduction is thought to be derived from coexisting water, while hydrogen in CH_4 produced by acetate fermentation is derived 25% from coexisting water and 75% from the methyl group of acetate, which is depleted in δD (Sugimoto and Wada, 1995; Waldron *et al.*, 1999; Chanton *et al.*, 2006). Further discrepancies arise from exchange of hydrogen between the acetate methyl group and water during final stages of methanogenic acetate metabolism accompanied by a presumed, but unknown isotopic

fractionation (Chanton *et al.*, 2006). Hydrogen concentration can also influence the δD of CH$_4$ (Burke, 1993; Sigimoto and Wada, 1995) with more enrichment occurring under conditions of low H$_2$ concentration. Finally, environmental water can influence the δD of organic matter, which in turn can affect the δD of acetate.

Using ebullition patchiness to estimate whole-lake and regional isofluxes for methane

We determined an accurate isotope signature of annual CH$_4$ emissions (isoflux) from two Siberian lakes by weighting the seasonal isotope signature of each component of the flux by the relative contribution of each component to whole lake annual emissions (Table 4-5). We used 95% of whole lake emissions in our calculations because the isotope signature of CH$_4$ emitted by molecular diffusion, which accounted for 5 ± 1% of the annual flux, was not determined in this study. This new method of weighting different bubble sources improves emission estimates for lakes because it accounts for the patchiness of ebullition flux, a parameter of natural lake and wetland emissions that is typically not addressed. If we had neglected the diversity in ebullition dynamics, including point source and hotspot emissions, our isotope results for North Siberian lakes would have been biased towards isotope signatures reflecting background bubbling and stirring of surface sediments, which are the only components of flux that most studies consider. This flux-weighted assessment of the contribution of the two main methanogenic pathways (16-23% acetate, 77-84% CO$_2$) shows CO$_2$ reduction to be the dominant pathway. This differs from the result that would be derived from measuring spotty background ebullition alone (37-51% acetate, 49-63% CO$_2$), where acetate fermentation contributes relatively more to the total CH$_4$ production. The ranges represent Cases 1 and 2 for ^{13}C values of acetate precursors based on assumptions of isotope signatures associated with labile and recalcitrant organic matter sources (see methods) (Nakagawa *et al.* 2002).

Similarly, considering the distribution of point-source and hotspot bubbling yielded a more accurate estimate of whole lake CH_4 isotope fluxes compared to what would otherwise be derived from disturbed surface sediments and sparse background ebullition sampling. Flux-weighted isotope signatures for whole-lake emissions based on detailed ebullition measurements are shown in Table 4-5. The point source-weighted distribution of CH_4 isotopes resulted in average whole-lake emissions isotope signatures of δD_{CH4} -428‰, $\delta^{13}C_{CH4}$ -70.3‰, and $^{14}C_{CH4}$ age 16,524 years (Table 4-5). The $\delta^{13}C_{CH4}$ was lighter in the whole-lake flux-weighted estimate than values derived by stirring surface sediments (-62.0‰) or trapping background bubbling (-63.4‰). The δD_{CH4} was not distinguishable between the different methods (stirring -414‰, background -432‰), probably reflecting large variation in differences in hydrogen availability or source water signatures at different depths within sediments. The radiocarbon age of CH_4 emissions was the parameter influenced most by the different measurement techniques. The more ancient flux-weighted estimate of 16,524 years reflects the importance of Pleistocene-age organic matter released from permafrost upon thaw of in deeper lake sediments (Zimov *et al.* 1997), while the much younger age of CH_4 in bubbles stirred from surface sediments (175 years for one sample from intensive study lakes, 998 ± 1,659 years, n=6 for all Siberian lakes) and background bubbling (4,271 ± 2,650 years, n=7) indicates contributions of younger organic matter sources in methanogenesis closer to the sediment surface. Radiocarbon age dating of lake sediment cores for 17 lakes in North Siberia supports this interpretation with modern ages of organic matter at the surface and Pleistocene-age (up to 48, 500 to 55,900 ± 6,170 years (^{14}C-dead)) organic matter in deeper sub-lake strata where yedoma thawed (data not shown).

The ability to improve lake CH_4 emission estimates by accounting for the patchiness of different bubble sources that have distinct isotopic compositions enables researchers to more accurately estimate whole lake and regional isofluxes. Assigning CH_4 isotope values to measured emissions (Chapter 2) yields isofluxes that can be used by inverse modelers to better constrain sources and sinks of atmospheric CH_4. In this study, extrapolating the whole-lake isoflux that includes point-source and hotspot

emissions from Siberian thermokarst lakes to the areal extent of yedoma territory (10^6 km^2), yielded isofluxes of δD_{CH4} -0.1115 Gt ‰$^{-1}$ yr^{-1}, $\delta^{13}C_{CH4}$ -0.0183 Gt ‰$^{-1}$ yr^{-1}, and $^{14}C_{CH4}$ age 4.3 x 10^{16} years (Table 4-4) for a large region of Siberia that has been underrepresented in global estimates of CH_4 emissions from wetlands and from which lake ebullition emissions have been altogether excluded (Mathews and Fung, 1986; Aselmann and Crutzen, 1989; Botch *et al.* 1995).

Recent results from two inverse modeling studies using CH_4 isotopes suggested that, compared with bottom-up estimates of current atmospheric CH_4 sources, the inverse estimates required larger tropical CH_4 fluxes from both bacterial and biomass burning sources with a simultaneous reduction of northern sources. The source-process inversion (Mikaloff Fletcher 2004a) attributed the decrease in northern hemisphere sources to a reduction in fossil-fuel and landfill emissions; while the regional inversion approach (Mikaloff Fletcher 2004b) assigned the largest CH_4-source decrease to boreal Eurasian wetlands (comparing bottom-up estimates of fluxes *vs.* prediction of the inverse model). Output from the inversion scenarios predicted emissions of 9-24 Tg CH_4 yr^{-1} from boreal Eurasia as a sum of all sources, which were grouped into three categories: bacterial CH_4, biomass burning, and fossil fuels. Our results from Siberia raise questions about the findings of Mikaloff Fletcher (2004b) because instead of a reduction of northern CH_4 sources, which is required by the inversions, we observed increased CH_4 emissions from Siberian thaw lakes (Chapter 1) and isofluxes from Siberian lakes that are more ^{13}C-depleted than values assumed by Mikaloff Fletcher (2004b). Inverse modeling must reconcile this additional source of high-latitude atmospheric CH_4 (lake bubbles), in particular from northern Eurasian yedoma lakes, which has now been characterized and whose $\delta^{13}C_{CH4}$ is depleted (-70.3 ‰) relative to the typical value used for northern wetland emissions (-58 ‰) and the annual mean value of atmospheric CH_4 (-47.3‰).

Our documentation of a large, ^{14}C-depleted CH_4 source from lake ebullition must also be considered in models, which until now have attributed high-latitude ^{14}C-free CH_4 and recent changes to high latitude CH_4 concentrations to leaky gas pipelines, coal mining and natural seepage from gas reservoirs in Siberia (Whalen *et al.* 1989,

Dlugokencky *et al.* 2003), not to aquatic sediments. Estimates of ^{14}C-CH_4 derived from fossil-fuel energy range from 95-110 Tg CH_4 yr^{-1} (IPCC 2001, Mikaloff Fletcher 2004). Annual emissions from Siberian lakes, 3.8 Tg CH_4 yr^{-1} with an average radiocarbon content of ~12 mMC (Chapter 1), are less than 3.5% of fossil-fuel CH_4 sources. However, radiocarbon ages up to 26,000 years (3.9 pMC) from Alaskan thaw lakes suggest that ^{14}C-depleted CH_4 ebullition is not unique to Siberia, and should be more thoroughly quantified for lakes and reservoirs globally. Given the large pool of organic matter locked up in boreal and arctic permafrost, continued warming of permafrost in the future (Sazonova *et al.*, 2004; Lawrence and Slater, 2005) could lead to accelerated release of ^{14}C-depleted CH_4 from expanding thaw lakes.

Conclusions

Based on the concentrations and isotopic compositions of gases in bubbles from North Siberian lakes we have distinguished two major types of bubbles, which represent two zones of CH_4 production in lakes (Fig. 4-10): (1) Bubbles stirred up from surface sediments in lakes or captured in randomly placed traps that represent background bubbling had young radiocarbon ages with stable isotope compositions and methane production pathways similar to other lakes and wetlands reported in the literature where similar methods of bubble collection are commonly used. These bubbles had lower concentrations of CH_4 and were formed by nearly equal contributions of CO_2 reduction and acetate fermentation. Their relatively young radiocarbon ages suggest that Holocene-age organic matter sources, at least in part, fueled methanogenesis. (2) We characterized, however, a second type of bubble source, which probably comes from deeper lake horizons based on ^{14}C depleted CH_4 signatures, high CH_4 concentrations, and high CH_4 emission rates. As CH_4 production exceeds its solubility limits, CH_4 bubbles come out of solution forcing their way through lake sediments to lower pressure states. We speculate that small streams of bubbles form pathways which merge into larger byways, like the

tributaries of rivers joining into the main flow. The deeper the site of CH_4 production, the stronger the stream of bubbles that coalesces from a large volume of sediments into a point source or hotspot of emission that exits through a small hole (several mm to <2cm diameter) at the sediment water interface. Continuous flux measurements and lake-bottom benchmarkers show that these vents remain in the same location for at least 3 years (Chapter 1). In contrast, background bubbling represents non- or weakly-channeled bubbling. Methane bubbles released as background flux likely form in small microsites closer to the sediment-water interface, so that a high pressure of gas is not required to push them through thick sediments.

The particular characteristics of hotspot bubbling are not unique to North Siberian yedoma lakes. Given that we found hotspots with CH_4 of high concentration and ^{14}C-depletion in Alaskan thermokarst lakes as well, we propose that these two distinct zones of CH_4 bubble production (deep point sources vs. shallow background) occur across geographical regions in all lakes in which thermokarst erosion delivers a large, labile source of organic substrate to deep anaerobic lake horizons. Thermokarst releases old organic matter from permafrost into lake sediments fueling methanogenesis. The ^{14}C-depleted CH_4 signature derived from ebullition associated with thermokarst erosion was previously considered unusual for natural ecosystem CH_4 emissions. Methane emissions typically reported from northern lakes and wetlands have modern radiocarbon ages, because, in wetlands recent plant productivity supplies labile organic matter from root exudates (King et al. 2002), and in lakes, the majority of samples have been collected by stirring surface sediments or using randomly placed traps that capture background ebullition of CH_4 released from shallow lake sediments whose relative input from modern aquatic and terrestrial plant productivity is high (Nakagawa et al. 2002, Chapter 2). Methane emissions depleted in ^{14}C from our study lakes in Siberia and Alaska appear to result from thermokarst erosion, particularly because hotspots of bubbling occurred only in lakes with thermokarst (Chapter 2). However, one might expect that CH_4 emitted from point-source bubbling in other non-thermokarst lakes would be relatively ^{14}C-depleted also, given the hypotheses presented above that CH_4 flux through bubble tributaries of

different sizes are related to the sediment depth where labile organic matter is supplied for methanogenesis. This is, however, a subject for future investigation.

In this study we characterized the distinct $\delta^{13}C_{CH4}$ and ^{14}C-depeted CH_4 signatures of arctic lake ebullition, combining them with improved bottom-up flux estimates (Chapters 1 and 2), to reveal a large new source of high-latitude atmospheric CH_4. Qualitative assessment of this new isotope CH_4 source contradicts patterns presented by recent inverse modeling, which predicted a reduction in boreal wetland sources in contrast to bottom-up source estimates. Instead of providing a Eurasian source-reduction scenario, we suggest an increase in boreal wetland sources with ^{14}C signatures that overlap with estimates of fossil fuel emissions. Since thermokarst erosion is a driving factor of CH_4 emissions in arctic lakes, and thaw lake area appears to be increasing in zones of continuous permafrost since 1970 (Smith *et al.*, 2005; Chapter 1), understanding the isotopic implications of further thermokarst lake expansion as permafrost in arctic regions continues to warm and thaw will help atmospheric modelers define CH_4 sources and predict changes.

References

Alperin *et al.* Factors that control the stable isotope composition of methane produced in an anoxic marine sediment, *Global Biogeochem. Cycles, 6*, 271-291, 1992.

Anderson, L., M. B. Abbott, B. P. Finney, and S. J. Burns, Regional atmospheric circulation change in the North Pacific during the Holocene inferred from lacustrine carbonate oxygen isotopes, Yukon Territory, Canada. *Quat. Res.* doi.:10.1016/j.yqres.2005.03.008, 2005.

Aselmann, I., and P. J. Crutzen, Global distribution of natural freshwater wetlands, rice paddies, their net primary productivity, seasonality, and possible methane emissions, *J. of Atm. Chem. 8*, 307-358, 1989.

Bartlett, K. B., P. M. Crill, R. L. Sass, R. C. Harriss, and N. B. Dise, Methane emissions from tundra environments in the Yukon-Kuskokwim Delta, Alaska, *J. Geophys. Res. 97*, 16,645-16,660, 1992.

Bastviken, D., J. Cole, M. Pace, and L. Tranvik. Methane emissions from lakes: Dependence of lake characteristics, two regional assessments, and a global estimate, *Global Biogeochem. Cycles 18*, GB3010, doi:10.1029/2004GB002238, 2004.

Botch, M. S., K. I. Kobak, T. S. Vinson, and T. P. Kolchugina. *Global Biogeochem. Cycles 9*, 37-46, 1995.

Casper, P., S. C. Maberly, G. H. Hall, and B. J. Finlay, Fluxes of methane and carbon dioxide from a small productive lake to the atmosphere, *Biogeochemistry 49*, 1-19, 2000.

Chanton, J. P., C. S. Martens, and C. A. Kelley, Gas transport from methane-saturated tidal freshwater and wetland sediments. *Limnol. and Oceanogr., 34*, 807-819, 1989.

Chanton, J., J. Bauer, P. Glaser, D. Siegel, E. Ramonowitz, S. Tyler, C. Kelley, A. Lazrus, Radiocarbon evidence for the substrates supporting methane formation within northern Minnesota peatlands. *Geochim. Cosmochim. Acta 59*, 3663-3668, 1995.

Chanton, J. P., L. C. Chasar, P. Glaser, and D. Siegel, Chapter 6, Carbon and hydrogen isotopic effects in microbial methane from terrestrial environments. In: Flanagan,L.B., Ehleringer, J.R., Pataki, D.E. (Eds.), Stable Isotopes and Biosphere-Atmosphere Interactions, Physiological Ecology Series. Elsevier-Academic Press, Amsterdam, pages 85-105, 2005.

Chanton, J. P., D. Fields, and M. E. Hines, Controls on the hydrogen isotopic composition of biogenic methane from high latitude terrestrial wetlands. *Journal of Geophysical Research—Biogeosciences*, 2006, *In review.*

Chasar, L. S., J. P. Chanton, P. H. Glaser and D. I. Siegel, Methane concentration and stable isotope distribution as evidence of rhizospheric processes: comparison of a fen and bog in the Glacial Lake Agassiz peatland complex. *Annals of Botany, 86,* 655-663, 2000a.

Chasar, L. S., J. P. Chanton, P. H. Glaser, D. I. Siegel, and J. S. Rivers, Radiocarbon and stable carbon isotopic evidence for transport and transformation of DOC, DIC and CH_4 in a northern Minnesota peatland. *Global Biogeochem. Cycles, 14,* 1095-1105, 2000b.

Coleman, M. L., T. J. Sheperd, J. J. Durham, J. E. Rouse and G. R. Moore, Reduction of water with zinc for hydrogen isotopic analysis. *Anal. Chem. 54,* 993-995, 1982.

Coleman, D. D., B. J. Risatti, and M. Schoell, Fraction of carbon and hydrogen isotopes by methane oxidizing bacteria, *Geochim. Cosmochim. Acta 45,*1033-1037, 1981.

Conrad, R., Control of methane production in terrestrial ecosystems in *Exchange of Trace Gases Between Terrestrial Ecosystems and the Atmosphere,* edited by M. O. Andreae and D. S. Schimel, pp. 39-58, John Wiley, New York, 1989.

Davis, N., *Permafrost: A guide to frozen ground in transition,* University of Alaska Press, Hong Kong (2001).

Dlugokencky, E. J., K. A. Masarie, P. M. Lang and P. P. Tans, Continuing decline in the growth rate of the atmospheric methane burden. *Nature 393,* 447-450, 1998.

Dlugokencky, E. J., S. Houweling, L. Bruhwiler, K. A. Masarie, P. M. Lang, J. B. Miller, and P. P. Tans, Atmospheric methane levels off: Temporary pause or a new steady-state? *Geophysical Research Letters 30*, 1992, doi: 1029/2003GL018126, 2003.

Duddleston, K. N., M. A. Kinney, R. P. Keine, and M. E. Hines, Anaerobic microbial biogeochemistry on a northern bog: Acetate as a dominant metabolic end product. *Global Biogeochem. Cycles 16*, 1063. doi.:10.1029/2001GB001402, 2002.

Dutta, K., E. A. G. Schuur, S. A. Zimov, J. T. Randerson, J. C. Neff, Potential carbon release from permafrost soils of Northeastern Siberia, Global Change Biology, *in prep.*

Fung, I. *et al.*, Three-dimensional model synthesis of the global methane cycle, *J. of Geophys. Res. 96*, 13,033- 13,065, 1991.

Hamilton, T. D. Glacial geology of the Toolik Lake and Upper Kuparuk River Regions. Institute of Arctic Biology, Biological Papers of the University of Alaska, Ed. D. A. Walker, Number 26 (2003).

Happell, J., J. P. Chanton, and W. Showers, The influence of methane oxidation on the stable isotope composition of methane emitted from Florida Swamp forests. *Geochem. Cosmochim. Acta 58*, 4377-4388, 1994.

Hein, R., P. J. Crutzen, and M. Heimann, An inverse modeling approach to investigate the global atmospheric methane cycle, *Global Biogeochem. Cycles, 11*, 43-76. 1997.

Hornibrook, E. R., F. J. Longstaffe, and W. S. Fyfe, Evolution of stable carbon isotope compositions from methane and carbon dioxide in freshwater wetlands and other anaerobic environments. *Geochem. Cosmochim. Acta 64*, 1013-1027, 2000.

Houweling, S., T. Kaminski, F. Dentener, J. Lelieveld, and M. Heimann, Inverse modeling of methane sources and sinks using the adjoint of a global transport model, *J. Geophy. Res. 104*, 26,137-26,160, 1999.

Intergovernmental Panel on Climate Change (IPCC), *The Scientific Basis,* Cambridge Univ. Press, New York, 2001.

Keppler, F., J. T. G. Hamilton, M. Brab, and T. Rockmann, Methane emissions from terrestrial plants under aerobic conditions, *Nature 439*, 187-191, 2006.

King, J.Y., W. S. Reeburgh, K. K. Theiler, G. W. Kling, W. M. Loya, L. C. Johnson, and K. J. Nadelhoffer, Pulse-labeling studies of carbon cycling in the Arctic tundra ecosystems: The contribution of photosynthates to methane emission. *Global Biogeochem. Cycles 16*, 1062, 2002.

Kipphut, G. W., and C. S. Martens, Biogeochemical cycling in an organic-rich coastal marine basin. 3. Dissolved gas transport in methane saturated sediments. *Geochim. et Cosmochim. Acta 46*, 2049-2060, 1982.

Kling, G., G. W. Kipphut, and M. C. Miller, The flux of CO_2 and CH_4 from lakes and rivers in arctic Alaska, *Hydrobiologia 240*, 23-36, 1992.

Landsdown, J. M., P. D. Quay, and S. L. King. CH_4 production *via* CO_2 reduction in a temperate bog: A source of 13C-depleted CH_4, *Geochim. Cosmochim. Acta, 56*, 3493-3503, 1992.

Lawrence, D. M., and A. G. Slater, A projection of severe near-surface permafrost degradation during the 21st century, *Geophysical Research Letters. 32*, doi:10.1029/2005GL025080, 2005.

Lowe, D. C., C. A. M. Brenninkmeijer, G. W. Brailsford, K. Lassey, A. J. Gomez, and E. G. Nisbet, Concentration and ^{13}C records of atmospheric methane in New Zealand and Antarctica: Evidence for changes in methane sources, *J. Geophys. Res. 99*, 16,913-16,925, 1994.

Martens, C. S., N. E. Blair, C. D. Green, and D. J. Des Marais, Seasonal variations in the stable carbon isotopic signature of biogenic methane in coastal sediment, *Science 233*, 1300-1303, 1992.

Mason, E. A. and T. R. Marrero. The diffusion of atoms and molecules, *Adv. At. Mol. Phys. 6*, 155-232, 1970.

Mathews, E. and I. Fung, Methane emission from natural wetlands: Global distribution, area, and environmental characteristics of sources, *Global Biogeochem. Cycles 1*, 61-86, 1987.

Mikaloff Fletcher, S. E., P. P. Tans, L. M. Bruhwiler, J. B. Miller, and M. Heimann, CH_4 source estimated from atmospheric observations of CH_4 and its $^{13}C/^{12}C$ isotopic ratios: 1. Inverse modelling of source processes. *Global Biogeochem. Cycles 18*, GB4004, doi:10.1029/2004GB002223, 2004a.

Mikaloff Fletcher, S. E., P. P. Tans, L. M. Bruhwiler, J. B. Miller, and M. Heimann, CH_4 source estimated from atmospheric observations of CH_4 and its $^{13}C/^{12}C$ isotopic ratios: 2. Inverse modelling of CH_4 fluxes from geographic regions. *Global Biogeochem. Cycles 18*, GB4004, doi:10.1029/2004GB002224, 2004b.

Nakagawa, F., N. Yoshida, Y. Nojiri, and V. N. Makarov, Production of methane from alasses in eastern Siberia: Implications from its ^{14}C and stable isotope compositions, *Global Biogeochem. Cycles 16*, doi.10.1029/2000GB001384, 2002.

Nozhevnikova, A. N., O. R. Kotsyurbenko, and M. V. Simankova, Aceteogenesis at low temperature, in *Acetogenesis*, Ed. H.L. Drake, Chapman and Hall, New York. pp. 416-431, 1994.

Quay, P. D., S. L. King, J. M. Landsdown, and D. O. Wilbur. Isotopic composition of methane released from wetlands: Implications for the increase in atmospheric methane, *Global Biogeochem. Cycles, 2*, 385-397, 1988.

Reeburgh, W. S., J. Y. King, S. K. Regli, G. W. Kling, N. A. Auerbach, and D. A. Walker, A CH_4 emission estimate for the Kuparuk River basin, Alaska., *J. Geophys. Res. 103*, 29,005- 29,013, 1998.

Roulet, N. T. *et al.*, Role of Hudson Bay lowland as a source of atmospheric methane. *J. Geophys. Res. 99*, 1439-1454, 1994.

Roulet, N. T., P. M. Crill, N. T. Comer, A. Dove, and R. A. Boubonniere, CO_2 and CH_4 flux between a boreal beaver pond and the atmosphere, *J. Geophys. Res. 102*, 29,313-29,3193, 1997.

Sazonova, T. S., V. E. Romanovsky, J. E. Walsh, and D. O. Sergueev, Permafrost dynamics in the 20th and 21st centuries along the East Siberian transect. *J. Geophys. Res. 109*, doi:10.1029/2003JD003680, 2004.

Smith, L. C., Y. Sheng, G. M. MacDonald, and L. D. Hinzman, Disappearing arctic lakes. *Science 308*, 1429, 2005.

Stuiver, M. and H. Polach, Reporting of ^{14}C data, *Radiocarbon, 19*, 355-363, 1977.

Sugimoto, A., and E. Wada. Carbon isotopic composition of bacterial methane in a soil incubation experiment: Contributions of acetate and CO2/H2, *Geochim. Cosmochim. Acta 59*, 1329-1337, 1993.

Vail'chuk, Y. K., A. C. Vasil'chuk, D. Rank, W. Kutschera and J. C. Kim, Rradiocarbon dating of d18O-dD plots in late pleistocene ice-wedges of the Duvanny Yar (lower Kolyma River, northern Yakutia), Radiocarbon, vol 43, Nr 2B, pp. 541-553. Proceedings of the 17th international ^{14}C conference, edited by I. Carmi and E. Boaretto, 2001.

Waldron, S., I. A. Hall, and A. E. Fallick, Enigmatic stable isotope dynamics of deep peat methane, *Global Biogeochem. Cycles, 13*, 93-100, 1999.

Walter, K. M., F. S. Chapin III, E. Schuur, and S.A, Zimov, Organic matter sequestration in peat beds of deep Siberian thermokarst lakes during the Holocene, Nature, *In prep.*

Wassmann, R. U.G., M. J. Thein, H.Whiticar, H. Rennenberg, S. Seiler, and J. W. Junk, Methane emissions from the Amazon floodplain: Characterization of production and transport, *Global Biogeochem. Cycles, 6*, 3-13, 1992.

Welp, L. R., J. R. Randerson, J. C. Finlay, S. P. Davidov, G. M. Zimova, A. I. Davidova, and S. A. Zimov, A high resolution time series of oxygen isotopes from the Kolyma

River: Implications for the seasonal dynamics of discharge and basin-scale water use. *Geophysical Research Letters 32*, LI4401, 2005.

Whalen, M., N. Tanaka, R. Henry, B. Deck, J. Zeglen, J. S. Vogel, J. Southon, A. Shemesh, R. Fairbanks, W. Broecker, Carbon-14 in methane sources and in atmospheric methane: Contribution from fossil carbon, *Science 245*, 286-290, 1989.

Whalen, S. C. and W. S. Reeburgh, A methane flux transect along the trans-Alaska pipeline haul road, *Tellus 42,* 237-249, 1990.

Whiticar, M. J., E. Faber, and M. Schoell, Biogenic methane formation in marine and freshwater environments: CO_2 reduction *vs*. acetate fermentation- Isotope evidence *Geochem. Cosmochim. Acta. 50,* 693-709, 1986.

Worthy, D. E., J. I. Levin, F. Hopper, M. K. Ernst, and N. B. A. Trivett, Evidence for a link between climate and northern wetland methane emissions. *J. Geophys. Res. 105*, 4031-4038, 2000.

Zhuang, Q. *et al.,* Methane fluxes between terrestrial ecosystems and the atmosphere at northern high latitudes during the past century: A retrospective analysis with a process-based biogeochemistry model. *Global Biogeochem. Cycles 18*, GB3010, doi:10.1029/2004GB002239, 2004.

Zimov, S. A. *et al.*, North Siberian lakes: A methane source- fueled by Pleistocene Carbon, *Science 277*, 800-802, 1997.

Zimov, S. A., Pleistocene Park: Return of the Mammoth's Ecosystem, *Science 308,* 796-798, 2005.
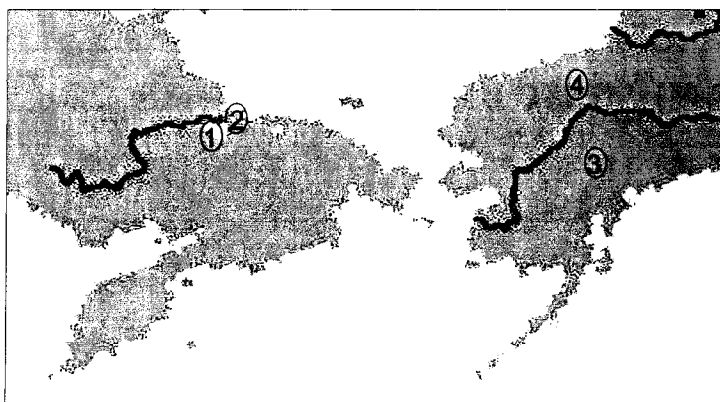
Figure 4-1. Location of boreal (1 and 3) and tundra (2 and 4) study sites in Siberia and Alaska.
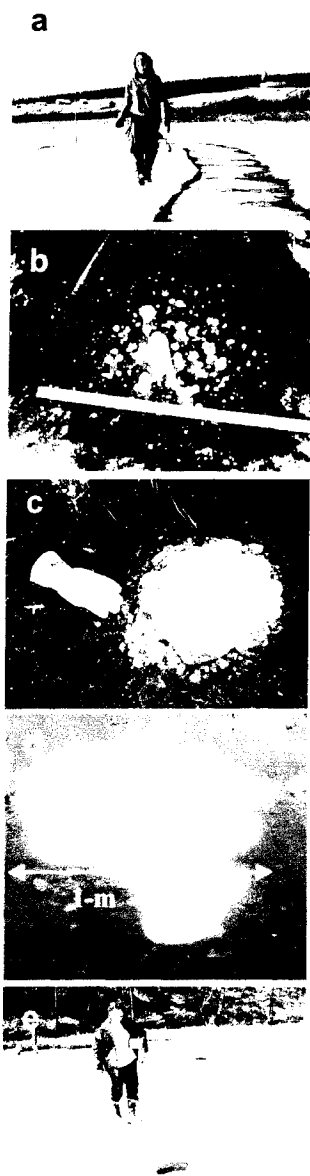
Figure 4-2. Photographs of point sources and hotspots visible in lake ice, whose distributions were measured using transects across lakes (a). Discrete ebullition points caused bubbles to stack-up in lake ice during winter (point sources, b-d). These are generally labeled 'ice koshkas' in the figures of this paper. Hotspots (e) are an extreme category of bubbling point sources with continuous, high flux rates sufficient to keep ice from freezing. This allows bubbles to escape year-round to the atmosphere through open holes in lake ice. Daily fluxes associated with each point source type and hotspots are presented in Chapter 1.
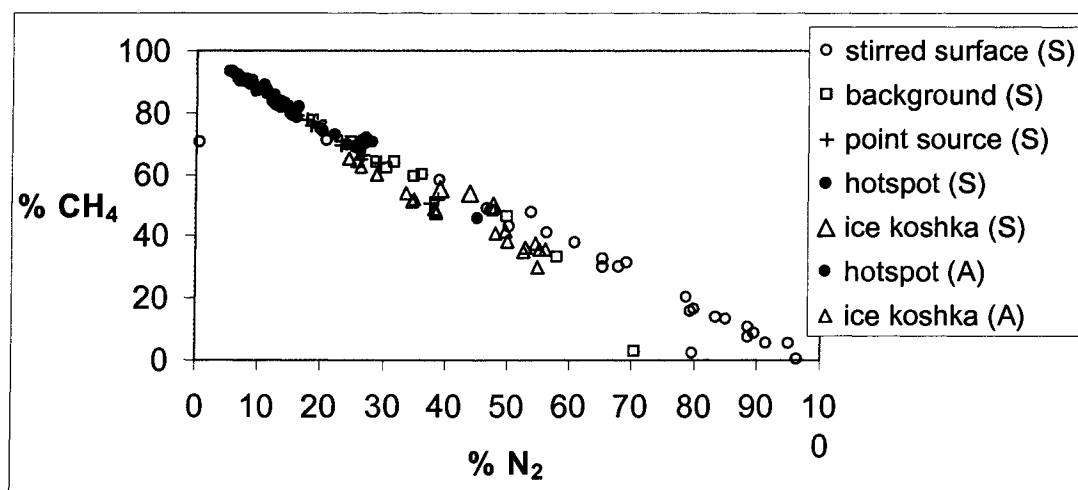
Figure 4-3. The concentrations of CH_4 and N_2 in bubbles collected from lakes in Alaska (A) and Siberia (S). The negative linear relationship is described by $[CH_4] = -1.03[N_2]) + 95.5$, $R^2 = 0.97$.
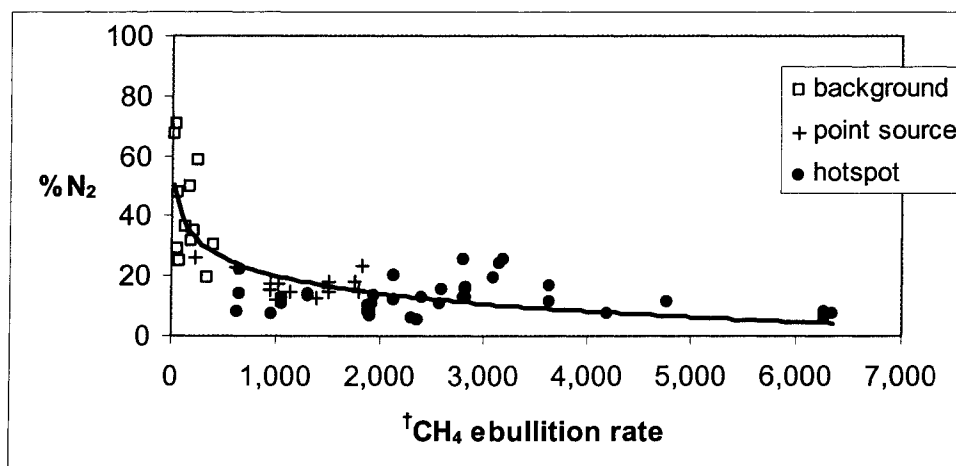
Figure 4-4. Methane ebullition rate *vs.* N_2 composition of background, point-source, and hotspot bubbles from Siberian lakes, expressed as $[N_2] = -8.5*ln(CH_4 \text{ flux}) + 79$, $r^2 = 0.63$. The data indicate that the N_2 content of bubbles is influenced by the rate of ebullition, whereby high bubbling rates strip N_2 from lake sediments.

[†] The units of ebullition measured with bubble traps are expressed as $mg\ CH_4\ m^{-2}\ d^{-1}$ for background bubbles, since the rates were a function of trap area; whereas units for point-source and hotspot bubbling are $mg\ CH_4\ spot^{-1}\ d^{-1}$ because emissions from discrete, small holes in lake sediments (<2 cm diameter) were independent of bubble trap area. All ebullition rates are the average rate during the 10-day period surrounding individual bubble collection dates for isotopic analysis.
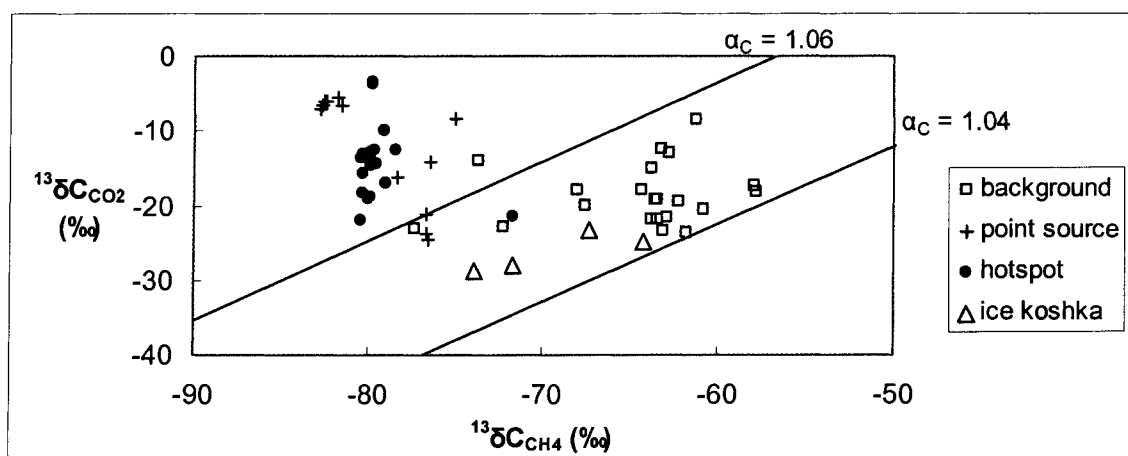
Figure 4-5. The $\delta^{13}C_{CO2}$ and $\delta^{13}C_{CH4}$ of different bubble sources collected from Shuchi Lake and Tube Dispenser Lake in Siberia. Solid lines are constant carbon isotopic fractionation (α_C) values of 1.04 and 1.06. The α_C values of bubbles indicate the pathway of CH_4 production, in which $\alpha_C > 1.06$ suggest CH_4 is produced mainly by CO_2 reduction and $\alpha_C < 1.055$ suggests CH_4 produced largely by acetate fermentation. A shift in the $\delta^{13}C_{CO2}$ and $\delta^{13}C_{CH4}$ of the ice koshkas (open triangles) represents alteration from the original point source signatures due to CH_4 oxidation in the ice.
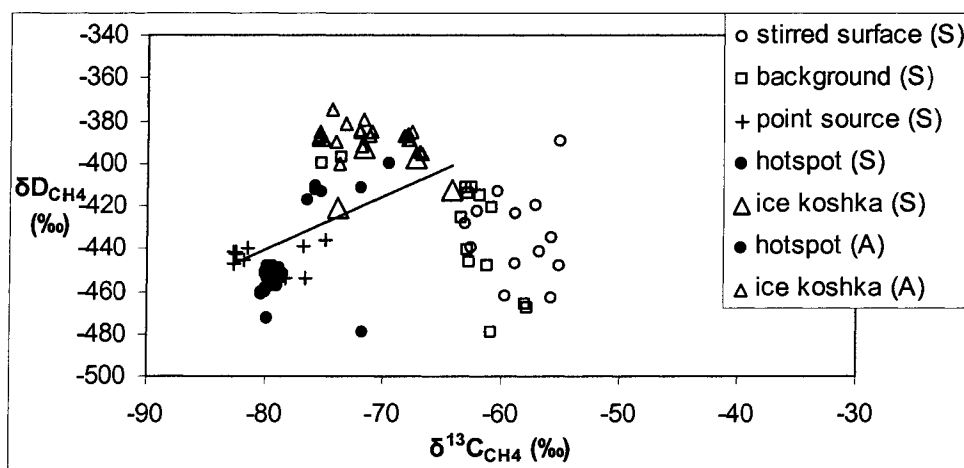
Figure 4-6. The $\delta^{13}C$ and δD of CH_4 in bubbles from Siberian (S) and Alaskan (A) lakes. The regression line for point sources (+) collected fresh from ebullition events with ice koshkas (Δ, point sources that are trapped all winter as bubble stacks in ice) is expressed as $\delta D_{CH4} = 2.5 * \delta^{13}C_{CH4} - 239$, $r^2 = 0.60$. The enrichment of both $\delta^{13}C$ and δD of CH_4 relative to point sources indicates CH_4 diffusion out of bubbles trapped in ice.
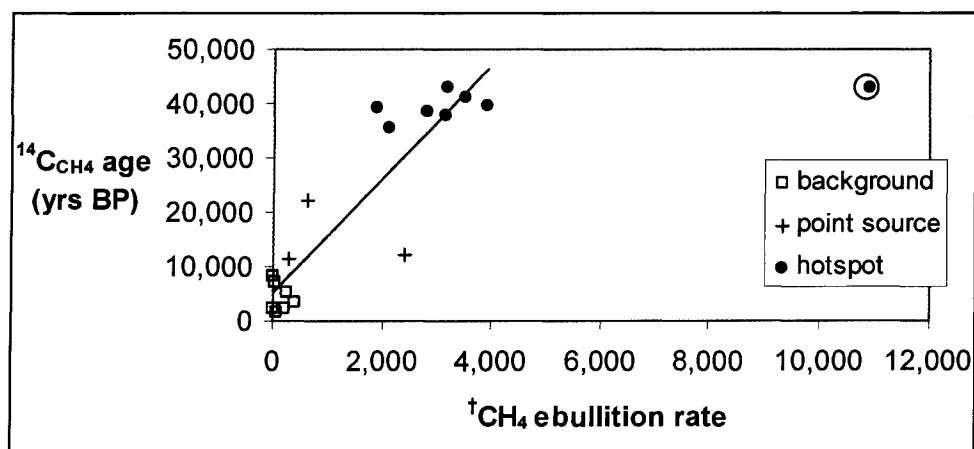
Figure 4-7. The radiocarbon age (years) and ebullition rates from Siberian lakes for age dating[Y]. The relationship is expressed by ^{14}C age = $10.5*CH_4$ flux + 4911, r^2 = 0.81, excluding the circled outlier.

[†] The units of ebullition measured with bubble traps are expressed as mg CH_4 m^{-2} d^{-1} for background bubbles, since the rates were a function of trap area; whereas units for point-source and hotspot bubbling are mg CH_4 $spot^{-1}$ d^{-1} because emissions from discrete, small holes in lake sediments (<2 cm diameter) were independent of bubble trap area. All ebullition rates are the average rate during the 10-day period surrounding individual bubble collection dates for isotopic analysis.

[Y]Table 4-3 shows additional $^{14}C_{CH4}$ ages of bubbles stirred from surface sediments in Siberian lakes. These data were not included in the correlation because they did not have a measured ebullition flux associated with them (methods).
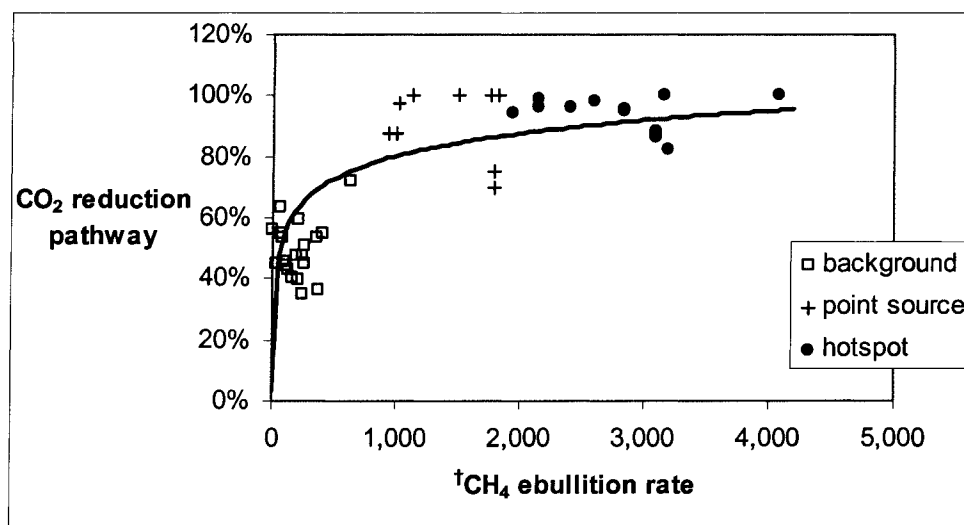
Figure 4-8. The proportion of CO_2 reduction pathway and the daily CH_4 ebullition flux averaged for 10 days surround the bubble sample collection date for North Siberian lakes. The regression equation is % CO_2 reduction pathway (Case 1) = 0.11*ln(CH_4 flux) + 0.07, R^2 = 0.56.

[†] The units of ebullition measured with bubble traps are expressed as $mg\ CH_4\ m^{-2}\ d^{-1}$ for background bubbles, since the rates were a function of trap area; whereas units for point-source and hotspot bubbling are $mg\ CH_4\ spot^{-1}\ d^{-1}$ because emissions from discrete, small holes in lake sediments (<2 cm diameter) were independent of bubble trap area.
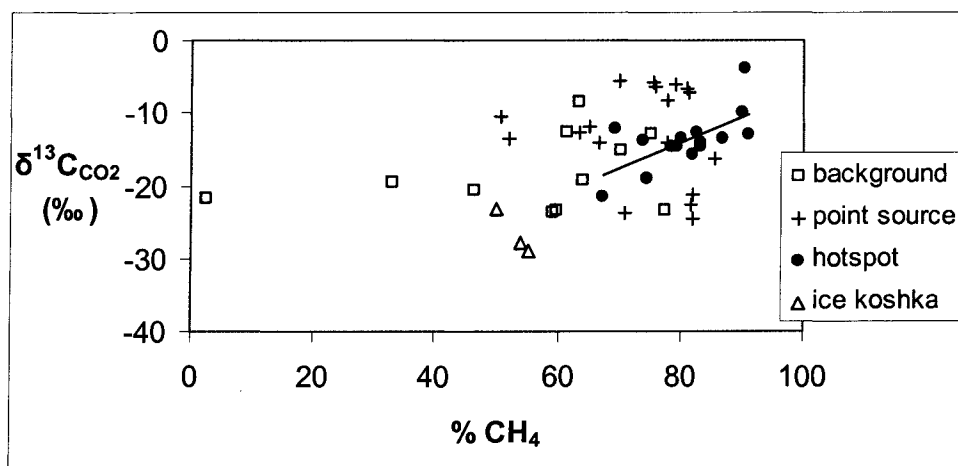
Figure 4-9. The $\delta^{13}C_{CO2}$ and CH_4 concentration in bubbles from North Siberian lakes. Regression lines are expressed as $\delta^{13}C_{CO2} = 0.07[CH_4] - 22$, $R^2=0.09$ (line not shown) for background traps, $\delta^{13}C_{CO2} = 0.12[CH_4] - 28$, $R^2 = 0.05$ (line not shown) for point sources, and $\delta^{13}C_{CO2} = 0.35[CH_4] - 42$, $R^2 = 0.43$ for ebullition hotspots (line shown).

¹⁴C age (years)	modern to 5,300	5,600 to 22,100	36,000 to 43,000
$\delta^{13}C_{CH4}$ (‰)	-58 to -63	-69 to -74	-79 to -80
Pathway (%ACE/%CO₂)	50/50	0/100	0/100
	'background' bubbling	point sources	hotspots
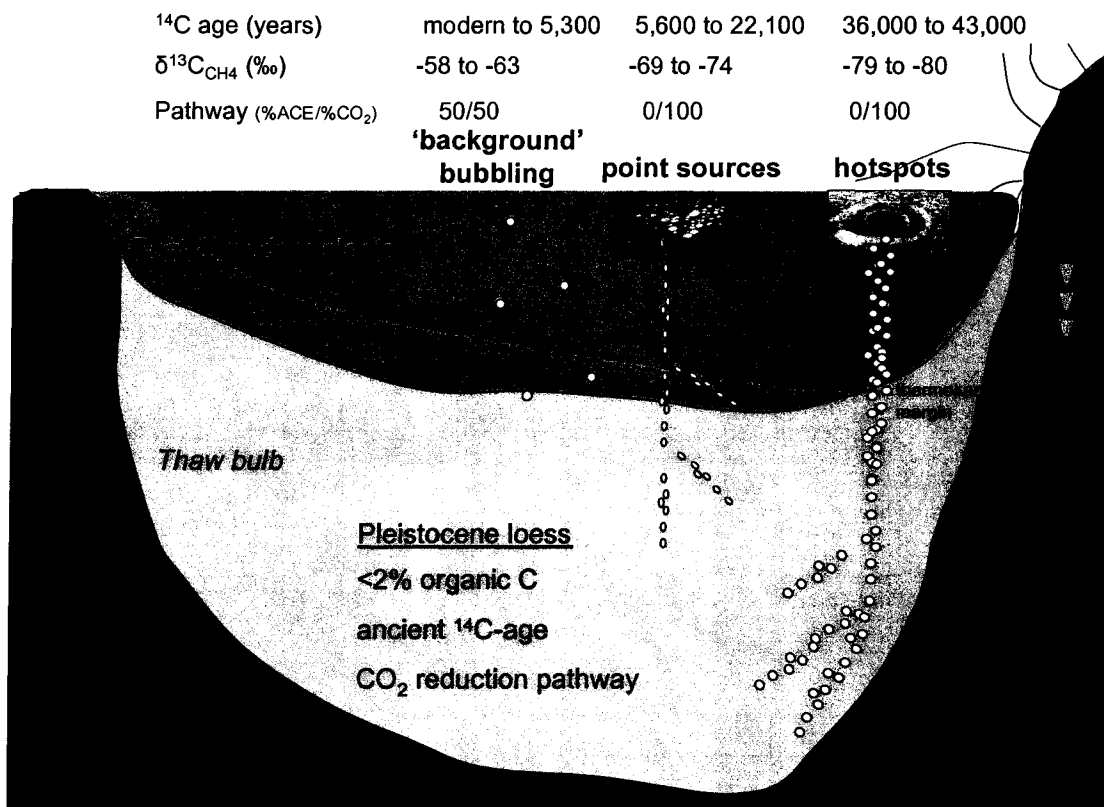
Figure 4-10. Schematic of CH_4 production and emission in North Siberian thaw lakes, summarizing isotopic information for background, point-source, and hotspot bubbling and hypothesizing sediment depth at which each bubbling source originates.

Table 4-1. Lake classification, degree of thermokarst activity, location, size, gas collection technique and sampling dates from study sites in Siberia and Alaska.

Region	Site	Classification[†]	Thermokarst	Bubble Collection Date	Area (m2)	Max Depth (m)	Collection Technique[v]
Northeast Siberia	Shuchi Lake	boreal, yedoma	moderate	July 2001, May 2003 - June 2004	58,051	11.0	S,N,IK
	Tube Dispenser Lake	boreal, yedoma	active	May 2003 - June 2004	110,175	16.5	N
	Grass Lake	boreal, yedoma	inactive	May 2003 - June 2004	5,363	12.5	N
	Station Rd Yedoma Pond 1	boreal, yedoma	active	July 2001	~225	1.8	S
	Tower Rd Yedoma Pond 2	boreal, yedoma	active	July 2001	~226	2.3	S
	Tower Rd Yedoma Pond 3	boreal, yedoma	active	July 2001	~227	2.3	S
	Kitchen Sand Pond 1	boreal, sand	none	July 2001	~228	1.3	S
	Volodya Sand Pond 2	boreal, sand	none	July 2001	~100	1.6	S
	Airport Sand Pond 3	boreal, sand	none	July 2001	~900	1.3	S
	Meadow Lake	boreal, HA-FD	moderate	July 2001		2.3	S
	Young Tundra Thaw Pond	tundra, yedoma	active	July 2001		no data	S
	No Fish Ambarchik Lake	tundra, yedoma	moderate	July 2001		no data	S
	Ambarchik Fish Lake	tundra, yedoma	moderate	July 2001		no data	S
	Tundra Floodplain Lake	tundra, HA-FD	moderate	July 2001		no data	S
Interior Alaska	Rosie Creek Beaver Pond	boreal, HA-RPL	active	Nov. 2004	6,324	1.5	N
	Goldstream Valley Lake	boreal, RPL	active	Nov. 2004	9,797		N
North Slope Alaska	Toolik Lake	tundra, GD	none	Oct. 2004	1,470,000	24.0	IK
	E1	tundra, GD	none	Oct. 2004	30,099	12.4	IK
	E5	tundra, GD	none	Oct. 2004	113,172	11.9	IK
	E6	tundra, GD	none	Oct. 2004	19,967	3.2	IK
	NE1	tundra, GD	none	Oct. 2004	21,502		IK
	N2	tundra, GD	none	Oct. 2004	13,663	10.7	IK
	N3	tundra, GD	none	Oct. 2004	9,349		IK

[†]**Substrate types abreviated:**

YEDOMA	Icy, organic-rich Pleistocene loess
SAND	sand, man-made
HA-FD	Holocene alluvium; flooplain deposits
HA-RPL	Hococene alluvium and reworked Pleistocene loess from Stage 3
RPL	Reworked Pleistocene Loess from Stage 3
GD	Glacial deposits

[v]**Collection Technique abbreviated:**

S	stirred surface sediments
N	natural bubbling into traps
IK	ice koshka

Table 4-2. Concentrations of major constituents (CH_4, N_2, CO_2, and O_2) and isotopes compositions ($\delta^{13}C_{CO_2}$, $\delta^{13}C_{CH_4}$, δD_{CH_4}, and δD_{H_2O}) of gas bubbles and lake water from Siberia and Alaska. Estimates are presented as mean ± standard deviation, n. For sample sizes of n=2, error estimates are half of the absolute difference between two measurements.

Region	Lake	Bubble source	$CH_4\%$	$N_2\%$	$CO_2\%$	$O_2\%$	$\delta^{13}C_{CO_2}$	$\delta^{13}C_{CH_4}$	δD_{CH_4}	δD_{H_2O} (depth)
Siberia	Shuchi Lake									-154±2.6, 3 (1-m)
										-159±2.9, 3 (10-m)
		stirred surface sediments	39.7±32.7, 5	48.8±36.9, 5	4.0±3.0, 5	9±10.6, 5			-62.0±5.1, 5	-414±17, 4
		background	63.8±16.1, 6	30.3±14.6, 6	0.3±0.3, 6	6.0±2.2, 6	-17.8±4.9, 10	-66.8±5.6, 10	-440±13, 3	
		point source	78.9±4.6, 14	16.6±3.4, 14	0.9±0.6, 15	3.9±1.4, 15	-11.1±6.9, 11	-79.7±3.1, 13	-444±6, 10	
		hotspot	84.3±6.9, 38	12.7±5.4, 38	0.7±0.3, 38	2.9±1.6, 38	-14.8±2.6, 24	-79.6±0.5, 35	-454±4, 32	
		ice koshka	53.0±2.7, 3	43.7±4.3, 3	0.3±0.1, 3	4.4±1.1, 3	-26.2±2.6, 4	69.3±4.3, 4	-406±13, 4	
	Tube Dispenser Lake									-161±8.1, 3 (15-m)
		background	55.0±7.1, 5	39.8±8.4, 5	0.2±0.1, 5	6.0±1.5, 5	-19.6±3.2, 11	-62.4±2.6, 14	-436±28, 9	
		hotspot	79.0±11.6, 2	16.5±9.9, 2	1.0±0.7, 2	3.9±2.6, 2	-9.6±10.3, 3	-77.1±4.7, 3	-476±4, 2	
	Grass Lake									-172±2.9, 3 (10-m)
		background	2.7, 1	68.9±1.7, 2	0.2±0, 2	30.1±1.4, 2		-58.6±24.3, 4	-399±1, 2	
	Station Road Yedoma Pond 1	stirred surface sediments						-56.1±2.5, 3		
	Tower Road Yedoma Pond 2	stirred surface sediments	29.8, 1	65.5, 1	4.5, 1	1.9, 1		-58.3±3.0, 3	-448±0, 2	
	Tower Road Yedoma Pond 3	stirred surface sediments						-62.0±6.3, 3	-461, 1	
	Kitchen Sand Pond 1	stirred surface sediments	11.8±1.1, 2	86.9±1.7, 2	1.3±0.1, 2	1.9±0.6, 2		-58.2±1.1, 2	-420, 1	
	Volodya Sand Pond 2	stirred surface sediments	10.7±8.2, 3	87.6±8.2, 3	1.9±1.3, 3	1.7±0.3, 3		-53.7±7.1, 3	-433±8, 2	
	Airport Sand Pond 3	stirred surface sediments	2.7±2.7, 2	94.1±2.5, 2	4.3±2.7, 3	2.0±0.9, 3		-57.7, 1		

130

Table 4-2 Cont.

	Meadow Lake	stirred surface sediments	37.1 ± 7.5, 4	62.3 ± 6.6, 4	1.8 ± 0.3, 4	1.3 ± 0.6, 4	-57.2 ± 5.2, 4	-449 ± 14, 2
	No Fish Ambarchik Lake	stirred surface sediments	24.1 ± 14.6, 3	72.0 ± 13.5, 3	3.5 ± 1.2, 3	1.6 ± 0.3, 3	-63.3 ± 2.1, 3	
	Ambarchik Fish Lake	stirred surface sediments	21.7 ± 7.9, 2	75.8 ± 7.9, 2	2.1 ± 0, 2	1.6 ± 0, 2	-60.2 ± 0.4, 2	
	Young Tundra Thaw Pond	stirred surface sediments	70.2 ± 0.6, 2	22.5 ± 1.7, 2	6.6 ± 1.2, 2	1.3 ± 0.1, 2	-56.1 ± 3.2, 2	
	Tundra Floodplain Lake	stirred surface sediments	49.7 ± 7.7, 3	45.6 ± 5.9, 3	4.2 ± 1.2, 3	1.8 ± 0.7, 3	-61.0 ± 2.0, 3	-432 ± 8, 2
Alaska	Rosie Creek Beaver Pond	hotspot	69.3 ± 12.3, 7	27.3 ± 10.2, 7	1.6 ± 0.3, 7	2.3 ± 2.7, 7	-75.5 ± 0.4, 5	-413 ± 2, 5
	Goldstream Lake	hotspot	88.7 ± 1.4, 3	9.5 ± 1.1, 3	0.8 ± 0.1, 3	1.2 ± 0, 3	-70.7 ± 1.2, 2	-406 ± 6, 2
	Lake E1	ice koshka	34.2 ± 2.8, 4	53.5 ± 1.4, 3	0 ± 0.1, 4	11.7 ± 2.0, 4	-73.5 ± 1.1, 4	-389 ± 10, 4
	Lake E6	ice koshka	59.7 ± 5.8, 7	28.7 ± 4.3, 7	0.2 ± 0.1, 7	11.1 ± 1.5, 7	-67.6 ± 0.6, 7	-390 ± 4, 7
	Lake N2	ice koshka	39.7 ± 1.1, 2	49.1 ± 1.0, 2	0.1 ± 0, 2	11.1 ± 0.4, 2	-75.2 ± 0.2, 2	-387 ± 2, 2
	Lake N3	ice koshka	49.5 ± 3.0, 4	37.2 ± 2.3, 4	0.1 ± 0, 4	12.8 ± 0.7, 4	-72.2 ± 0.7, 4	-383 ± 2, 4
	Lake NE1	ice koshka	38.4 ± 2.9, 5	53 ± 3.1, 5	0.1 ± 0, 5	8.6 ± 0.4, 5	-73.8 ± 2.4, 5	-387 ± 1, 5

[†]We have not presented the $\delta^{13}C_{CO2}$ of samples collected in 2001 because we cannot trust that CH_4 oxidation did not occur in the refrigerated sample bottles during storage. Data on $\delta^{13}C_{CO2}$ of Alaskan gases were not collected.

Table 4-3. Radiocarbon content of CH_4 (and CO_2) in lake bubbles from Siberia and Alaska presented as percent modern carbon (pmC) and ^{14}C age (years). Error symbols represent standard deviation of accelerator mass spectrometer analyses for each sample.

	Lake name	Margin type	Bubble Trap No.	Depth (m)	Bubble source	Freshness	Field Date	$^{14}C_{CH4}$, pmC	±	$^{14}C_{CH4}$ age (yrs)	±	$^{14}C_{CO2}$, pmC	±	$^{14}C_{CO2}$ age (yrs)	±
Siberia	Shuchi Lake	Non-thermokarst	-	0.75	surface, stirred	fresh	July 12, 2001	97.8%	0.2%	175	20	95.7%	0.2%	355	25
		Non-thermokarst	21	1.4	background	not fresh	Aug. 7, 2003	84.6%	0.3%	1,345	30				
		Thermokarst	20	1.8	background	not fresh	July 23, 2003	51.4%	0.1%	5,350	25				
		Thermokarst	4	2.25	hotspot	fresh	May 12, 2003	0.5%	0.1%	42,800	1,400				
		Thermokarst	4		hotspot	fresh	June 16, 2003	0.8%	0.1%	38,670	860				
		Thermokarst	4		hotspot	fresh	July 23, 2003	0.9%	0.1%	37,920	780				
		Thermokarst	4		hotspot	fresh	Sept. 6, 2003	1.2%	0.1%	35,570	590				
		Thermokarst	4		hotspot	fresh	Oct. 15, 2003	0.8%	0.1%	39,120	920				
		Thermokarst	4		hotspot	fresh	Dec. 27, 2003			42,900	2,200				
		Thermokarst	4		hotspot	fresh	Feb. 21, 2004			41,200	1,800				
		Thermokarst	4		hotspot	fresh	April 27, 2004			39,500	1,400				
		Thermokarst	23	1.75	point source	not fresh	July 23, 2003	49.9%	0.1%	5,590	20				
		Thermokarst	23	1.75	point source	fresh	July 29, 2003	24.3%	0.1%	11,355	40				
		Thermokarst	5	4.75	point source	fresh	May 10, 2003	6.4%	0.1%	22,050	120				
		Thermokarst	8	0.8	point source	fresh	July 23, 2003	21.7%	0.1%	12,285	40				
		Thermokarst	33	1.5	background	not fresh	July 23, 2003	66.3%	0.2%	3,305	20				
	Tube Dispenser Lake	Thermokarst	33		background	not fresh	July 29, 2003	74.5%	0.3%	2,360	30				
		Thermokarst	44	3.1	background	not fresh	July 23, 2003	41.1%	0.1%	7,145	30				
		Thermokarst	11	5	hotspot	fresh	May 10, 2003	1.2%	0.1%	35,260	570				
	Grass Lake		16	12	background	not fresh	June 17, 2003	36.1%	0.2%	8,185	40				
			16		background	not fresh	Sep. 10, 2003	76.0%	0.2%	2,210	20				
	Tower Road Yedoma Pond 2		-	0.75	surface, stirred	fresh	July 28, 2001	105.2%	0.3%	>modern	20				
	Tower Road Yedoma Pond 3		-	0.75	surface, stirred	fresh	July 28, 2001	109.4%	0.2%	>modern	20				
	Tundra Floodplain Lake		-	0.35	surface, stirred	fresh	July 20, 2001	63.1%	0.2%	3,695	20	60.9%	0.1%	3,980	20
			-		surface, stirred	fresh	July 20, 2001	79.0%	0.2%	1,890	25	77.9%	0.3%	2,010	30
Alaska	Rosie Creek Beaver Pond		-	1.5	hotspot	fresh	Nov. 1, 2004	15.9%	0.1%	14,760	35				
			-	1.5		fresh	Nov. 1, 2004	11.2%	0.1%	17,585	40				
	Goldstream Valley Lake		-	1.3	hotspot	fresh	Nov. 1, 2004	3.9%	0.1%	26,020	100				

Table 4-4. Estimation of CO_2 reduction and acetate fermentation contributions to CH_4 production of different bubble sources in two Siberian lakes. Carbon isotopic fractionation α_C values exceeding 1.060 indicate CH_4 production by CO_2 reduction, while α_C less than 1.055 suggests acetate fermentation (Table a). Cases 1 and 2 (Table b) assume $\delta^{13}C$ of acetate derived from labile and recalcitrant sediment organic matter respectively. Mean values are reported with standard deviation and n number of samples.

(a) Lake	Bubble source	α_c	$\delta^{13}C_{CH4}$	$^{13}CH_{4,CO2}$
Shuchi Lake	background	1.051 ± 0.005, 9	-66.8 ± 5.6, 10	-85.0 ± 4.6, 9
	point source	1.072 ± 0.011, 13	-79.7 ± 3.1, 13	-78.4 ± 6.4, 11
	hotspot	1.070 ± 0.003, 18	-79.6 ± 0.5, 35	-81.8 ± 2.4, 24
Tube Dispenser Lake	background	1.046 ± 0.005, 11	-62.4 ± 2.6, 14	-86.3 ± 3.0, 11
	hotspot	1.073 ± 0.017, 3	-77.1 ± 4.7, 3	-76.9 ± 9.6, 3

(b) Lake	Bubble source	Case 1		Case 2	
		CO2%	Ace%	CO2%	Ace%
Shuchi Lake	background	57%	43%	69%	31%
	point source	100%	0%	100%	0%
	hotspot	94%	6%	96%	4%
Tube Dispenser Lake	background	45%	55%	60%	40%
	hotspot	100%	0%	100%	0%

Table 4-5. Ebullition flux-weighted estimates of CH_4 isotope emissions from two intensively studied Siberian lakes. (Table a) Methane fluxes reflect the mean and standard deviation of year-long continuous measurements of ebullition and diffusion at two Siberian lakes (Chapter 1). Mean isotope values are reported with standard deviation and n number of samples. The regional total (‰$^{-1}$ Gt CH_4 region^{-1} yr^{-1}) was determined by multiplying the lake total isoflux by 11% lake cover of $10^6 km^2$ for yedoma territory (Table b). The stable isotope, radiocarbon age and proportion of CO_2 reduction (%CO_2) and acetate fermentation (%Ace) pathways (Table c) for bubble samples collected from ebullition flux component (background, point source, and hotspots) during summer and winter are weighted by the contribution of each component to total annual whole lake emissions. Cases 1 and 2 in Table c assume $\delta^{13}C$ of acetate derived from labile and recalcitrant sediment organic matter respectively.

(a) Season 2003-04	Flux component	Whole lake (g CH_4 m^{-2} of lake yr^{-1})	% of annual flux	Mean			
				δD_{CH4} (‰)	$\delta^{13}C_{CH4}$ (‰)	$\Delta^{14}C_{CH4}$ (‰)	$^{14}C_{CH4}$ age (years)
Summer	background	5.7 ± 2	22 ± 6%	-431.8 ± 26.3, 14	-63.4 ± 9.4, 28	-390 ± 186, 7	4,271 ± 2,650, 7
	point source	6.2 ± 0.7	25 ± 5%	442.6 ± 3.8, 9	-74.2 ± 8.8, 15	-683 ± 155, 3	9,743 ± 3,627, 3
	hotspots	1 ± 0.7	4 ± 2%	-457.3 ± 3.3, 6	-79.9 ± 0.5, 12	-991 ± 2, 4	37,820 ± 1,580, 4
	molecular diffusion	1.3 ± 0.1	5 ± 1%				
Winter	background[b]	0.5 ± 0	2 ± 0%	-393.2	-58.2	-390 ± 186, 7	4,271 ± 2,650, 7
	point source[c]	8.3 ± 0.9	34 ± 7%	-405.9 ± 13.2, 4	-69.3 ± 4.3, 4	-936	22,050, 1
	hotspots	2 ± 1.3	8 ± 5%	-454.3 ± 7.1, 28	-79.2 ± 1.6, 26	-993 ± 3, 5	40,332 ± 3,157, 5
Whole lake total		25	100%	-427.5	-70.3	-738.5	16,524

Table 4-5 cont.

(b) Season 2003-04	Flux component	Isoflux[a] (‰ g CH_4 m^{-2} of lake yr^{-1})		
		δD_{CH4} (‰)	$\delta^{13}C_{CH4}$ (‰)	$\Delta^{14}C_{CH4}$ (‰)
Summer	background	-2461.3	-361.5	-2221.9
	point source	-2744.1	-460.0	-4231.9
	hotspots molecular diffusion	-457.3	-79.9	-990.9
Winter	background[b]	-196.6	-29.1	-194.9
	point source[c]	-3368.6	-574.8	-7770.5
	hotspots	-908.6	-158.4	-1986.0
Whole lake total		-10,137	-1,664	-17,396

		‰ Gt CH_4 $region^{-1}$ yr^{-1}		
Regional total		-1.115	-0.183	-1.914

(c) Season 2003-04	Flux component	Case 1			Case 2			
		% CO_2	% Ace	±	% CO_2	% Ace	±	n
Summer	background	49%	51%	9%	63%	37%	7%	20
	point source	100%	0%	16%	100%	0%	11%	8
	hotspots molecular diffusion	96%	4%	4%	97%	3%	3%	10
Winter	background[b]	49%	51%	9%	63%	37%	37%	20
	point source[c]	76%	24%	8%	82%	18%	6%	4
	hotspots	92%	8%	12%	97%	3%	13%	11
Whole lake total		74%	21%		80%	15%		

[a]The isoflux is calculated as the sum of each isotope signature (‰) multiplied by the CH_4 flux (g CH_4 m^{-2} of lake yr^{-1}).

[b]Isotopes of background bubble samples were not measured for winter. Summer values were used in the calculations. We assume the error is insignificant given that background bubbling accounts for only 2% of annual emissions.

[c]We used stable isotope values measured from ice koshka gas collected in spring to incorporate any oxidation or diffusion effects on emission signals from point sources that are trapped during long periods of time in ice. Radiocarbon age and calculated CH_4 production pathways for point sources of all seasons reflect isotope signatures of bubbles collected freshly in traps.

SUMMARY

By quantifying the magnitude and patchiness of methane (CH_4) ebullition (bubbling) fluxes from arctic thaw lakes, this work showed that such emissions are important at the global scale. Methane is the most abundant organic gas in the Earth's atmosphere, a key molecule in tropospheric chemistry, and an important greenhouse gas responsible for ~20% of the direct radiative forcing from all long-lived greenhouse gases (Cicerone and Oremland 1989, IPCC 2001). The concentration of atmospheric CH_4 has more than doubled since the beginning of the industrial revolution. Anthropogenic sources such as ruminant animal husbandry, rice agriculture, natural gas production, biomass burning, and landfills account for ~60% of total sources and are the primary cause of the rapid increase in atmospheric methane concentration (AMC) over the past 150 years. Natural wetlands, however, are another important source (~15-47% of total emissions; IPCC 2001), which has yet to be more narrowly defined given large uncertainties in wetland extent and the spatial and temporal variability associated with extrapolating short-term local CH_4 emission measurements to regional scales (Reeburgh et al., 1998, Mikaloff Fletcher et al., 2004a,b).

Much of atmospheric CH_4 originates in high northern latitudes, where the concentration of atmospheric CH_4 is highest (Steele et al. 1987, Fung et al. 1991). However, the relative contribution of various northern CH_4 sources is still poorly understood (Nisbet et al. 1989, Mikaloff Fletcher 2004). The most extensive cover of wetlands on Earth occurs at high latitudes of the Northern Hemisphere (Mathews and Fung et al. 1987, Aselmann and Crutzen 1989), and the North has been an important source of atmospheric CH_4 for thousands of years prior to the industrial revolution (Rasmussen and Khalil 1984, Severinghaus and Brook 1999, Smith et al. 2004). Since warming in the Arctic is predicted to enhance CH_4 emissions from wetlands during the next century (IPCC 2001), improving the estimate of northern wetland contribution to atmospheric CH_4 has been identified as an important research objective (Mathews and Fung 1989, Nisbet et al. 1989, Reeburgh et al. 1998, Dlugokencky et al. 2001, Mikaloff Fletcher 2004).

Although lakes are a prominent landscape feature in the North, occupying up to 30% of the land surface area in some regions, they have been largely ignored with regards CH_4 emissions in biogeochemical and inverse models of the global atmospheric methane budget. The primary reason is that most process-based studies of lake emissions employ techniques to quantify emission by molecular diffusion during the open water season (summer) without measuring ebullition, which presents logistical difficulties owing to its patchiness. Studies that have measured ebullition often extrapolate short-term measurements from randomly placed bubble traps or floating chambers to an annual estimate. My work shows that the techniques used in previous studies systematically underestimated the magnitude of lake emissions. By assessing the patchiness of ebullition through mapping of bubbling 'point sources' and 'hotspots', types of bubbling that had never been quantified, I demonstrated that including ebullition increases previous estimates of CH_4 flux from the same lakes 5-fold in Siberia [from 6.8 g m^{-2} yr^{-1} (Zimov et al. 1997) to 34 g m^{-2} yr^{-1} (this study)] and 2.5- to 14-fold fold in Alaska [from 0.6 g m^{-2} yr^{-1} based on molecular diffusion (Kling et al. 1992) to 1.6-9.3 g CH_4 m^{-2} yr^{-1} based on point-source ebullition (this study)].

I linked year-long continuous field measurements of lake ebullition with aerial photographs and geographical information systems analyses to scale lake emissions to the 10^6 km^2 extent of the Pleistocene-aged yedoma ice-complex in North Siberia, yielding a conservative regional estimate of 3.8 Tg CH_4 yr^{-1} from lakes. An independent mass-balance approach based on carbon loss from North Siberian yedoma lake sediments due to methanogenesis yielded a similar estimate (4-5 Tg CH_4 yr^{-1} averaged over the past 10,000 to 13,000 years). This significantly increases current estimates of northern wetland contributions (<6-40 Tg yr^{-1}) (Roulet et al. 1994, Reeburgh et al. 1998, Worthy et al. 2000, IPCC 2001, Mikaloff Fletcher 2004) to the atmospheric CH_4 budget.

By assessing the spatial distribution of bubbling point sources and hotspots, I identified thermokarst (thaw) erosion along lake margins as the primary driver of CH_4 emissions from Siberian yedoma lakes. Permafrost thaw and ground-surface collapse, a process known as thermokarst, release organic matter into anaerobic lake bottoms fueling

methanogenesis. Thermokarst margins of lakes (15- to 30-m wide band) accounted for 79-90% of total emissions from Siberian lakes. Geographical information systems analysis showed a 14.7% increase in lake area in our North Siberia study region between 1974 and 2000. This is similar to the lake expansion observed during the same period in the West Siberian Lowlands (Smith *et al.* 2005). Calculation suggests that the 14.7% lake expansion led to an increase in lake CH_4 emissions by 58%. If this is true, thermokarst activity is a positive feedback to climate warming. The Pleistocene age of CH_4 (^{14}C age 35,570-42,800 years) emitted from hotspots along active thermokarst margins of lakes demonstrates that recruitment of a previously sequestered carbon source is a large cause of this positive feedback to climate warming.

I combined maps of bubble-source distributions in lakes with long-term, continuous flux measurements and isotope compositions of bubbles to provide annual whole-lake and regional CH_4 isofluxes (flux-weighted average of isotope signatures). In contrast to typical values used in inverse models of atmospheric CH_4 for northern wetland sources ($\delta^{13}C_{CH4}$ = -58‰, ^{14}C age modern), I show that this large, new source of high latitude CH_4 from aquatic ecosystems (thaw lake ebullition) is isotopically distinct ($\delta^{13}C_{CH4}$ = -70‰, ^{14}C age 16,500 yrs). Inverse modeling of atmospheric methane attributes ^{14}C -dead CH_4 to fossil fuel sources; however, ^{14}C ages of 14,760-26,020 years measured from bubbling hotspots in boreal thaw lakes in Alaska suggest that the ^{14}C-depleted CH_4 signature of ebullition is not unique to Siberian yedoma lakes, and more thorough quantification of this natural ^{14}C-depleted CH_4 source in the Arctic should be conducted.

Finally, this work considered the role of thaw lakes on the yedoma ice-complex of Siberia in atmospheric CH_4 dynamics during the last deglaciation. Though specific sources of late-Quaternary atmospheric CH_4 are poorly constrained, ice core records of the interpolar CH_4 gradient suggest that an arctic/boreal source was responsible for >30% of the abrupt increases of global atmospheric CH_4 concentration during deglacial climate warming. Until now the two major hypotheses that have been advanced to explain millennial-scale variations in AMC, each with limitations, are: 1) CH_4 emissions from

northern wetlands increased in response to climate warming (wetland hypothesis Chappellaz *et al.* 1993, Smith *et al.* 2004), and 2) catastrophic release of methane hydrates in sea floor sediments caused rapid increases in AMC ('clathrate gun hypothesis' Kennett *et al.* 2003). Based on 1) high rates of CH_4 bubbling from modern thaw lakes in the Arctic, 2) CH_4 production potentials of organic matter from frozen, unconsolidated deposits of late Pleistocene age, and 3) estimates of the changing extent of these deposits as sea level rose and thaw lakes developed during deglaciation, I advanced a new hypothesis: CH_4 bubbling from newly forming thaw lakes contributed 32-70% of the high-latitude increases in AMC that accompanied rapid climate warming at the Pleistocene-Holocene boundary. This hypothesis complements the two previous hypotheses and contributes to an improved understanding of the patterns of climate warming during previous deglaciations.

About 425 Gt C are still preserved in the yedoma ice complex in North Siberia. If the yedoma region with its high-ice-content permafrost warms more rapidly in the future, as projected (Sazonova *et al.* 2004), and lakes respond by rapid expansion, ebullition from thermokarst lakes could serve as a powerful positive feedback to high-latitude warming, as it may have during deglacial climate warming at the onset of the Holocene. Expansion of yedoma thaw lakes during recent decades in North Siberia suggests that this positive feedback is already underway. This important source of atmospheric CH_4 is not currently considered in climate-change projections.

LITERATURE CITED

Arctic Climate Impact Assessment (ACIA): Overview Report. Cambridge Univ. Press, New York. Cambridge Univ. Press, New York.

Aselmann, I. and Crutzen, P. J. Global distribution of natural freshwater wetlands, rice paddies, their net primary productivity, seasonality, and possible methane emissions. *J. of Atm. Chem.* 8, 307-358 (1989).

Bastviken, D., Cole, J., Pace, M., & Tranvik, L. Methane emissions from lakes: Dependence of lake characteristics, two regional assessments, and a global estimate. *Global Biogeochem. Cycles* 18, GB3010, doi:10.1029/2004GB002238 (2004).

Casper, P., Maberly, S. C., Hall, G. H., & Finlay, B. J. Fluxes of methane and carbon dioxide from a small productive lake to the atmosphere. *Biogeochemistry* 49, 1-19 (2000).

Chappellaz, T., Bluniert, T., Raynaud, D., Barnola, J. M., Schwander, J., and Stauffert, B. Synchronous changes in atmospheric CH_4 and Greenland climate between 40 and 8 kyr BP. *Nature* 366, 443-445 (1993).

Cicerone, R. J., and Oremland, R. S. Biogeochemical aspects of atmospheric methane, *Global Biogeochem. Cycles* 2(4):299-327 (1988).

Dlugokencky, E. J., Walter, B. P. , Masarie, K. A., Lang, P. M., and Kasischke, E. S. Measurements of an anomalous global methane increase during 1998. *Geophysical Research Letters* 28(3): 499-502 (2001).

Ethridge, D. M., Steele, L. P., Francey, R. J., and Langenfelds, R. L. Atmospheric methane between 1000 A.D. and present: Evidence of anthropogenic emissions and climate variability, *J. Geophys. Res.* 103: 15,979-15,993 (1998).

Fung, I., John, J., Lerne, J., Mathew, E., Prather, M., Steele, L. P., and Fraser, P. J. Three-dimensional model synthesis of the global methane cycle. *J. Geophys. Res* 96: 13,033-13,065 (1991)

Hinkel, K. M., Eisne, W. R., Bockheim, J. G., Nelson, F. E., Peterson, K. M., Dai, X. Spatial extent, age, and carbon stocks in drained thaw lake basins on the Barrow Peninsula, Alaska. *Arctic. Antarctic and Alpine Research* 35: 291-300 (2003).

Intergovernmental Panel on Climate Change (IPCC). *The Scientific Basis.* Cambridge Univ. Press, New York (2001).

Jorgenson, M. T., Racine, C. H., Walters, J. C., and Osterkamp, T. E. Permafrost degradation and ecological changes associated with a warming climate in central Alaska. *Climatic Change* 48: 551-579 (2001).

Kennett, J. P., Cannariato, K. G., Hendy, I. L., and Behl, R. J. Methane Hydrates in Quaternary Climate Change. Book. American Geophysical Union, Washington DC, (2003).

Kling, G. W., Kipphut, G. W., and Miller, M. C. The flux of CO2 and CH4 from lakes and rivers in arctic Alaska. *Hydrobiologia* 240: 23-36 (1992).

Mathews, E., and Fung, I. Methane emission from natural wetlands: Global distribution, area, and environmental characteristics of sources. *Global Biogeochem. Cycles* 1: 61-86 (1987).

Mikaloff Fletcher, S. E., Tans, P. P., Bruhwiler, L. M., Miller, J. B., and Heimann, M. CH_4 source estimated from atmospheric observations of CH_4 and its $^{13}C/^{12}C$ isotopic ratios: 1. Inverse modelling of source processes. *Global Biogeochem. Cycles* 18, GB4004, doi:10.1029/2004GB002223 (2004a).

Mikaloff Fletcher, S. E., Tans, P. P., Bruhwiler, L. M., Miller, J. B., & Heimann, M. CH_4 source estimated from atmospheric observations of CH_4 and its $^{13}C/^{12}C$ isotopic ratios: 2. Inverse modelling of CH_4 fluxes from geographic regions. *Global Biogeochem. Cycles* 18, GB4004, doi:10.1029/2004GB002224 (2004b).

Nisbet, E. G. Some northern sources of atmospheric methane: production, history, and future implications. *Can. J. Earth Sci.* 26: 1603-1611 (1989).

Osterkamp, T. E., Viereck, L., Shu, Y., Jorgenson, M. T., Racine, C., Doyle, A., and Boone, R. D. Observations of thermokarst and its impact on boreal forests in Alaska, U.S.A. *Arctic, Antarctic, and Alpine Research* 32: 303-315, (2000).

Rasmussen, R. A. and Khalil, M. A. K. Atmospheric methane in the recent and ancient atmospheres: concentrations, trends and interhemispheric gradient. *J. Geophys. Res.*, 89: 11,599-11,605 (1984).

Reeburgh, W. S. *et al.* A CH_4 emission estimate for the Kuparuk River basin, Alaska. *J. Geophys. Res.* 103, 29,005- 29,013 (1998).

Roulet, N. T. *et al.* Role of Hudson Bay lowland as a source of atmospheric methane. *J. Geophys. Res.* 99, 1439-1454 (1994).

Rudd, J. W. M., and Hamilton, R. D. Methane cycling in a eutrophic shield lake and its effects on whole lake metabolism. *Limnol. Oceanogr.* 23: 337-348 (1978).

Sazonova, T. S., Romanovsky, V. E., Walsh, J. E. and Sergueev, D. O. Permafrost dynamics in the 20th and 21st centuries along the East Siberian transect. *J. Geophys. Res.* 109, doi:10.1029/2003JD003680 (2004).

Severinghaus, J. P., and Brook, E.J. Abrupt climate change at the end of the Last Glacial Period inferred from trapped air in polar ice. *Science* 286:930-934 (1999).

Smith, L. C., MacDonald, G. M., Velichko, A. A., Beilman, D. W., Borisova, O. K., Frey, K. E., Kremenetski, K. V., and Sheng, Y. Siberian peatlands a net carbon sink and global methane source since the early Holocene. *Science* 303: 353-356 (2004).

Smith, L. C., Sheng, Y., MacDonald, G. M., and Hinzman, L. D. Disappearing arctic lakes. *Science* 308: 1429 (2005).

Steele, L. P., Conway, T. J., Fraser, P. J., Rasmussen, R. A., and Khalil, M. A. K.. The global distribution of methane in the troposphere, J. *Atmos. Chem.* 5:125-171 (1987).

Whalen, S. C., and Reeburgh, W. S. A methane flux transect along the trans-Alaska pipeline haul road. *Tellus* 22B: 237-249 (1990).

Worthy, D. E., Levin, J., I., Hopper, F., Ernst, M. K., and Trivett, N. B. A. Evidence for a link between climate and northern wetland methane emissions. *J. Geophys. Res.* 105, 4031-4038 (2000).

Zhuang, Q., Melillo, J., Kicklighter, D.W., Prinn, T.G., McGuire, A.D., Steudler, P.A., Felzer, B.S. and Hu, S. Methane fluxes between terrestrial ecosystems and the atmosphere at northern high latitudes during the past century: A retrospective analysis with a process-based biogeochemistry model. *Global Biogeochem. Cycles* 18, GB3010, doi:10.1029/2004GB002239 (2004).

Zimov, S. A., Voropaev, Y. V., Semiletov, I. P., Davidov, S. P., Prosiannikov, S. F., Chapin III, F. S., Chapin, M. C., Trumbore, S. and Tyler, S. North Siberian lakes: A methane source- fuelled by Pleistocene Carbon. *Science* 277, 800-802 (1997).

Zimov, S. A. 2005. Pleistocene Park: Return of the Mammoth's Ecosystem. *Science* 308, 796-798.